MYCORRHIZAS AND THE CONTEXT DEPENDENCY OF MUTUALISM: EFFECTS OF SOIL PHOSPHORUS AVAILABILITY AND COMMUNITY COMPOSITION OF ARBUSCULAR MYCORRHIZAL FUNGI ON PLANT PERFORMANCE AND SYMBIOSIS WITH THE GRASSLAND FORB *GAILLARDIA ARISTATA* ACROSS ITS NORTHERN RANGE

A Thesis
Submitted to the Graduate Faculty
of the
North Dakota State University
of Agriculture and Applied Science

By

Alison Long

In Partial Fulfillment of the Requirements
for the Degree of
MASTER OF SCIENCE

Major Program:
Environmental and Conservation Sciences

May 2021

Fargo, North Dakota

North Dakota State University
Graduate School

Title

MYCORRHIZAS AND THE CONTEXT DEPENDENCY OF MUTUALISM: EFFECTS OF SOIL PHOSPHORUS AVAILABILITY AND COMMUNITY COMPOSITION OF ARBUSCULAR MYCORRHIZAL FUNGI ON PLANT PERFORMANCE AND SYMBIOSIS WITH THE GRASSLAND FORB *GAILLARDIA ARISTATA* ACROSS ITS NORTHERN RANGE

By

Alison Long

The Supervisory Committee certifies that this ***disquisition*** complies with North Dakota State University's regulations and meets the accepted standards for the degree of

MASTER OF SCIENCE

SUPERVISORY COMMITTEE:

Laura Aldrich-Wolfe
Chair

Ylva Lekberg

Caley Gasch

Deirdre Prischmann-Voldseth

Approved:

11/19/2021
Date

Craig Stockwell
Department Chair

ABSTRACT

Arbuscular mycorrhizal fungi (AMF) colonize roots and provide phosphorus as well as other benefits to hosts in exchange for photosynthate. I explored how the symbiosis between AMF and the native prairie forb *Gaillardia aristata* differed regionally among sites that varied in soil phosphorus availability (SPA). In the field, plant biomass and shoot phosphorus concentration were correlated with SPA and hyphal length. AMF community composition in roots correlated with distance between sites, SPA, temperature, and precipitation. To test the hypothesis that AMF from sites varying in SPA would differ in effectiveness at provisioning phosphorus to their host, I grew *G. aristata* in the greenhouse with soil inoculum from sites low and high in SPA and fertilized with or without phosphorus. *Gaillardia aristata* benefited equally from both inocula and phosphorus fertilization, while root AMF communities differed between inocula but not with fertilization. AMF from varying SPA appear to be equally effective mutualists.

ACKNOWLEDGEMENTS

I first must thank Dr. Laura Aldrich-Wolfe for accepting me as a member of her lab and giving me the opportunity to change my career path and enter the fascinating world of mycorrhizal fungi. Without her support and guidance scholastically, professionally, and personally, my graduate school experience would not have been nearly as successful nor enjoyable. My collaborator Ylva Lekberg was invaluable in providing mentorship, perspective, and time in addition to resources at MPG Ranch. Moreover, Kelly Laflamme and Lorinda Bullington from MPG Ranch contributed their expertise to the molecular portion of this research. The remainder of my committee, Caley Gasch and Deirdre Prischmann-Voldseth, provided similar necessary insight, support, and tools for this work. I appreciate the kind assistance of Joel Bell in training and support needed for completion of phosphatase assays and Jeff Kittilson with setup of a vacuum filtration system. Stefanie Vink provided indispensable guidance in bioinformatics pipelines.

I need to thank the incredible community that is the Biological Sciences department, particularly all the fellow grad students who became lifelong friends. Many thanks to Libby Sternhagen, a light in the darkness, my lab mate, and grad school guru. I could not have survived without the friendship of Christine Cornish, Alicia Schlarb, Rebecca Jones, and Hanna Karevold and am appreciative of their help in refining presentations and data visualization. I thank Lydia Nixon for always being there for me. My lab mates Ankita Sawant and Jeffrey Lackmann provided helpful feedback on this thesis. Many undergraduate students in the Aldrich-Wolfe lab, particularly Marley Lund, Breann Adamek, Kenzie Vinje, Hanna Zastoupil, Michael Fisher, and Zach Tarble helped to process the copious plant and fungal samples collected for this research and I am grateful for their contributions. Special thanks to Jesse Gallagher and Keith Stueve, who participated in fieldwork as well as labwork and ensured there was never a dull moment.

I am very grateful for financial support from the Environmental and Conservation Sciences (ECS) program, especially its chair, Dr. Craig Stockwell, the Biological Sciences

department, and the College of Science and Mathematics for supporting me not only in conducting my research, but also by allowing me to attend conferences where I was able to present my research. Portions of this project were funded by the J. E. Weaver Grant from the Nebraska Chapter of The Nature Conservancy and NSF ND EPSCoR Track 1 Award OIA-1355466. I am indebted to the ranchers who allowed me to sample on their land as well as MPG Ranch for their generosity in sharing time and resources with me. This work used resources of the Center for Computationally Assisted Science and Technology (CCAST) at North Dakota State University, which were made possible in part by NSF MRI Award No. 2019077. I appreciate everyone at NDSU who has guided me through the grad school process, particularly Wendy Leach and the Graduate School administrative employees who have answered all my endless questions.

The support of my family and friends, especially Sarah Illing, over the last three years means so much to me. Most importantly, this thesis and degree would not have happened without the love, sacrifice, and encouragement of my amazing wife. From moving to North Dakota with me so I could pursue this degree, to harvesting and washing root samples late into the night, to cooking me delicious meals while I worked long hours, to believing in me before I believed in myself, her generosity and support are well remembered and appreciated more than she knows.

PREFACE

"In nature, nothing exists alone." ~Rachel Carson, *Silent Spring* (1962)

"How delicate is the mechanism by which the balance of power is maintained among members of the soil population." ~Mabel Rayner, *Trees and Toadstools* (1945)

"Each step that we make in the more intimate knowledge of nature leads us to the entrance of new labyrinths." ~Alexander von Humboldt, *Cosmos: A Sketch of a Physical Description of the Universe, Volume 1* (1845)

TABLE OF CONTENTS

LIST OF TABLES

LIST OF FIGURES

LIST OF ABBREVIATIONS

AMF .....Arbuscular Mycorrhizal Fungi

ANOVA .....Analysis of Variance

ASV .....Amplicon Sequence Variant

BB.....B-B Ranch

BF .....Blackfoot

BI .....Bicentennial Prairie

BW .....Beckman WMA

CEC.....Cation Exchange Capacity

CG .....Central Grasslands

CL .....Clearwater

CN .....Clearwater New

DB .....Delbert Berntson

HSD .....Honestly Significant Difference

ITS.....Internal Transcribed Spacer

KL .....Kleinschmidt

LP .....Lone Ponderosa

MS .....Mt. Sentinel

NCBI .....National Center for Biotechnology Information

NMS .....Non-metric Multidimentional Scaling

OM .....Organic Matter

OTU.....Operational Taxonomic Unit

P.....Phosphorus

PERMANOVA.....Permutational Multivariate Analysis of Variance

PCR .....Polymerase Chain Reaction

SC.....Sheep Camp

VT .....Virtual Taxon

LIST OF APPENDIX TABLES

LIST OF APPENDIX FIGURES

CHAPTER 1. VARIATION IN COMMUNITES OF ARBUSCULAR MYCORRHIZAL FUNGI AND PLANT PERFORMANCE OF *GAILLARDIA ARISTATA* ACROSS SITES OF DIFFERING SOIL PHOSPHORUS AVAILABILITY IN THE NORTHERN GREAT PLAINS

1.1. Abstract

Arbuscular mycorrhizal fungi (AMF) are root endosymbionts that provide nutrients such as phosphorus (P) to their plant hosts in exchange for lipids and sugars. I sought to address how patterns of mycorrhizal abundance and formation and AMF community composition might vary with spatial variability of abiotic factors, including P, that should influence the importance of the symbiosis to the plant. I measured plant biomass, plant and soil nutrients, length of extraradical hyphae in the soil, and root colonization by AMF for *Gaillardia aristata*, a native prairie forb and species of special concern in Minnesota, at each of 12 sites from Montana to Minnesota that ranged in mean soil P availability from 2 to 38 ppm. I identified AMF species present in roots using next-generation DNA sequencing. Plants from soils with higher P availability were larger and had more P in their aboveground tissues. Greater plant P was associated with greater hyphal length in the soil but not with greater AMF colonization of roots. At the mid-continental scale, AMF community composition varied with spatial distance, soil P availability, temperature, and precipitation. These results suggest that soil P availability and mycorrhizas may be related to growth and P status in *G. aristata* and that AMF community composition is shaped by climate and soil.

1.2. Introduction

Arbuscular mycorrhizal fungi (AM fungi or AMF) are obligate symbionts that associate with the roots of most terrestrial plants (Smith & Read 2008). Within the symbiosis, these Glomeromycetes (Cavalier-Smith 1998) provide mineral nutrients and services to their plant hosts in exchange for photosynthate in the form of carbohydrates and lipids (Wright *et al*. 1998; Pfeffer *et al*. 1999; Luginbuehl *et al*. 2017; Jiang *et al*. 2017). Along with nutrient acquisition (Rovira 1969; Baker & Cook 1974) and protection from pathogens (Newsham *et al*. 1995; Pozo & Azcón-Aguilar 2007), the fungal symbionts can provide tolerance to

drought (Augé 2001), salinity (Porcel *et al*. 2012) and heavy metal stress (Joner *et al*. 2000).

By enhancing plant nutrient uptake and protecting their hosts from biotic and abiotic stressors, AMF can greatly influence plant performance. Plant performance, or the ability to obtain resources and survive stressful environments and competitors, is generally quantified via survival, growth, and reproduction. It is often strongly positively correlated with growth rate and reproductive success (Harper and White, 1974; Bazzaz *et al*., 1987; Herms and Mattson, 1992). Nutrient status is an important contributor to plant performance. Plants acquire nutrients from their soil environments and accumulate these nutrients in their tissues. Essential nutrients must be present at a sufficient concentration for metabolic functions of the plant to occur; poor plant performance can result from lack of these nutrients (Epstein 1972).

The provisioning of phosphate is a fundamental role of AMF in this relationship and they can provide up to 100% of a plant's phosphorus (P) requirement (Pearson & Jakobsen 1993; Smith *et al*. 2003). Phosphorus is an essential plant macronutrient important in enzyme reactions and regulation of metabolic pathways (Theodorou & Plaxton 1993), and is a necessary component of nucleic acids, phospholipids, and adenosine triphosphate (ATP). However, P is highly immobile in soil, which often makes it limiting for plant growth (Schachtman *et al*. 1998). AM fungal hyphae emanate from the roots, forming an extensive network that increases the surface area available for nutrient absorption (Bisleski 1973), mines the soil for P beyond the rhizosphere depletion zone (Owusu-Bennoah & Wild 1979; Schachtman *et al*. 1998; Smith *et al*. 2011), and scavenges P from soil pores too small for roots to access (Allen 2011).

While AMF can be important contributors to plant performance, the community composition of these belowground endosymbionts may influence how they interact with their hosts. Most plant species are simultaneously colonized by multiple AMF partners which are functionally diverse in the benefits they provide (Johnson *et al*. 1997; Jones & Smith

2004), and the composition of these AMF communities may affect the extent to which AMF benefit plant fitness and defense (Klironomos 2000; Bever 2002; Klironomos 2003; Klironomos *et al*. 2004). AMF communities can differ in the relative abundances of different taxa, and families of AMF may differ in their morphology and function (Hart & Reader 2002). For example, Gigasporaceae may colonize soil more heavily than roots, while Glomeraceae tend to have more intraradical biomass and Acaulosporaceae colonize both spaces less heavily relative to members of the other two families (Hart & Reader 2002). The presence of Glomeraceae inside roots may reduce infection of roots by pathogens, while hyphal networks of the Gigasporaceae in the soil increase nutrient and water uptake (Newsham *et al*. 1995). Shifts in community composition may indicate shifts in the relative importance of different functions within AMF and plant communities.

Understanding how communities assemble and the forces that shape their composition is a central theme of community ecology (MacArthur & Wilson 1967). Soil characteristics such as pH, nutrient content, texture, and organic matter, as well as climatic variables like temperature and moisture, have been correlated with changes in AMF community composition (Lekberg *et al*. 2007; Hazard *et al*. 2013; Chaudhary *et al*. 2014; Davison *et al*. 2015). Land use histories, soil microclimates, and seasonality are additional forces that shape which species of AMF are present and in what quantities (Davison *et al*. 2015). Dispersal limitation and genetic drift also structure AMF communities (Koch *et al*. 2004; Lekberg *et al*. 2007).

Here I aim to expand on previous work examining AMF communities associated with a single plant species by focusing on sites chosen for differences in P availability across a large geographic range. Because plant host species has been shown to influence AMF community composition (Martinez-Garcia *et al*. 2015), sampling the assemblages of only one plant species eliminates possible variation in AMF community composition arising from plant species identity and allows for a clearer picture of the environmental variables shaping these communities. Given the well-established role of AMF in provisioning P to plants, I

sought to explore changes in AMF community composition and mycorrhizal relationships within the context of varying soil characteristics, that also differed in P availability.

To investigate how root communities of AMF vary at the mid-continental scale, I sampled those associated with the native forb *Gaillardia aristata* Pursh (blanketflower) from remnant prairies in Montana, North Dakota, and Minnesota. This taprooted, perennial plant in the Asteraceae family does well in a variety of soils and its distribution extends across North America, encompassing sites with low and high soil P availability (USDA PLANTS Database https://plants.sc.egov.usda.gov/home/plantProfile?symbol=GAAR). In the first season, seedlings form a rosette of alternate, rough and variously lobed leaves. The following spring, the stem elongates to form a terminal inflorescence (Koning 2018). The species grows to approximately 60 cm in height (Minnesota DNR Rare Species Guide https://www.dnr.state.mn.us/rsg/profile.html?/rsg/profile.html?action=elementDetail&selectedElement=PDAST3Y030). *Gaillardia aristata* has been identified as a species of special concern in Minnesota due to loss of habitat, particularly in the state's western mixed and tall grass prairies (Minnesota DNR Rare Species Guide https://www.dnr.state.mn.us/rsg/profile.html?/rsg/profile.html?action=elementDetail&selectedElement=PDAST3Y030).

The goal of this field study was to examine how mycorrhizal associations of *G. aristata* differ along a mid-continental transect of varying soil P availability from populations in montane grasslands of western Montana across the northern Great Plains to Minnesota, and to identify which environmental factors may be important for these differences. Specifically, I investigated the following questions:

1. Is soil P availability related to *G. aristata* performance and association with AMF?
2. Are differences in P availability among sites associated with changes in AMF community composition?
3. Which environmental variables are most important for explaining differences in AMF community composition?

If soil P availability is important for the performance of *G. aristata,* then plants should be larger and have better P status in high P soils. I expected to see that *G. aristata* plants at higher P sites would have greater biomass and higher P content and concentration in their aboveground tissues than plants at sites with lower P availability. I also predicted that plants in low soil P availability would have a similar P concentration in their tissues as plants in soils high in P availability because their AMF would allow them to meet their demand for P. I hypothesized that if mycorrhizas are important for P status in *G. aristata*, then plants in low P environments would have greater amounts of extraradical hyphae in the soil and greater root colonization by AMF than plants at sites with high P availability.

Conversely, I expected that plants in high P soils would be less dependent on AMF to meet their P requirements, and therefore might allocate a lower proportion of photosynthate to their fungal partners, and consequently be less colonized by AMF, host fewer AMF species, and be associated with AMF that grow fewer hyphae in the soil. When analyzing AMF community composition among sites, I did not expect the communities to differ with soil P environment if the same AMF community was equally effective at provisioning P to *G. aristata* regardless of P availability. However, if some members of the AMF community were more important for P uptake, then I would have expected those taxa to be overrepresented at low P sites.

While I expected soil P availability to shape AMF communities, I also predicted that if there were other environmental variables that structured the communities I sampled, then those drivers would be correlated with differences in community composition. The soil ecosystem is a complex environment where many physical, chemical, and biological processes, not only P availability, interact to shape the microbial communities present.

1.3. Methods

1.3.1. Study region

Twelve sites in the temperate grasslands of Montana, North Dakota, and Minnesota were sampled June 12-28, 2018 (Figure 1.1). Sites were chosen based on suspected soil P

levels and similar latitude. However, they varied in their climate (Table 1.1), soil, and vegetation (Table 1.2).

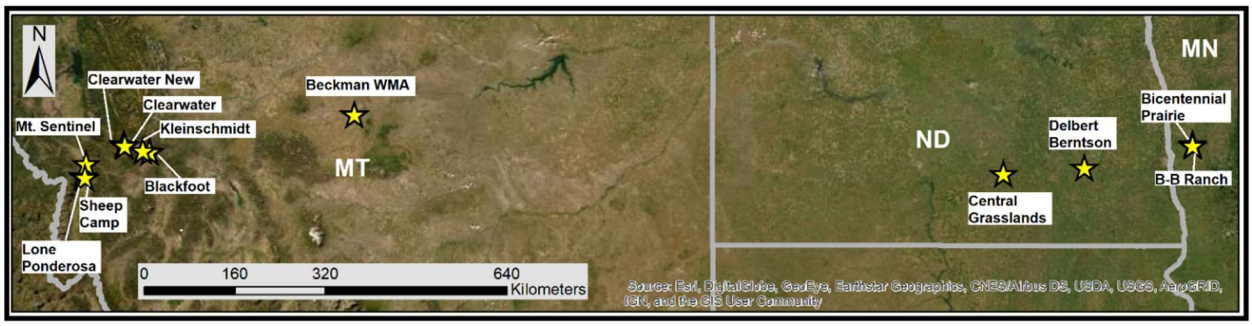

Figure 1.1. Map of the twelve study sites.
Note: Ten *Gaillardia aristata* plants and their associated soil were collected at each of 12 field sites across Montana (from west to east: Sheep Camp, Lone Ponderosa, Mt. Sentinel, Clearwater New, Clearwater, Kleinschmidt, Blackfoot, Beckman WMA), North Dakota (Central Grasslands and Delbert Berntson), and Minnesota (B-B Ranch and Bicentennial Prairie) in June 2018.

Table 1.1. Site summary data for elevation, temperature and precipitation.

Site	Latitude	Longitude	Mean Elevationm	Mean MAT C	Mean MWMT C	Mean MCMT C	Mean MAPmm	Mean MSPmm
Sheep Camp	46.70	-114.02	1119	7	19	-4	403	191
Lone Ponderosa	46.69	-113.99	1371	6	18	-5	525	223
Mt. Sentinel	46.84	-113.97	1227	6	18	-4	532	235
Clearwater New	47.05	-113.38	1293	5	17	-6	426	195
Clearwater	47.03	-113.36	1265	5	17	-6	402	188
Kleinschmidt	46.98	-113.07	1304	5	17	-6	381	191
Blackfoot	46.97	-112.96	1363	5	17	-6	393	196
Beckman WMA	47.37	-109.72	1090	7	20	-5	361	248
Central Grasslands	46.73	-99.43	610	5	21	-12	462	338
Delbert Berntson	46.79	-98.15	453	5	21	-12	519	352
B-B Ranch	47.03	-96.43	323	5	21	-13	604	414
Bicentennial Prairie	47.05	-96.43	321	5	21	-13	604	413

Note: Geographical and climatic means for 12 sites that were sampled for *Gaillardia aristata* and associated AMF communities in June 2018. Sites listed west to east. Temperature and precipitation data from ClimateNA (1981-2010 averages). MAT = mean annual temperature; MWMT = mean warmest month temperature; MCMT = mean coldest month temperature; MAP = mean annual precipitation; MSP = May to September precipitation.

Table 1.2. Dominant soil type and vegetation classification for each site.

Site	Dominant soil type	Vegetation classification
Sheep Camp	Bigarm gravelly loam (Loamy-skeletal, mixed, superactive, frigid Typic Haploxeroll)	Central Rocky Mountain Lower Montane, Foothill & Valley Grassland
Lone Ponderosa	Bigarm gravelly loam (Loamy-skeletal, mixed, superactive, frigid Typic Haploxeroll)	Central Rocky Mountain Lower Montane, Foothill & Valley Grassland
Mt. Sentinel	Minesinger (Clayey-skeletal, mixed, superactive, frigid Typic Argixeroll)-Bigarm (Loamy-skeletal, mixed, superactive, frigid Typic Haploxeroll) complex	Central Rocky Mountain Lower Montane, Foothill & Valley Grassland
Clearwater New	Perma variant-Perma complex (Loamy-skeletal, mixed, superactive, frigid Typic Haplustoll)	Central Rocky Mountain Lower Montane, Foothill & Valley Grassland
Clearwater	Perma variant stony silt loam (Loamy-skeletal, mixed, superactive, frigid Typic Haplustoll)	Central Rocky Mountain Lower Montane, Foothill & Valley Grassland
Kleinschmidt	Quigley (Fine-loamy, mixed, superactive, frigid Typic Haplustoll)-Straw (Fine-loamy, mixed, superactive, frigid Cumulic Haplustoll)-Water complex; Perma gravelly loam (Loamy-skeletal, mixed, superactive, frigid Typic Haplustoll)	Central Rocky Mountain Lower Montane, Foothill & Valley Grassland; Intermountain Mountain Big Sagebrush Steppe & Shrubland; Intermountain Dry Tall Sagebrush Steppe & Shrubland
Blackfoot	Perma gravelly loam and Perma cobbly loam (Loamy-skeletal, mixed, superactive, frigid Typic Haplustolls)	Central Rocky Mountain Lower Montane, Foothill & Valley Grassland
Beckman WMA	Tally fine sandy loam (Coarse-loamy, mixed, superactive, frigid Typic Haplustoll) and Tally-Flasher (Mixed, frigid, shallow Typic Ustipsamment) complex	Great Plains Sand Grassland
Central Grasslands	Wabek (Sandy-skeletal, mixed, frigid Entic Haplustoll)-Appam (Sandy, mixed, frigid Typic Haplustoll) complex	Pasture & Hay Field Crop; Northern Great Plains Mixedgrass Prairie
Delbert Berntson	Buse (Fine-loamy, mixed, superactive, frigid Typic Calciudoll)-Barnes (Fine-loamy, mixed, superactive, frigid Calcic Hapludoll) loams	Pasture & Hay Field Crop
B-B Ranch	Sioux sandy loam (Sandy-skeletal, mixed, frigid Entic Hapludoll)	Pasture & Hay Field Crop; Row & Close Grain Crop Cultural Formation
Bicentennial Prairie	Sioux sandy loam (Sandy-skeletal, mixed, frigid Entic Hapludoll)	Row & Close Grain Crop Cultural Formation

Note: Taxonomic class of dominant soil type and vegetation classification for 12 sites sampled for *Gaillardia aristata* and associated AMF communities in June 2018. Sites are listed from west to east. Dominant soil types from USDA NRCS Official Soil Series and vegetation types from the National Vegetation Classification System.

1.3.2. Sample collection and processing

Ten individuals of *Gaillardia aristata* were selected haphazardly at each site. To ensure that plants of this clonal species were genetically distinct, a distance of > 2 m

between plants was maintained when possible. The actual distance between plants sampled within a site ranged from 0.76 to 515 m with a mean of 68.4 m; there were three instances where plants sampled were less than 2 m apart. The area sampled ranged from 595 m^2 at Lone Ponderosa (LP) to 43,550 m^2 at Clearwater (CL). The mean area sampled was 6,450 m^2 and the median was 1,664 m^2. Global positioning system (GPS) coordinates and elevation were recorded at each sampling location with a Garmin eTrex Basic GPS unit (Olathe, Kansas, USA). Individuals were destructively sampled using shovels to remove an intact root ball approximately 30 cm in diameter, including the plant and surrounding soil, to a depth of approximately 30 cm. The soil from the root ball was sifted through a 2-mm sieve in the field and placed in an unsealed plastic bag. Soil particles were brushed from sieves between samples to minimize cross-contamination. The roots, shoots, and leaves of each individual were placed in an unsealed plastic bag, and both the soil and plant samples were kept on ice in coolers in the field and stored at 4 °C until processed.

All samples were processed < 24 h after being collected. Shoots were separated from roots and dried to constant mass at 60 °C. A 2-mL soil sample from each individual was frozen at -20 °C, shipped on dry ice, and stored at -20 °C prior to DNA extraction. The remainder of the soil sample from each individual was air dried in a paper bag at room temperature for soil nutrient analysis and estimation of hyphal length in the soil. Roots were rinsed to remove any remaining soil and weighed before being cut from the taproot, which was not included in subsequent analyses. A root sample of approximately 80 mg for each plant was frozen at -20 °C for DNA extraction. Approximately 50 mg of root tissue from each sample was placed in a microcassette and stored in 1% (*w*/*v*) KOH solution at 4 °C for microscopic analysis of AMF root colonization.

Dried shoots and soils were sent to Ward Laboratories, Inc. (Kearney, Nebraska, USA) for grinding and nutrient analysis. All 10 soil samples from each site were analyzed for Mehlich III P availability and five of the 10 samples from each site were analyzed for soil nutrients and pH. The samples chosen were those with volumes sufficient for analysis. Soil

samples were analyzed for pH, soluble salts, organic matter, cation exchange capacity (CEC), and ammonium-nitrogen (NH_4-N) and nitrate-nitrogen (NO_3-N). Aboveground plant tissue analysis was conducted on the same plants for which soil nutrients were analyzed. Both sample types were analyzed for P, calcium, magnesium, potassium, zinc, iron, manganese, copper, sulfate, and sodium. Nitrogen, molybdenum, and boron content were analyzed for plant tissue. Descriptions of these analyses are in Appendix A.

1.3.3. Root colonization by AMF

To visualize AM fungal structures in roots, microcassettes with roots were placed in 10% KOH (*w*/*v*) at 95 °C for 6 min on a stirring hot plate to clear cell contents, rinsed in tap water for 5 min, acidified in 2% HCl (*v*/*v*) at room temperature for 15 min, and stained with 0.05% trypan blue (*w*/*v*) in a 1:1:1 solution of tap water, glycerol, and lactic acid for 5 min (modified from Grace & Stribley 1991). Samples were rinsed in tap water for a minimum of 2 h to clear excess stain, stored in destain solution (1:1:1 solution of tap water, glycerol, and lactic acid) at 4 °C, and mounted in polyvinyl lactoglycerol on microscope slides. Samples were scored for root colonization via the magnified intersect method (McGonigle *et al*. 1990) by examining slides at 200× magnification and evaluating each of 100 intersections for the presence of AM hyphae, vesicles and arbuscules, and non-AM hyphae. Counts of AM fungal structures were summed for each sample and divided by 100 to obtain an estimate of the proportion of the root length colonized by AMF.

1.3.4. Extent of extraradical hyphae in the soil

From each site, five of the 10 samples were chosen for hyphal length analysis. When there was sufficient soil, the samples chosen for nutrient analysis were also used for hyphal length so that relationships between nutrient status and the extent of the hyphal network could be explored. Otherwise, the hyphal length sample was taken from another individual at the site. Hyphal length was quantified following a protocol modified from Jakobsen *et al*. (1992). Twelve milliliters of sodium hexametaphosphate solution (*w*/*v*; 35 g L^{-1}) was added to 100 mL tap water and used to disperse clay particles from hyphae in each 4 g soil sample

by mixing end-over-end for 30 s followed by a 30 min resting period at room temperature. Soil was wet-sieved with a 38 µm sieve to remove clay particles. After shaking the sample for 5 s, a 2-mL aliquot was pipetted onto a 47-mm gridded mixed cellulose ester membrane disc filter (GN-6 Metricel; Pall Corporation, Ann Arbor, Michigan, USA) on a Büchner funnel under vacuum. Approximately 1 mL of 0.05% (*w*/*v*) trypan blue stain was applied to the membrane for 5 min to stain hyphae and subsequently removed via vacuum filtration. Fifty intersections where the vertical and horizontal lines of the grid meet were chosen randomly, centered in the field of view of a dissecting scope at 50× magnification, and scored for the presence or absence of hyphae. Because septae were not necessarily visible at this magnification, all hyphae were counted.

For each field of view, each hypha that touched or crossed either the vertical or horizontal lines of the gridded membrane was recorded. If a hypha crossed or touched both, it was scored twice. An estimate of hyphal length (*R*, in mm) per g of soil was calculated according to the formula:

$$R = \frac{N \times A \times \pi}{2 \times H \times 4}$$

where *N* is the number of hyphal intersects with the membrane's gridded lines, *A* is the area of the membrane (here, 173.5 mm^2), and *H* is the cumulative length of the grid that the hyphae had the opportunity to cross (here, 470 mm).

1.3.5. DNA extraction, amplification, and sequencing

Frozen root samples were ground on a TissueLyser II (QIAGEN, Germantown, Maryland, USA) under liquid nitrogen for 30 s at 30 Hz with one 6.35 mm diameter chrome steel bead (Biospec Products, Bartlesville, Oklahoma, USA) to maintain low temperatures and prevent DNA degradation, while breaking apart cells to make DNA available for extraction. Roots that were not fully ground after the initial 30 s period were re-frozen and re-ground in 30 s increments up to 90 s total.

DNA was isolated from roots with the DNeasy Plant Mini Kit (QIAGEN, Germantown, Maryland, USA) following the manufacturer's protocol (except with two elution volumes of 75 µL each). Eluates were stored at -20 °C until shipment on dry ice to MPG Ranch, where template DNA, along with extraction negative controls, were amplified via polymerase chain reaction (PCR).

Two PCR products were amplified, one using general fungal primers for the ITS2 and one using AMF-specific primers. To characterize the root fungal community of *G. aristata*, the internal transcribed spacer 2 (ITS2) region of fungal nuclear ribosomal DNA was amplified using the fITS7 and ITS7o forward primers (Ihrmark *et al*., 2012; Kohout *et al*. 2014) and the ITS4 (White *et al*., 1990) reverse primer. The ITS2 region is often chosen for sequencing of fungal DNA since it contains sufficient sequence variation for distinguishing species (Turenne *et al*. 2000). Likewise, the 18S region was sequenced for molecular identification of AMF due to high specificity and coverage of AM fungal taxa (Öpik *et al*. 2014). When other fungi are present, AMF taxa may not amplify well with ITS2 primers (Lekberg *et al*. 2018). Additionally, the 18S is conserved enough to allow for construction of phylogenies, so it is useful for phylogenetic placement of AMF taxa. Specifically, a 550-600 bp segment of the 18S gene was amplified using AMF-specific primers, the WANDA forward primer (Dumbrell *et al*. 2011) and the AML2 reverse primer (Lee *et al*., 2008).

Primers were modified with 22 bp Fluidigm universal tags CS1 or CS2 (Fluidigm Inc. San Francisco, California, USA). PCR1 reactions were performed in 12.5 µL reaction volumes comprised of 1 µL of DNA template, 4.25 µL of PCR H_2O, 0.5 µL of BSA (10 mg/mL), and 20 pmol of each primer in 1X GoTaq® Green Master Mix [(Green GoTaq® Reaction Buffer, 200 µM dATP, 200 µM dGTP, 200 µM dCTP, 200 µMdTTP and 1.5 mM $MgCl_2$); Promega, Madison, Wisconsin, USA]. Each reaction was carried out in duplicate in a SimpliAmp™ Thermal Cycler (Thermo Fisher Scientific, Waltham, Massachusetts, USA) with 2 min activation at 94 °C for ITS2, followed by 35 cycles at 94 °C for 30 sec, 57 °C for 30 sec, 72 °C for 30 sec, and a final elongation of 72 °C for 7 min. Amplification of the 18S gene was performed with

2 min activation at 95 °C, followed by 35 cycles at 95 °C for 1 min, 59 °C for 1 min, 72 °C for 1 min, and a final elongation of 72 °C for 10 min.

The presence or absence of PCR products, including extraction and PCR negative controls, were confirmed by 1.5% agarose gel electrophoresis with a 100 bp ladder (O'GeneRuler DNA Ladder, Thermo Scientific, Waltham, Massachusetts, USA). PCR1 products were used as template in PCR2 after being diluted 1:10 in dH_2O and were combined with the same Fluidigm tags as PCR1 primers, 8 bp Illumina barcodes (Illumina, San Diego, California, USA), and Illumina adapters (see Appendix B for barcodes and primers). PCR2 was performed using 1 µL of template and 20 pmol of each primer in 1X GoTaq® Green Master Mix for a total reaction volume of 25 µL. Reactions were carried out in duplicate on a SimpliAmp™ Thermal Cycler under the following conditions: 95 °C for 1 min followed by 15 cycles of 95 °C for 30 sec, 60 °C for 30 sec, 68 °C for 1 min with a final elongation at 68 °C for 5 min. PCR2 amplicons were purified with AMPure XP beads (Beckman Coulter Genomics, Beverly, Massachusetts, USA) and their concentration was quantified by Qubit® 2.0 fluorometer (Invitrogen, Waltham, Massachusetts, USA). Samples were pooled in equimolar DNA concentration prior to sequencing, which was done via Illlumina MiSeq platform at the University of Montana Genomics Core (http://hs.umt.edu/dbs/labs/genomics/; Missoula, Montana, USA).

1.3.6. ITS2 bioinformatics for fungal root communities

Bioinformatics analyses were performed on the Thunder Cluster at North Dakota State University's Center for Computationally Assisted Science and Technology. After sequencing, the PIPITS pipeline version 2.5.0 (Gweon *et al*. 2015) was used with default settings to determine operational taxonomic units (OTUs) based on ITS2 sequences of 6,439,036 raw forward and reverse reads. Because field DNA extracts were amplified and sequenced with the greenhouse DNA extracts described in Chapter 2, the number of reads reported here includes those from both sample types. Out of 3,562,189 read pairs joined with PEAR 0.9.8 (Zhang *et al*. 2014), 58,647 low-quality reads were removed with

FASTQ_QUALITY_FILTER (FASTX-Toolkit; http://hannonlab.cshl.edu/fastx_toolkit). The remaining 3,503,542 quality filtered reads were converted to FASTA format via FASTQ_TO_FASTA (FASTX-Toolkit). After ITSx 1.1.1 (Bengtsson-Palme *et al*. 2013) extracted the ITS2 subregion from the sequences, vsearch v2.14.2 (Rognes *et al*. 2016) was used to dereplicate sequences, remove short (<100 bp) and unique sequences, and cluster the remaining sequences at 97% identity. After chimeras were detected and removed using the UCHIME 7.2 reference dataset (Nilsson *et al*. 2018), taxonomy was assigned to the remaining sequences with the UNITE trained database version 04.02.2020 and the RDP Classifier 2.12 (Wang *et al*. 2007) based on the Warcup_retrained v2 ITS training dataset (Deshpande *et al*., 2016). FUNGuild (Nguyen *et al* 2016) was used to assign OTUs to guilds. Counts observed in negative controls (1,881 sequences in 149 OTUs) were subtracted out from other samples (including field soil, field root, and greenhouse root samples). A PCR negative control (PCRNEG-2) was inadvertently contaminated prior to amplification and consequently its counts were removed from both ITS2 and 18S datasets. A field root sample from the Central Grasslands site (FRCG-119) was omitted from further analysis due to having only three sequences detected.

1.3.7. 18S bioinformatics for arbuscular mycorrhizal fungi

18S sequences from Illumina MiSeq were processed with QIIME2 version 2020.6 (Bolyen *et al*. 2019). Forward reads were imported into QIIME2 and demultiplexed before trimming primers, trimmed to 200 bp (by trimming 25 bp from the beginning and truncating to 225 bp) to remove low quality regions (with reads truncated at a quality score ≤ 5), denoising, dereplicating, and clustering into exact amplicon sequence variants (ASVs) representing 100% sequence similarity with DADA2 version 1.16 (Callahan *et al*. 2016). These ASVs were filtered to remove those that did not align with known AMF in the MaarjAM (Öpik *et al*. 2010) database (accessed 10/1/2020) at 85% identity or higher. Taxonomy was assigned with the MaarjAM classifier (from Lorinda Bullington dated 5/6/2019) at a confidence of 90%. After excluding the Ascomycete outgroup and filtering out unassigned

sequences and sequences assigned to unknown fungi, counts observed in negative controls (20 sequences belonging to 3 Glomus ASVs) were subtracted out from field root, field soil, and greenhouse root samples. For the final field root 18S dataset, 357,638 sequences assigned to 866 AMF ASVs were included. One root sample (FRCL-80) was excluded from further analysis due to low sequence count (9 sequences total). For some analyses, ASVs were clustered *de novo* at 97% identity in QIIME2, resulting in 103 OTUs. A rooted phylogeny was created by alignment using MAFFT version 7.475 (Katoh *et al*. 2013) and FastTree (Price *et al*. 2010).

1.3.8. Statistical analyses

Plant P content was calculated as P concentration × biomass. Differences in soil nutrient availability among sites were tested by one-way analysis of variance (ANOVA) with site as the factor followed by Tukey's honestly significant difference (HSD) test (JMP®, Version Pro 15. SAS Institute Inc., Cary, North Carolina, USA) on data that were transformed to meet model assumptions. Zinc, iron, and Mehlich III P availability were $\log_{10}$ transformed. Soil salts, manganese, and cation exchange capacity (CEC) were square root transformed. Sulfate, calcium, and sodium were reciprocal transformed. Copper, magnesium, and nitrate-nitrogen were reciprocal root transformed. Organic matter content, potassium, ammonium-nitrogen, and pH were not transformed since they already displayed a normal distribution.

Data for hyphal length, plant shoot biomass and P content, and the ratio of hyphal length to aboveground biomass were $\log_{10}$ transformed to meet model assumptions. Shoot P concentration data were not transformed since they exhibited a bimodal distribution. Percent root length colonized by AMF was arcsine square root transformed and, because observer strongly influenced values (data not shown), only data from a single observer were analyzed. Therefore, *n* was reduced to 73 for this response variable. Differences among sites in plant performance and root length colonized by AMF were tested by one-way ANOVA with site as the factor followed by Tukey's honestly significant difference (HSD) test (JMP®,

Version Pro 15. SAS Institute Inc., Cary, North Carolina, USA) on data that were transformed to meet model assumptions. Because the ratio of hyphal length to aboveground biomass did not meet assumptions about equal variance when testing site differences, a nonparametric Kruskal-Wallis one-way ANOVA was performed.

Linear regression analysis was performed in R 4.0.5 (R Core Team 2021) to examine relationships between soil P availability and plant shoot P; between plant shoot biomass and shoot P; between extent of extraradical hyphae and shoot biomass; and between extent of extraradical hyphae and shoot P. Nonmetric multidimensional scaling (NMS) ordinations were performed in PC-ORD 7.08 (Wild Blueberry Media, Corvallis, OR, USA) to visualize AMF community composition across sites. Ordinations were carried out using the Sorenson distance measure, a random starting configuration, and 500 runs each with randomized and real data. OTU and ASV abundances were Hellinger-transformed in PC-ORD to downweight low-abundance sequences (Buttigieg & Ramette 2014). NMS ordinations for 18S dataset were performed with ASVs clustered to 97% identity to reduce noise and stress.

PC-ORD was used to test for correlations of environmental data with the NMS ordination for AMF community composition. Longitude, latitude, and elevation data were collected with my samples and were included in the environmental matrix. Climate data were obtained with the ClimateNA v5.21 software package, available at http://tinyurl.com/ClimateNA based on the methodology described by Wang *et al.* (2016). Long-term (1981-2010) averages for mean temperature and total precipitation in June, the month in which sampling occurred, were included in the environmental matrix. Long-term data for June were chosen instead of similar climatic data collected over other time periods, such as average temperature and total precipitation during May 2018, June 2018, 2017, and 1981-1990, because long-term June data were the most strongly associated with the ordination axes. Area sampled at each site and distance between *G. aristata* individuals were calculated in ArcGIS Pro 2.8.2 (Esri, West Redlands, California, USA).

To test whether AMF communities in root samples at the same site were more similar to each other than they were to samples at other sites, permutational multivariate analysis of variance (PERMANOVA; Anderson 2001) was performed in QIIME2 with 999 permutations. Pairwise comparisons were performed with $q = 0.05$, where q-values were calculated from Benjamini-Hochberg false discovery rate-corrected p-values. Rarefaction was not performed (McMurdie & Holmes 2014; Beule & Karlovsky 2020) for datasets used in NMS, PERMANOVA, or chi square analysis. Rarefaction curves and richness and evenness metrics for OTUs were generated in R 4.0.5 (R Core Team 2021) using the vegan package (Oksanen *et al*. 2020). ASV diversity analyses to assess richness and Pielou's evenness done in QIIME2 used a sampling depth of 546 ASVs to maximize the number of sequences retained per sample while excluding as few samples as possible. A chi square test was used to determine if taxonomic distribution of ASVs differed between sites. A statistically significant test was followed by calculation of adjusted standardized residuals (Sharpe 2015) to identify which taxa differed between sites.

1.4. Results

1.4.1. Soil P availability correlated with *Gaillardia aristata* growth and P status

Soils under *G. aristata* differed in their P availability among sites ($F_{11,108} = 70.49$, $p < 0.0001$). My sampling captured a range of soil P levels that generally decreased from west to east (Figure 1.2). All four sites in eastern ND and western MN had very low soil P availability (2-3 ppm) under *G. aristata*, while sites in MT displayed generally higher but more variable soil P availability. Lone Ponderosa (LP) was the site with the highest mean soil P. Clearwater (CL) and Beckman WMA (BW) had the lowest soil P availability of the sites in MT, although BW is the site farthest east (in central MT) in that state (Fig. 1.1). Site means for other soil chemical properties that differed among sites are provided in Appendix D.

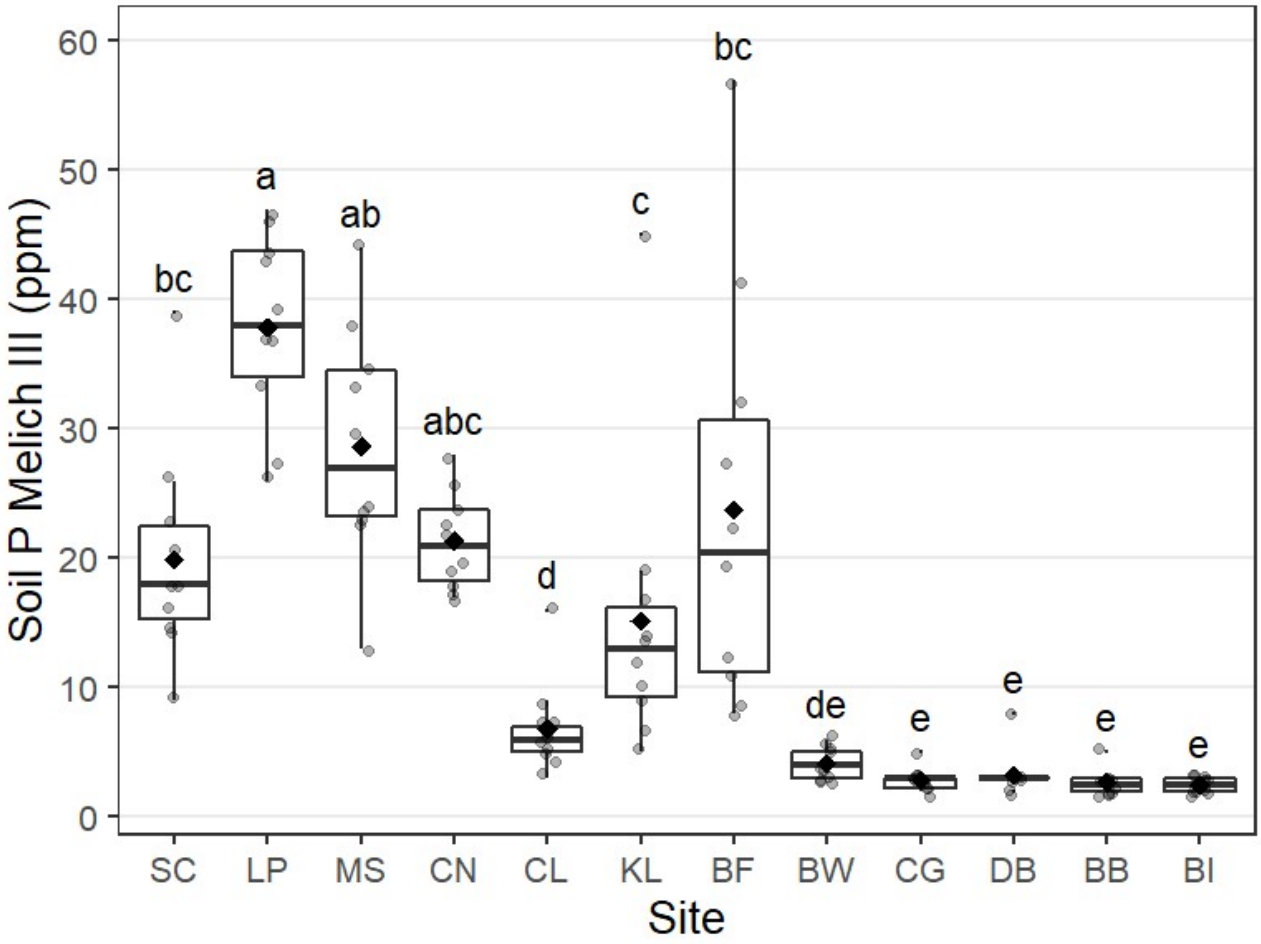

Figure 1.2. Soil P availability by site.
Note: Soils around the roots of individual *G. aristata* plants (n = 10) were collected at 12 sites from Montana to Minnesota in June 2018. Sites are arranged from west to east. Means with the same letter are not statistically different. The box and whisker plots display the median (center horizontal line) flanked by the 25th and 75th percentiles. The upper whisker extends from the 75th percentile line to the largest value no further than 1.5 * IQR from the 75th percentile (where IQR is the inter-quartile range, or distance between the first and third quartiles). The lower whisker extends from the 25th percentile line to the smallest value at most 1.5 * IQR of the hinge. Black diamonds represent means.

Shoot biomass of *G. aristata* increased with soil P availability (R^2 = 0.08, p = 0.0012, n = 119). Similarly, shoot P content (R^2 = 0.35, p < 0.0001, n = 60) and concentration (R^2 = 0.74, p < 0.0001, n = 60) increased with soil P availability (Figure 1.3). *Gaillardia aristata* plants with higher soil P availability had higher P content and concentration in their shoots.

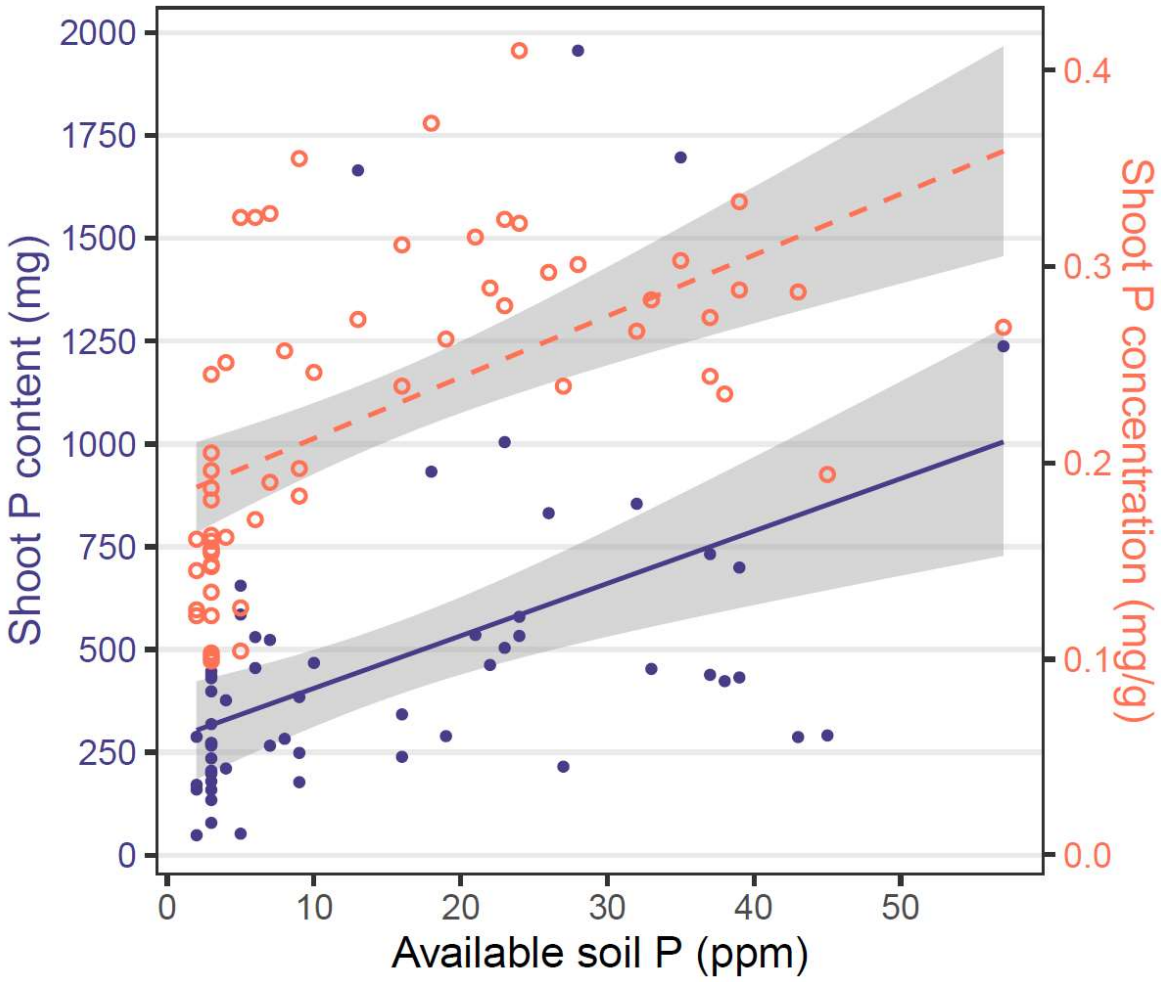

Figure 1.3. Relationship between *Gaillardia aristata* shoot P content and concentration and soil P availability.
Note: *Gaillardia aristata* and its associated soils were collected at 12 sites from Montana to Minnesota in June 2018. Soil P availability was measured with Mehlich III protocol. Regression lines describe how response variables change with soil P availability. Data for shoot P content are displayed as closed navy points with solid regression line, while those for shoot P concentration are shown as open orange points with dashed regression line. Gray regions flanking regression lines represent 0.95 confidence interval.

Some site differences in plant biomass were observed ($F_{11,108} = 3.17$, $p = 0.0009$; Figure 1.4). On average, *Gaillardia aristata* sampled at Beckman WMA (BW) were larger than those at Delbert Berntson (DB) and Bicentennial Prairie (BI). For the remainder of the sites, average plant size did not differ statistically.

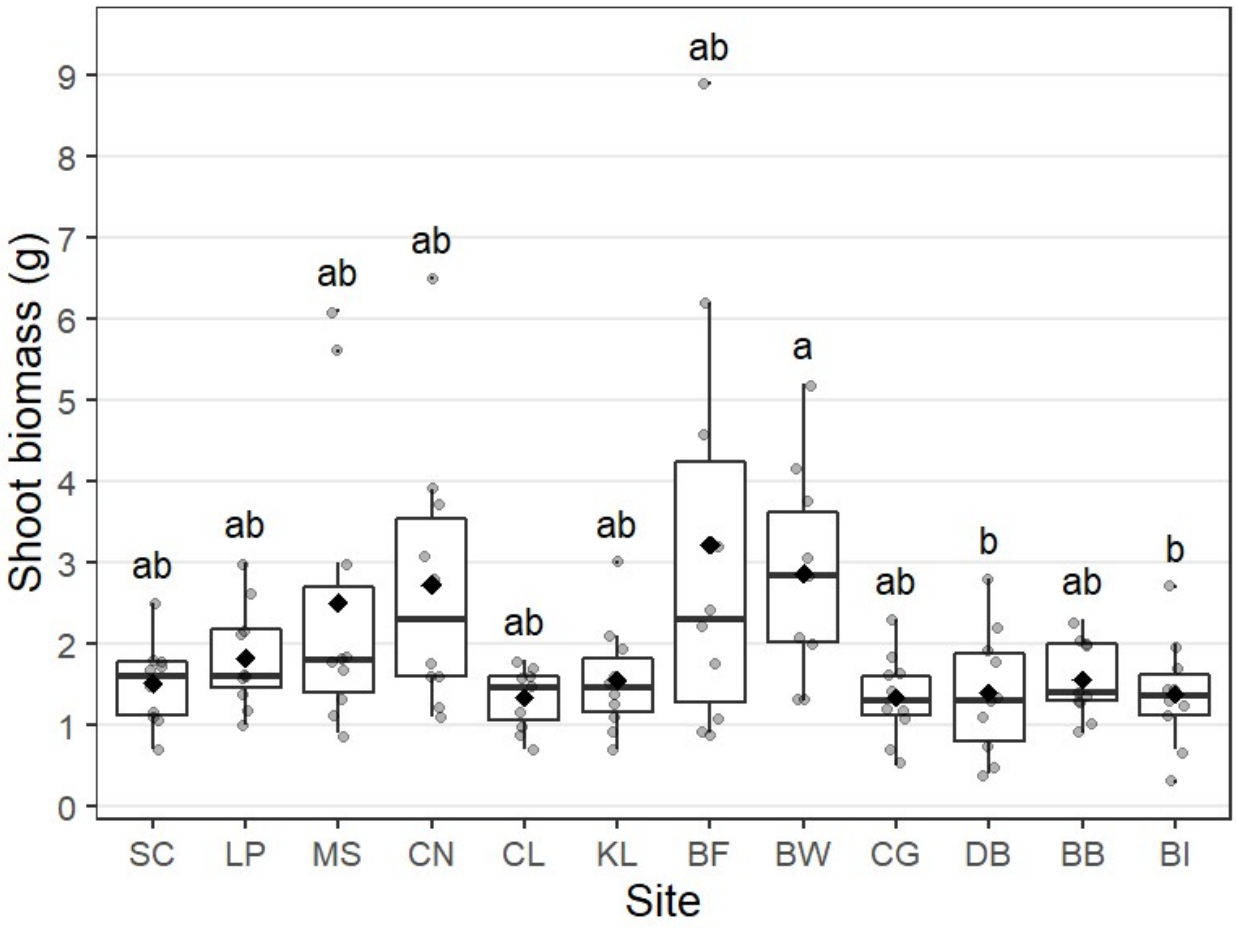

Figure 1.4. *Gaillardia aristata* shoot biomass by site.
Note: *Gaillardia aristata* and its associated soils were collected at 12 sites from Montana to Minnesota in June 2018. Sites arranged from west to east (n = 10). Means with the same letter are not statistically different. The box and whisker plots display the median (center horizontal line) flanked by the 25th and 75th percentiles. The upper whisker extends from the 75th percentile line to the largest value no further than 1.5 * IQR from the 75th percentile (where IQR is the inter-quartile range, or distance between the first and third quartiles). The lower whisker extends from the 25th percentile line to the smallest value at most 1.5 * IQR of the hinge. Black diamonds represent means.

No relationship between shoot biomass and P concentration was observed (R^2 = 0.02, p = 0.3426, n = 60; data not shown). *Gaillardia aristata* had similar concentration of P in its shoots regardless of its size. However, concentration of P in the shoot tissue of *G. aristata* did differ by site ($F_{11,48}$ = 19.06, p < 0.0001; Figure 1.5). On average, sites in western Montana had plants with higher P concentrations in their shoots than those in eastern Montana (BW), North Dakota (CG and DB), and Minnesota (BB and BI).

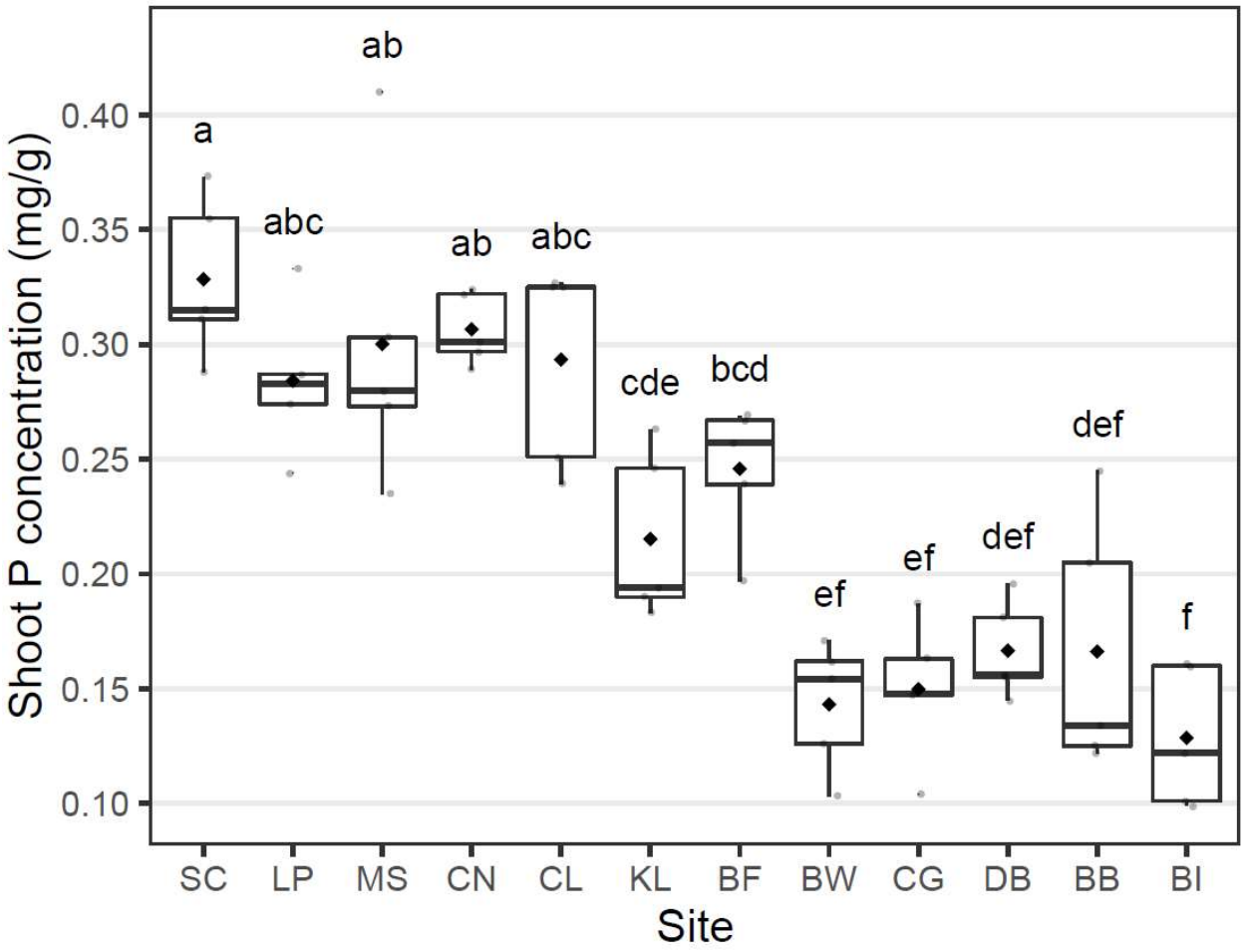

Figure 1.5. *Gaillardia aristata* shoot P concentration by site.
Note: *Gaillardia aristata* and its associated soils were collected at 12 sites from Montana to Minnesota in June 2018. Sites arranged from west to east (n = 10). Means with the same letter are not statistically different. The box and whisker plots display the median (center horizontal line) flanked by the 25th and 75th percentiles. The upper whisker extends from the 75th percentile line to the largest value no further than 1.5 * IQR from the 75th percentile (where IQR is the inter-quartile range, or distance between the first and third quartiles). The lower whisker extends from the 25th percentile line to the smallest value at most 1.5 * IQR of the hinge. Black diamonds represent means.

1.4.2. Mycorrhizas and P uptake in *Gaillardia aristata*

The presence of more hyphae in the soil was associated with greater shoot P content (R^2 = 0.25, p < 0.0233, n = 20) and greater shoot biomass (R^2 = 0.22, p < 0.0002, n = 60) in *G. aristata* (Figure 1.6). However, the amount of extraradical hyphae did not differ with soil P availability (R^2 = 0.04, p = 0.1127, n = 60) or shoot P concentration (R^2 = 0.03, p = 0.502, n = 20).

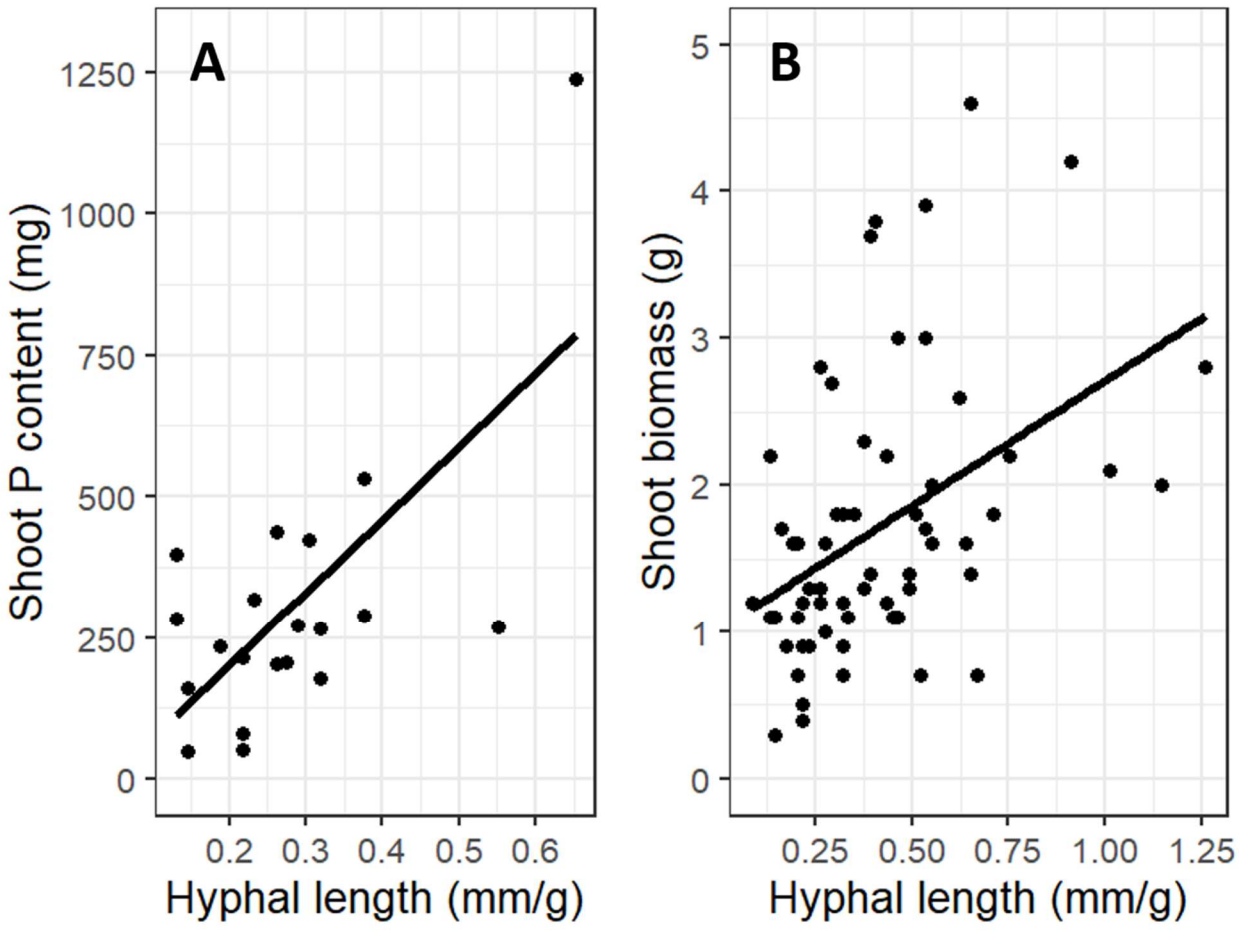

Figure 1.6. Relationship between length of extraradical hyphae and shoot P content (A) and biomass (B).
Note: *Gaillardia aristata* and its associated soils were collected at 12 sites from Montana to Minnesota in June 2018. Regression line describes how shoot P content (n = 20) and biomass (n = 60) change with hyphal length in the soil. Hyphal length is measured in m per g of soil.

The amount of extraradical hyphae differed among sites ($F_{11,48}$ = 3.72, p = 0.0007; Figure 1.7). There were more hyphae in soils under *G. aristata* at Beckman WMA (BW) than at Clearwater (CL), Delbert Berntson (DB), and Bicentennial Prairie (BI), with intermediate amounts of hyphae at the other sites. When examining the relative investment by testing the ratio of hyphal length to aboveground biomass, no differences among sites were observed (χ^2 = 4.87, df = 11, p = 0.9373; Figure 1.7).

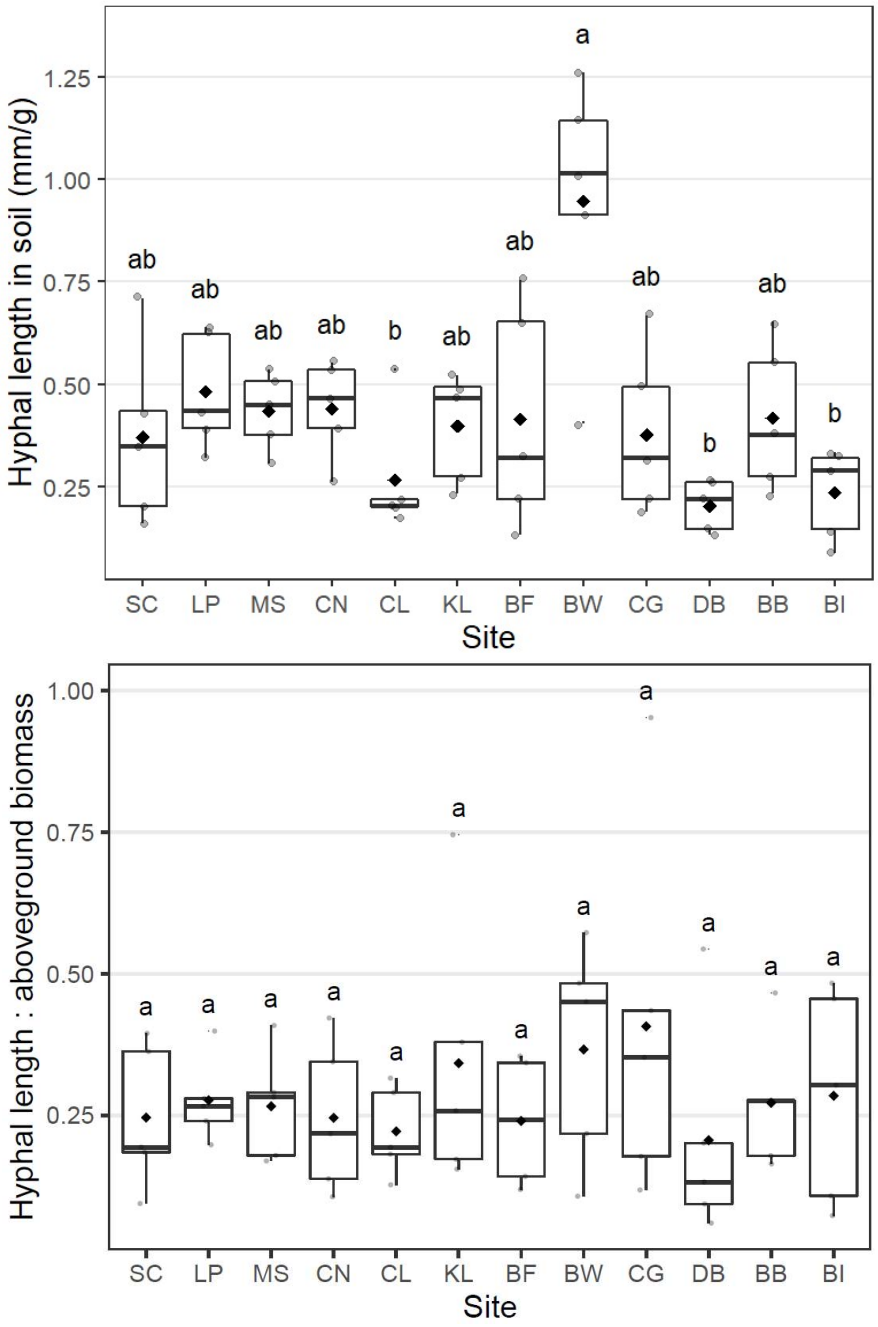

Figure 1.7. Site differences in extraradical hyphae in the soil.
Note: *Gaillardia aristata* and its associated soils were collected at 12 sites from Montana to Minnesota in June 2018. Hyphal length is measured in m per g of soil (n = 5) and is displayed by itself and as a ratio with aboveground biomass. The box and whisker plots display the median (center horizontal line) flanked by the 25th and 75th percentiles. The upper whisker extends from the 75th percentile line to the largest value no further than 1.5 * IQR from the 75th percentile (where IQR is the inter-quartile range, or distance between the first and third quartiles). The lower whisker extends from the 25th percentile line to the smallest value at most 1.5 * IQR of the hinge. Black diamonds represent means.

Proportion of root length colonized by AMF varied by site ($F_{11,62} = 3.05$, $p = 0.0026$; Figure 1.8). On average, the roots most heavily colonized by AMF were sampled at Beckman WMA (BW). *Gaillardia aristata* at Blackfoot (BF) and Delbert Berntson (DB) had significantly less root colonization by AMF than those at Beckman WMA, while *G. aristata* at Bicentennial Prairie (BI) had the lowest mean root colonization. However, there was no relationship between root colonization and soil P availability ($R^2 = 0.03$, $p = 0.1559$, $n = 74$), plant P content ($R^2 = 0.08$, $p = 0.0737$, $n = 39$), plant P concentration ($R^2 = 0.04$, $p = 0.2510$, $n = 39$), plant biomass ($R^2 = 0.03$, $p = 0.1760$, $n = 74$), or hyphal length in the soil ($R^2 = 0.02$, $p = 0.4701$, $n = 35$; data not shown).

When examining the presence of mycorrhizas by site, some patterns emerged. *Gaillardia aristata* plants at Beckman WMA (BW) had the greatest extent of extraradical hyphae (Figure 1.7) and had the most heavily colonized roots (Figure 1.8). The eastern-most site, Bicentennial Prairie (BI), had the lowest proportion of root length colonized by AMF and was one of the sites with the lowest hyphal length in the soil.

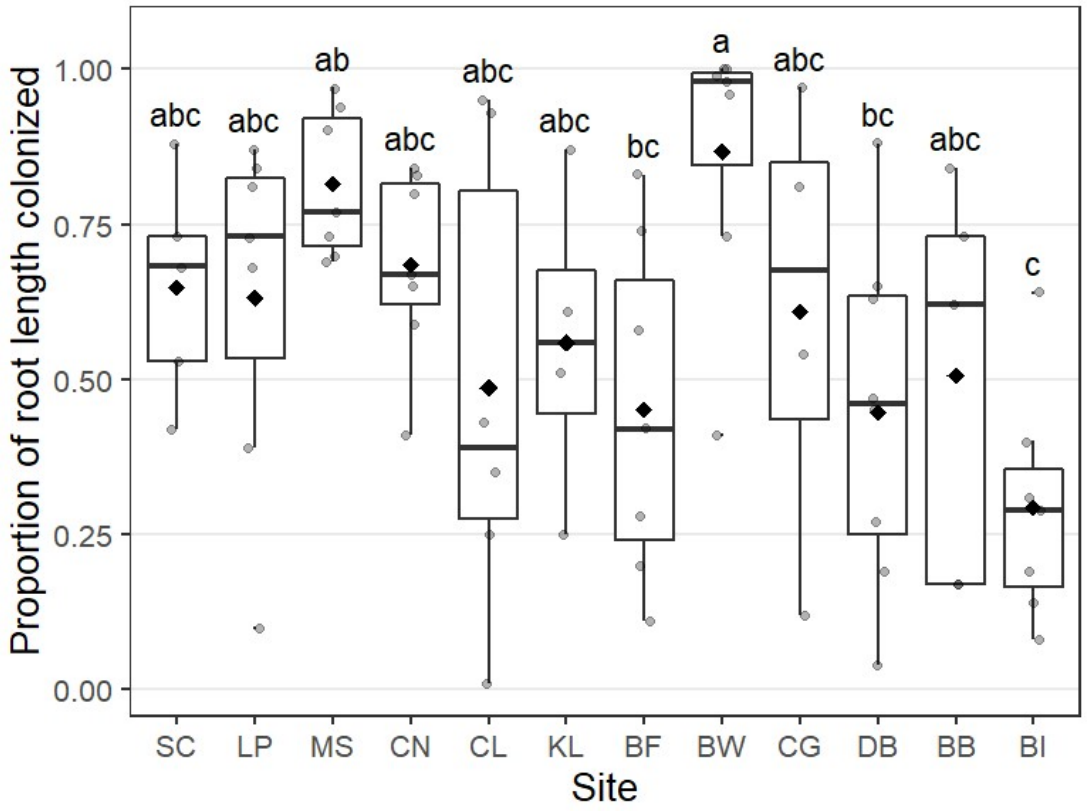

Figure 1.8. Site differences in proportion of root length colonized by AMF.
Note: *Gaillardia aristata* and its associated soils were collected at 12 sites from Montana to Minnesota in June 2018. Roots from each sample were observed microscopically at 100 points for presence of AMF structures. The box and whisker plots display the median (center horizontal line) flanked by the 25th and 75th percentiles. The upper whisker extends from the 75th percentile line to the largest value no further than 1.5 * IQR from the 75th percentile (where IQR is the inter-quartile range, or distance between the first and third quartiles). The lower whisker extends from the 25th percentile line to the smallest value at most 1.5 * IQR of the hinge. Black diamonds represent means.

There was no relationship between richness of AMF and soil P availability (R^2 = 0.01, p = 0.2066, n = 119) for 18S ASVs, but ITS2 OTU richness increased with soil P availability (R^2 = 0.07, p = 0.0040, n = 118). ASV and OTU richness of AMF differed among sites ($F_{11,108}$ = 4.03, p < 0.0001, $F_{11,107}$ = 3.82, p < 0.0001, respectively; Figure 1.9). ASV richness in roots was higher at Beckman WMA (BW), with a mean of 31 ASVs per sample, than at most other sites. Sheep Camp (SC) and Clearwater New (CN) had AMF assemblages intermediate in ASV richness, and AMF communities at B-B Ranch (BB) were the least diverse, with a mean of 15 ASVs per sample. OTU richness followed a similar pattern, with root AMF communities at Beckman WMA displaying the highest richness, Sheep Camp (SC),

B-B Ranch (BB), and Bicentennial Prairie (BI) displaying intermediate levels of richness, and the rest of the sites having the lowest OTU richness. Some site differences in evenness were observed, with Central Grasslands (CG) having higher and B-B Ranch (BB) having lower ASV evenness than other sites. Root communities at Delbert Berntson (DB) had higher OTU evenness than those at other sites, while Mt. Sentinel (MS), Clearwater (CL), and BB had lower OTU evenness (Appendix D).

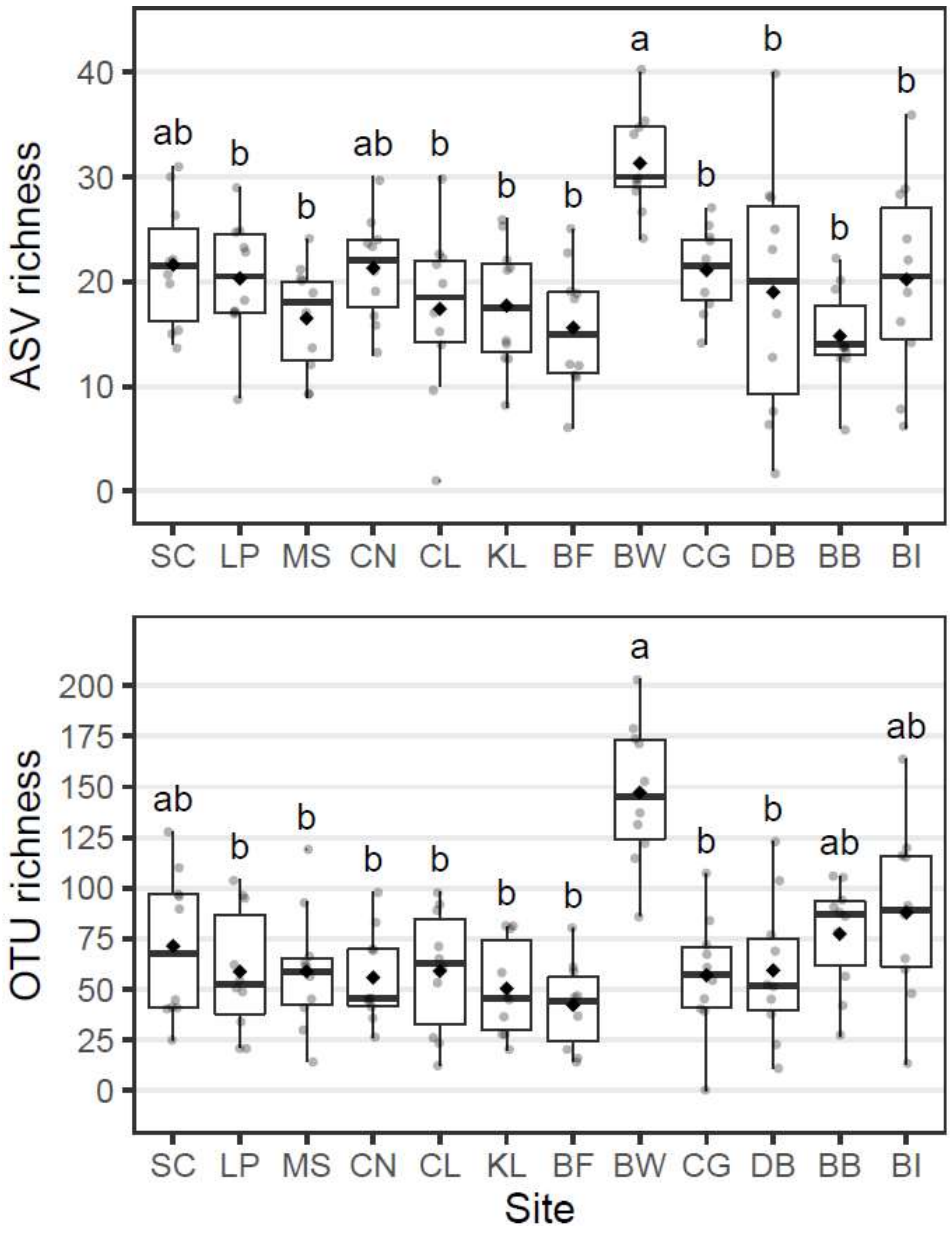

Figure 1.9. Site differences in OTU and ASV richness of AMF.
Note: DNA was extracted from roots of *Gaillardia aristata* collected at 12 sites from Montana to Minnesota in June 2018. Sites are arranged from west to east. OTU (top) and ASV (richness) measured as the number of unique taxa observed in each sample. The box and whisker plots display the median (center horizontal line) flanked by the 25th and 75th percentiles. The upper whisker extends from the 75th percentile line to the largest value no further than 1.5 * IQR from the 75th percentile (where IQR is the inter-quartile range, or distance between the first and third quartiles). The lower whisker extends from the 25th percentile line to the smallest value at most 1.5 * IQR of the hinge. Black diamonds represent means.

1.4.3. Soil P availability and site differences in community composition of AMF

The final OTU table for all fungi detected in the roots of *G. aristata* consisted of 808,433 counts of 3,373 OTUs. Of these, 253,722 sequences belonging to 1,009 OTUs at 97% identity were assigned to the Glomeromycetes. The final 18S dataset was composed of 357,638 sequences which were grouped into 866 ASVs. Accumulation curves reached an asymptote for some ASVs and most OTUs (Figure 1.10). Sites low in soil P availability generally exhibited higher OTU accumulation than those high in P, while accumulation curves for ASVs did not appear to differ by P availability. Despite the diversity of AMF observed, there were several OTUs and ASVs that were sampled across all sites, and these are listed in Appendix D.

According to MaarjAM taxonomic assignment, all four orders in Glomeromycota were represented. However, for the nine families represented, only one genus was observed in each family. Of the 866 ASVs in the dataset, 445 were assigned to a species (including virtual taxa (VTs)). Of the remaining ASVs, 373 could only be assigned to genus, while 48 could only be assigned to the Glomeromycetes. A phylogeny constructed with the observed ASVs is shown in Figure 1.11. The majority of the ASVs classified as unknown Glomeromycetes are most closely related to *Claroideoglomus*, according to the phylogeny.

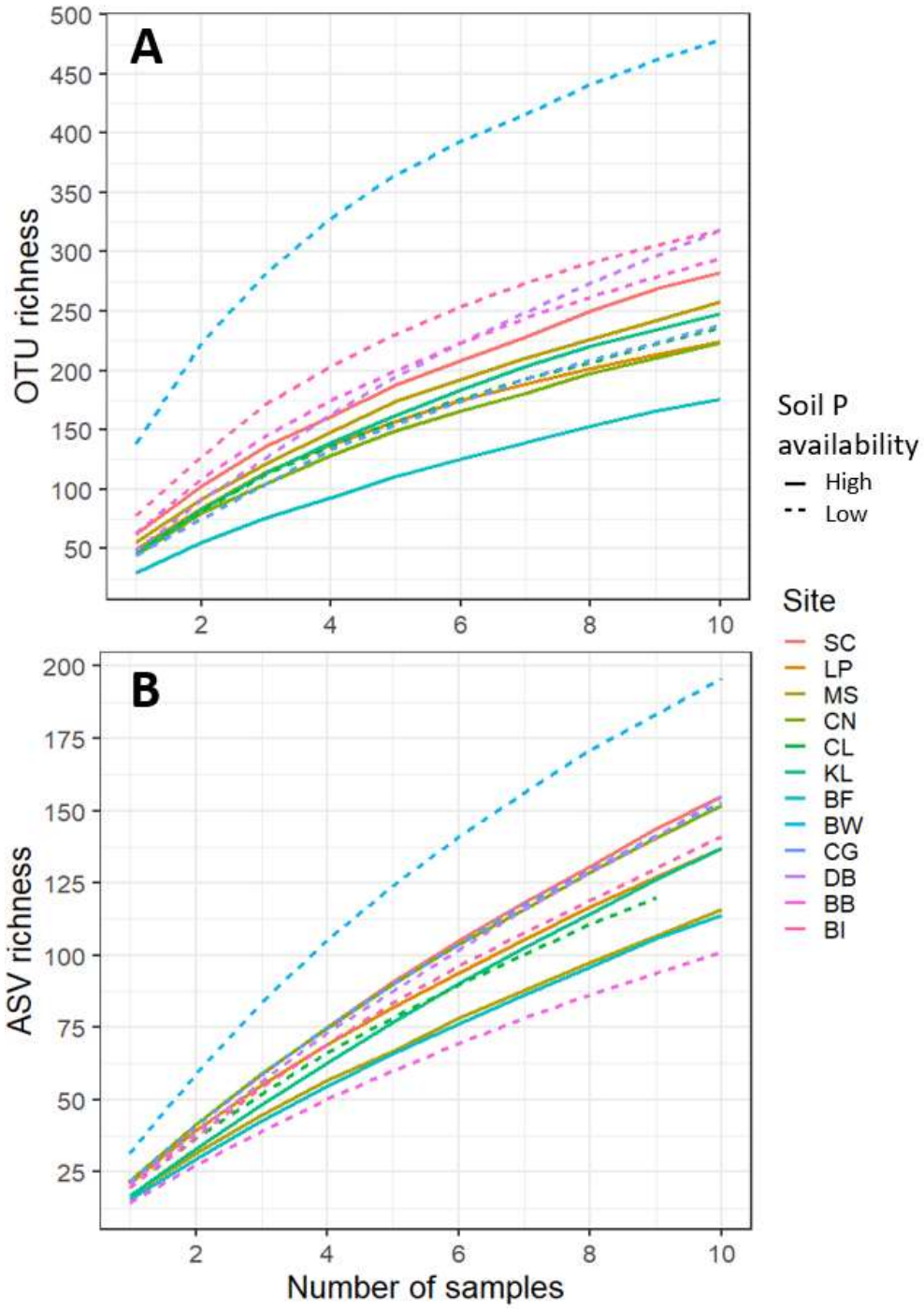

Figure 1.10. Randomized accumulation curves of samples at each site of OTUs (A) and ASVs (B).
Note: Each curve represents the cumulative OTU (top) and ASV (bottom) richness of AMF taxa observed at a site based on the number of samples. DNA was extracted from roots of *Gaillardia aristata* collected at 12 sites from Montana to Minnesota in June 2018. Sites listed in legend from west to east. Sites categorized as having high soil P availability are shown with solid lines, while those categorized as having low soil P availability are shown with dashed lines.

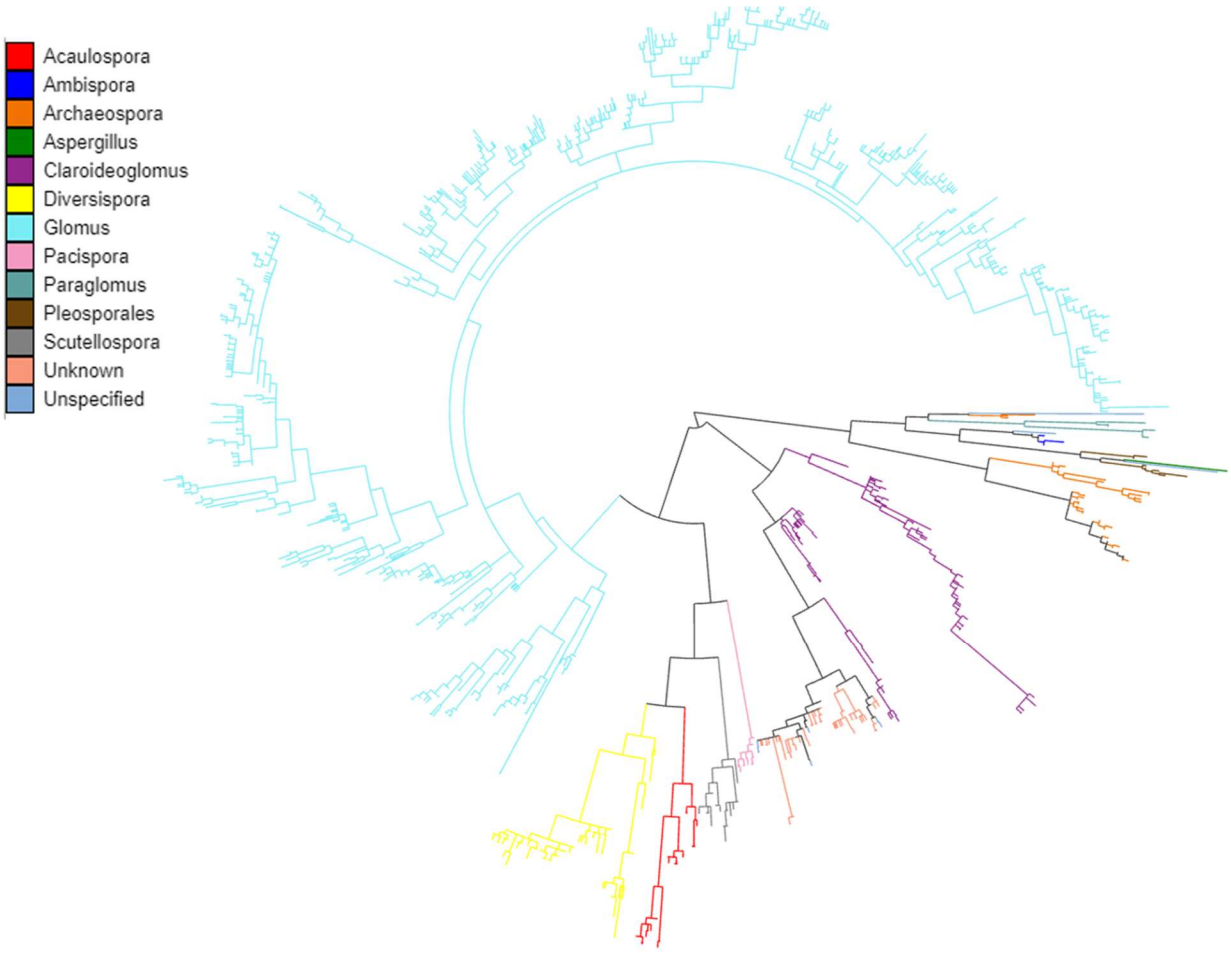

Figure 1.11. Phylogeny of observed AMF sequences.
Note: Phylogenetic tree of AMF sequences with Ascomycete outgroup. The phylogeny includes ASVs from field root samples of *G. aristata* collected in June 2018 as well as ASVs from associated soil samples and root communities from a related greenhouse experiment. Aspergillus and Pleosporales are the outgroup used to construct the phylogeny. Unknown ASVs are those that lack a species identification.

The detected number of 18S AMF sequences per site ranged from 23,471 (at Delbert Berntson) to 41,055 (at Beckman WMA) with a mean of 29,804 and median of 28,835 sequences. Although roots at all sites were dominated by *Glomus* taxa, relative abundances of genera differed by site (χ^2 = 26115.41, *df* = 99, $p < 0.0001$). Approximately 75% of the sequences in *G. aristata* roots at Clearwater (CL) and over 80% at all other sites were identified as *Glomus*, with samples from B-B Ranch (BB) almost completely composed of *Glomus* (Figure 1.12). This genus was overrepresented in western sites relative to eastern sites. The opposite pattern was observed for *Claroideoglomus* and *Diversispora*, which were

seen in the roots of *G. aristata* at western sites more frequently than in the North Dakota and Minnesota sites (Appendix D). *Ambispora* was only observed at one site (Clearwater New). ASVs assigned to *Acaulospora*, *Paraglomus*, and *Scutellospora* were observed only in the roots sampled from western Montana sites (i.e. excluding Beckman WMA). Glomeromycetes of unknown genera were present at almost all sites and comprised approximately 0-4% of ASVs at each site.

Some AMF root communities, like those at B-B Ranch, were much simpler phylogenetically than those at other sites. At B-B Ranch, the community was almost entirely dominated by *Glomus* (27,548 sequences), with 142 sequences assigned to *Claroideoglomus*, 26 sequences assigned to unknown AMF, and 3 sequences of *Diversispora*. The other site at the eastern end of the sampling range, Bicentennial Prairie, was similarly simple. At this site, there were 26,125 sequences assigned to *Glomus*, 349 assigned to *Diversispora*, 49 assigned to *Claroideoglomus*, 14 to *Archaeospora*, and 7 assigned to unknown AMF. In contrast, western sites had more genera represented and more sequences of non-*Glomus* genera. Of the AMF genera currently described, 16 were not observed at the sites I sampled. Four of these absent genera belong to Glomeraceae, four belong to Gigasporaceae, and four to Diversisporaceae. Some AMF families contain only one genus, and of those families, *Sacculospora* was not captured by my sampling.

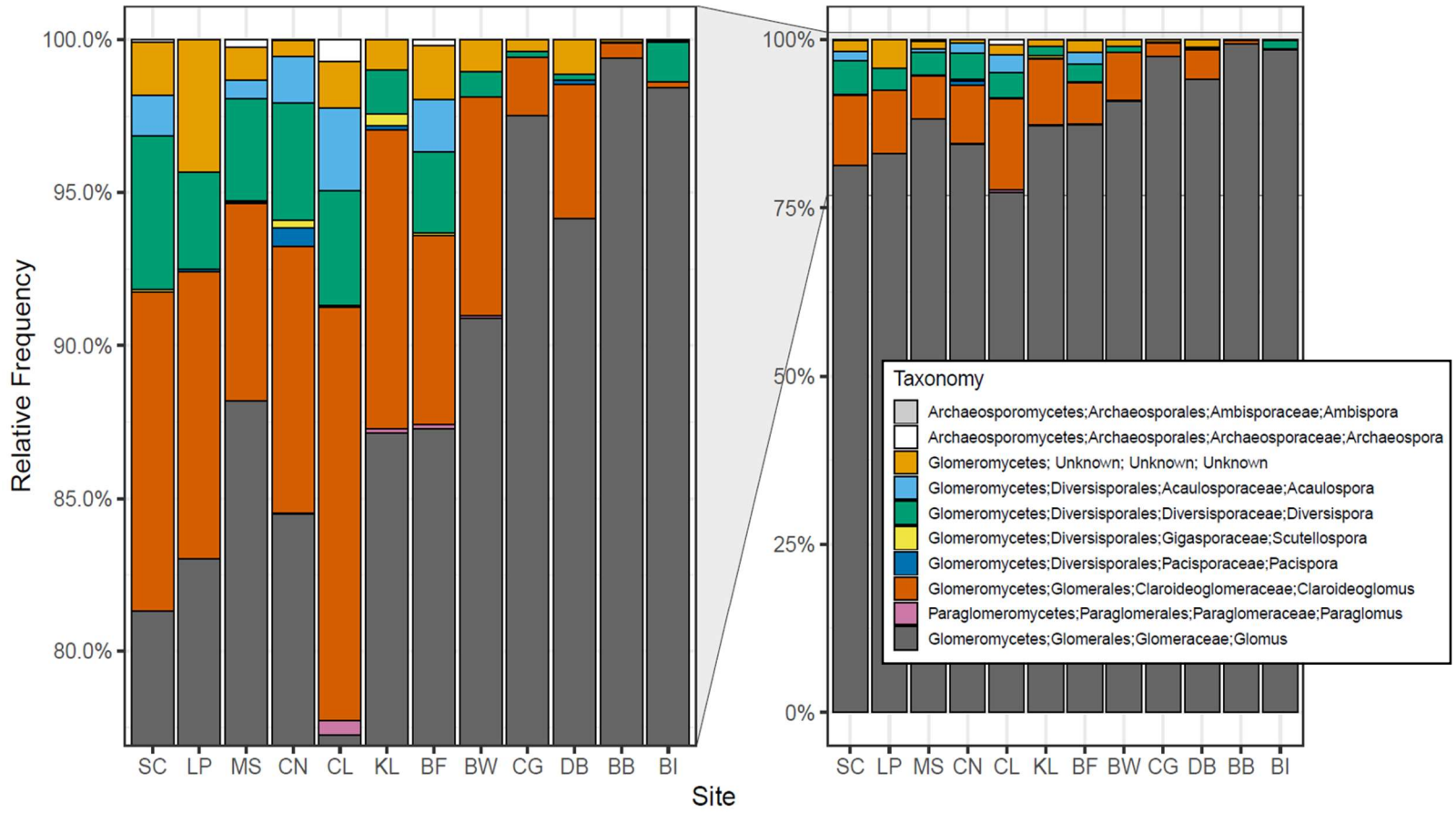

Figure 1.12. Relative frequency of each genus of AMF by site.
Note: Taxonomic distribution of ASVs for each site, with the figure on the left showing relative abundances greater than 0.75 since all sites were composed of at least that proportion of *Glomus* taxa. Sites are arranged from west to east. 18S sequences were extracted from *Gaillardia aristata* roots sampled across Montana (SC, LP, MS, CN, CL, KL, BF, BW), North Dakota (CG and DB), and Minnesota (BB and BI).

PERMANOVA revealed that AMF community composition differed among the sites (*Pseudo-*$F_{11,108}$ = 3.97, p = 0.001). Each AMF community in the roots of *G. aristata* at Bicentennial Prairie, Beckman WMA, and Lone Ponderosa was more similar to other communities at the same site than to those at any other site (Figure 1.13). AMF communities in *G. aristata* roots at Delbert Berntson did not differ in composition from those at Central Grasslands and B-B Ranch. Communities at Blackfoot, Kleinschmidt, Clearwater, Clearwater New, and Mt. Sentinel were not significantly different from each other, and the same was true for Mt. Sentinel and Sheep Camp.

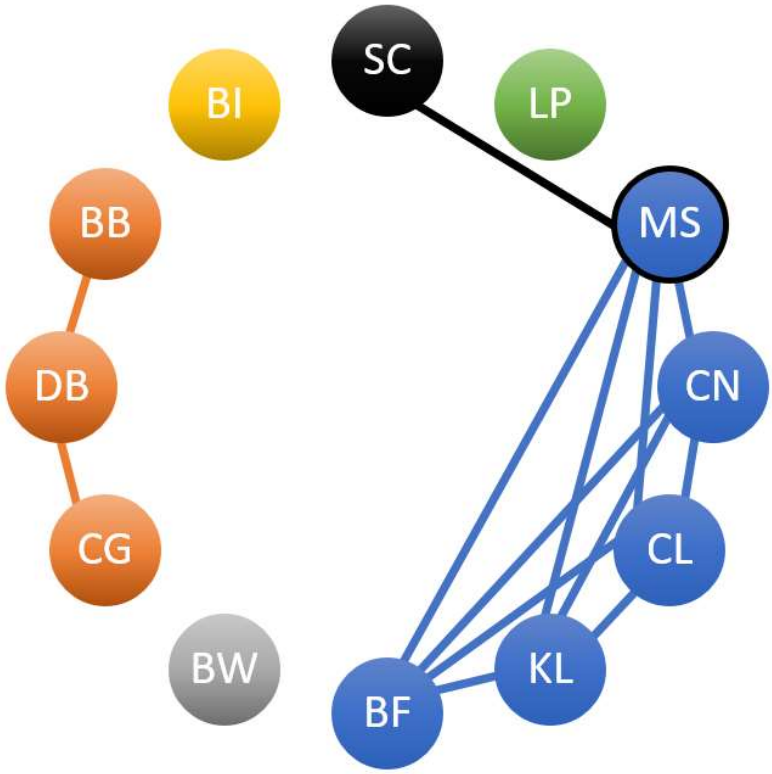

Figure 1.13. Diagram of similarity of AMF communities in roots of *G. aristata* among sites. Note: PERMANOVA test for beta group significance comparing AMF communities sampled from the roots of *Gaillardia aristata* across Montana (Sheep Camp, Lone Ponderosa, Mt. Sentinel, Clearwater New, Clearwater, Kleinschmidt, Blackfoot, Beckman WMA), North Dakota (Central Grasslands and Delbert Berntson), and Minnesota (B-B Ranch and Bicentennial Prairie). Sites arranged from west to east, beginning at the 12 o'clock position. Sites which are not connected by color and lines have statistically different AMF community composition.

Ordination with NMS visually represented relationships among root AMF communities at the 12 sites (Figure 1.14). Clear geographical structuring was observed along Axis 1, with AMF assemblages at sites in Montana generally grouping on the left side of the ordination and those in North Dakota and Minnesota grouping to the right. Longitude correlated with this axis (r = 0.78), as did elevation (r = -0.75), soil P availability (r = -0.75), temperature (r = 0.76), and precipitation (r = 0.77). Communities differed from each other on Axis 2, yet this axis was not associated with most of the environmental variables measured.

The AMF communities in *G. aristata* roots at Kleinschmidt (KL) and Blackfoot (BF), two sites in Montana, displayed greater variation along Axis 1 than did the communities at other Montana sites. Some of the AMF communities at these two sites were closer in ordination space to the North Dakota and Montana communities, indicating that they were more similar to these eastern communities. Some variation along Axis 2 was also observed among the Montana AMF communities, with those at Lone Ponderosa (LP) being the least similar to those at Blackfoot (BF) and Clearwater (CL). AMF communities at Clearwater (CL), a Montana site, clustered with nearby Montana sites, despite the lower soil P availability under *G. aristata* at this site relative to others in western Montana (Figure 1.14).

Beckman WMA (BW), a site in eastern Montana, displayed AMF root communities that did not cluster with those at the other Montana sites (Figure 1.13). Instead, they separated from the other Montana AMF communities along Axis 1 and were more similar to those in North Dakota and Minnesota. However, they did separate from these eastern communities along Axis 2. One community at Delbert Berntson (DB), located in southeastern ND, was observed to be more similar to Montana communities than to other eastern communities. Otherwise, the AMF assemblages in eastern ND and western MN were very similar to each other. An ordination including soil nutrient variables (which, other than P, were only analyzed for half of the root samples) is shown in Appendix D.

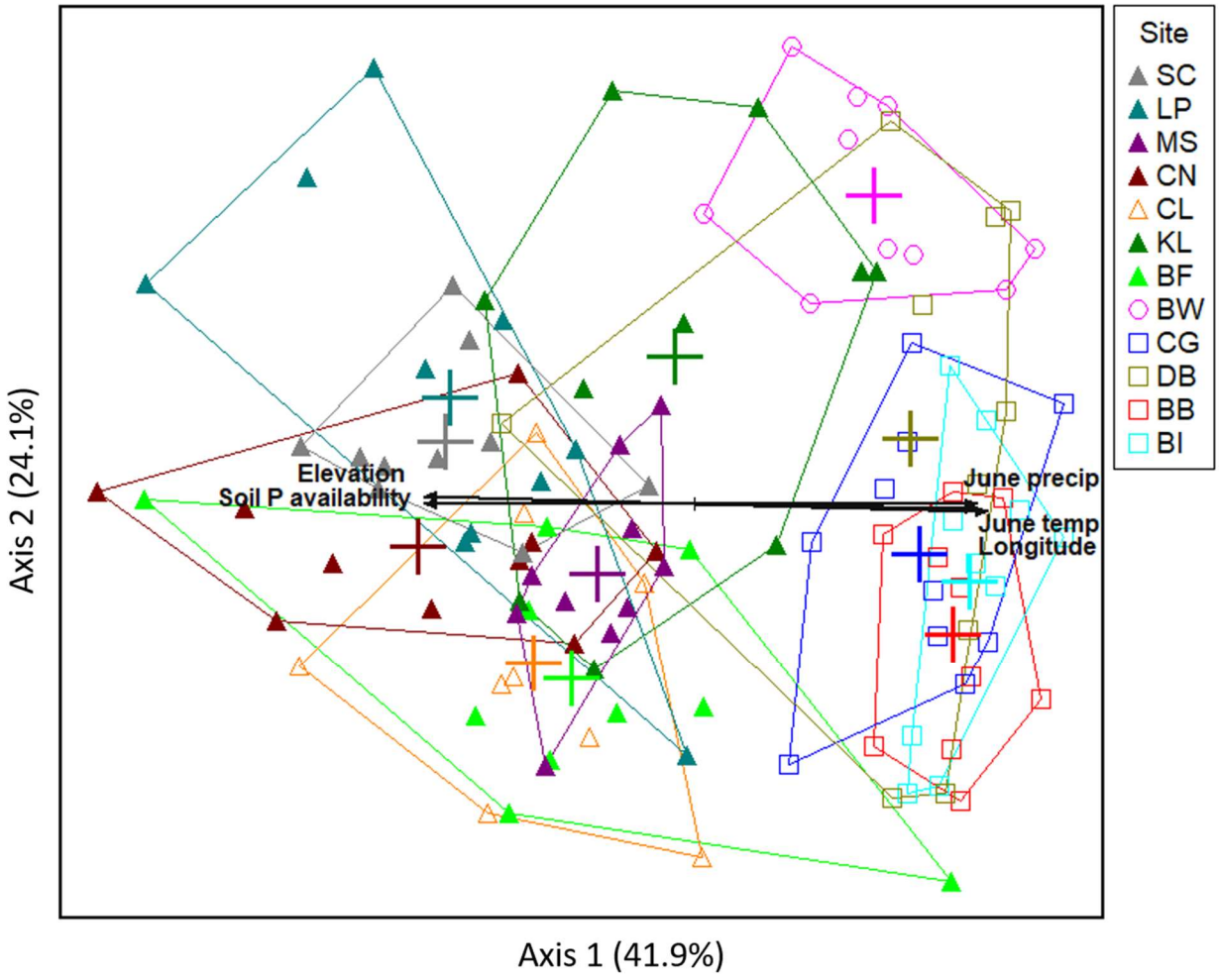

Figure 1.14. NMS of 18S AMF communities in *G. aristata* roots by site.
Note: AMF communities were sampled from the roots of *Gaillardia aristata* in June 2018. Each point represents the fungal community associated with a single plant's roots. Sites are listed from west to east, with closed shapes representing sites high in soil P availability and open shapes representing low soil P sites. Sites in western Montana are displayed as triangles, sites in North Dakota are displayed as squares, and the site in eastern Montana is shown as a circle. Black arrows represent environmental variables correlated with the axes of the ordination ($r > 0.50$). Ordination was performed on Hellinger-transformed ASV abundance table. The final stress for the three-dimensional ordination was 15.4.

1.5. Discussion

This field study provides strong evidence for spatial and environmental structuring of AMF communities associated with *G. aristata* across the Northern Great Plains. In particular, AMF community composition was shaped by soil P availability, precipitation, temperature, elevation, and spatial distance. *Glomus* was dominant at all sites, but more strongly in eastern than western sites. Plant P and biomass increased with hyphal length, which

provides correlational evidence that AMF may be important for P uptake and performance in this plant species.

1.5.1. Soil P availability and performance of *Gaillardia aristata* and mycorrhizas

I sampled *G. aristata* at sites that varied in their soil P availability, and this nutrient seemed to be important for the performance of this species. Plants in soils with higher P availability were larger and had greater P concentration in their aboveground tissue (Figure 1.3). With more P available in their soils, plants were able to grow larger and achieve better P status. The importance of this macronutrient for plant functioning has been well-documented (Theodorou & Plaxton 1993; Schachtman *et al*. 1998).

Because larger plants generally perform better than smaller ones, which results in greater reproductive output and fitness than their competitors, biomass is often used as a proxy for plant performance or fitness (Younginger *et al*. 2017). However, biomass in the field is reflective of many environmental variables beyond P, such as other soil nutrients, precipitation, and photoperiod (Chatzistathis & Therios 2013). Therefore, it is difficult to attribute the differences in biomass I observed to soil P only.

Plants in low P soils typically exhibit greater amounts of extraradical hyphae (Koide & Kabir 2000; Wallander *et al*. 2010; Smith & Smith 2011) than plants in soils with adequate P availability. While mycorrhizas are important for P uptake, they also are capable of providing a range of additional nutrients and services to plants (Newsham *et al*. 1995; Pozo & Azcón-Aguilar 2007; Augé 2001; Porcel *et al*. 2012; Joner *et al*. 2000). Especially when sufficient soil P is available directly to plant roots, it is likely that AMF are provisioning something other than P. I observed no relationship between soil P availability and extent of extraradical hyphae, which suggests that the AMF associated with *G. aristata* may have been providing nutrients or services beyond P. Root colonization also did not vary with soil P availability, which may be because presence of AMF in the roots instead of the soils where P can be scavenged indicates that the AMF species colonizing roots may have a function other than P uptake (Hart & Reader 2002).

Greater hyphal length in the soil was associated with greater shoot biomass and P content, which provides support for the idea that having more extraradical hyphae mining the soil for P results in greater plant P uptake which allows the plant to grow larger. However, I measured all hyphae, not just those of AMF, so my data may not necessarily reflect patterns of AMF hyphal length specifically. Conversely, it could also be argued that larger plants have more carbon to invest in their hyphae and therefore their fungal partners can grow more hyphae.

1.5.2. Soil P availability and AMF community composition

Because the main role of AMF is to provide P (Smith & Read 2008), I expected plants in high P soils to be less dependent on their mycorrhizas for P uptake, and therefore host fewer AMF species. This relationship was not observed for ASV richness, but I found evidence of greater OTU richness with lower soil P availability. The assumption underlying my prediction was that being more dependent on mycorrhizas would necessitate more AMF species when, in fact, it is more likely that the AMF species best at provisioning P are needed. When comparing AMF diversity among sites, Beckman WMA (BW) had the greatest number of ASVs and OTUs. While there is no clear pattern for ASV richness, sites low in soil P availability generally showed greater OTU richness than those high in P.

Currently, there is not a strong understanding of what drives AMF richness. In plants, aboveground richness is often greatest at intermediate levels of aboveground biomass (Grime 1973), but it is unknown if this pattern extends to microbial richness. Plant community is thought to play an important role in AMF richness, possibly due to differences in resource supply by plants or differences in which AMF taxa are hosted (Lekberg *et al*. 2013). It is also possible that AMF richness is driven by stochastic processes, fungal interactions, or unknown environmental factors (Lekberg *et al*. 2013). Beckman WMA was the site where *G. aristata* hosted the greatest AMF richness, and was also the site with the lowest levels of ammonium, potassium, iron, manganese, and zinc. Perhaps such a diversity

of AMF species was needed to provision these various nutrients to the plant. Soils sampled at this site were also lowest in organic matter and cation exchange capacity.

The relative abundance of the most common AMF genera appeared to vary by geography, with the prevalence of *Glomus* increasing towards the east and the prevalence of *Claroideoglomus* and *Diversispora* increasing towards the west. Since sites where *Glomus* was the most predominant in *G. aristata* roots were also those with the lowest soil P availability, it is possible that *Glomus* species were the AMF that charged the least C per unit P and small plants could not afford the other Glomeromycetes. However, it is also possible that the soil P availability at these eastern sites was so low (2-3 ppm) that the non-*Glomus* taxa were unable to thrive there (Teste *et al*. 2016). *Ambispora*, *Acaulospora*, and *Paraglomus* were entirely absent from sites in North Dakota and Minnesota, while *Archaeospora* was observed at only one of these eastern sites (Bicentennial Prairie).

Generally, Glomeraceae are thought to colonize roots more heavily than soil and play a role in protection from pathogens, while the converse may be true for Gigasporaceae, whose function may be the provisioning of nutrients and water (Hart & Reader 2002). No genera in Gigasporaceae were observed in the roots of *G. aristata. Glomus*, a genus within Glomeracae, was dominant at all sites but especially at eastern sites, where soil P availability was lowest. This is the opposite of what I might have expected, since taxa prevalent in the soil instead of roots that can scavenge for nutrients would likely be most important in nutrient-poor soils. Other site differences, such as number of plant pathogens present, may be causing this effect.

It is also possible that soil P was not associated with the site differences in relative abundance. Clearwater (CL), the only western site with low soil P availability, had more *Claroideoglomus* and fewer *Glomus* ASVs, just like the other western sites. If it were soil P driving these differences, I might have expected the relative abundances of ASVs sampled from Clearwater to look more like those of the eastern sites. Other possible drivers of these patterns include temperature and precipitation gradients.

1.5.3. Environmental structuring of AMF communities

The NMS showed separation of AMF communities in *G. aristata* roots depending on soil P availability, but also elevation, longitude, temperature, and precipitation. These variables are all strongly correlated with each other and Axis 1 of the NMS. Temperature, precipitation, latitude, and elevation have been identified as important drivers of AMF community composition (Hazard *et al*. 2013; Chaudhary *et al*. 2014; Davison *et al*. 2015). It should be noted that some of these variables may be proxies for other forces. For example, longitude in itself is unlikely to structure AMF communities, and is more likely to represent the spatial distance between these communities. It should also be noted that AMF communities in *G. aristata* roots could be structured by forces other than those that I measured. For example, length of the growing season and competitive interactions with plants in close proximity to the *G. aristata* individuals I sampled could also shape these communities. Land management practices can influence AMF community composition (Martinez & Johnson 2010; Řezáčová *et al*. 2019).

Allen *et al*. (1995), in perhaps the first study focusing on only one plant species, observed that the AMF species that associated with the sagebrush species *Artemisia tridentata* varied across the plant's range. Spatial structuring, or the differences in community composition due to geographic distance, has been observed in many studies in addition to this one (Kivlin *et al*. 2011; van der Gast *et al*. 2011; Jansa *et al*. 2014; Xu *et al*. 2017). Rasmussen *et al*. (2018) identified six studies examining how AMF communities associated with the same host species were structured spatially, with some finding evidence of spatial autocorrelation, or spatially closer communities being more similar (Lekberg *et al*. 2007; Chaudhary *et al*. 2014), and spatial structure explaining AMF community variation (Horn *et al*. 2017) while some found no evidence of spatial autocorrelation (Friese & Koske 1991; Hazard *et al*. 2013). These studies reported a wide range of environmental variables that were associated with community structure. Rasmussen *et al*. (2018) conducted a study that found support for spatial autocorrelation driving AMF community composition, as well

as environmental variables such as soil pH, neighboring vegetation, non-AM root fungi, NO_3, total N, temperature, and relative humidity (Rasmussen *et al*. 2018).

The type of ecosystem may also affect which AMF species are present. In another study which sampled grassland AMF communities on only one plant species, the authors found that these molecularly-identified AMF assemblages were structured spatially as well as by pH, water content, C, N, C:N ratio, P, and dehydrogenase activity (Horn *et al*. 2017). The authors collected samples from *Festuca brevipila* in the semi-arid grasslands of Germany; macroplots were 20 to 500 km apart with plots 9 to 15 m apart.

Environmental conditions and dispersal limitations are two mechanisms for explaining the spatial structuring of AMF communities. Like other sessile organisms, AMF have propagules that originate from an immobile source and require an agent to transport them to new hosts (Paz *et al*. 2020). Wind, water, mammals, invertebrates and humans have all been documented as dispersal agents for AMF (Paz *et al*. 2020). However, Kivlin *et al*. (2014) found that at regional scales, environmental filtering affects community composition of soil fungi more than dispersal limitations. Because soil P availability differs geographically, community composition may reflect both dispersal limitations and differences in P availability.

The results of the PERMANOVA largely confirmed the site differences in AMF community composition observed in the NMS ordination. AMF communities at five of the sites in western Montana (MS, CN, CL, KL, and BF) were not statistically different from each other. These included the site with low soil P availability (CL), which provides further support for the idea that other environmental variables, such as spatial proximity, may be more important for structuring AMF communities than soil P. The PERMANOVA showed that AMF communities at Bicentennial Prairie and Lone Ponderosa were more similar to other communities at the same site than they were to those at any other site.

Beckman WMA had the largest *G. aristata* plants that were the most heavily colonized by AMF and grew the most hyphae in the soil. The AMF communities at this site

displayed the greatest OTU and ASV richness and were more similar to each other than they were to communities at other sites. This site was the only one located in eastern Montana and was distant from all other sites spatially. Its sandy loam soils and Great Plains Sand Grassland vegetation were also distinct from other sites (Table 1.2). Soils sampled under *G. aristata* at this site were the lowest in ammonium-nitrogen, potassium, iron, manganese, zinc, and organic matter and highest in pH (Appendix D).

1.5.4. Limitations and conclusions

Some limitations of this field study restrict my ability to draw conclusions. I sampled the plants in the east later than those in the west, and although the phenology of the plants was similar, there were variations in the life stage of individuals, and seasonality of AMF could also be a confounding factor (Lutgen *et al*. 2003). While plant biomass is a cumulative record of the entire growing season, soil microbial communities experience high turnover and the AMF species associated with the *G. aristata* individuals I harvested may have been very different if sampled a week earlier or later, which makes conclusions about the AMF communities more speculative.

Species richness is expected to increase with sampling area, which was not constant among my sites. The largest sampling area was almost tenfold that of the smallest, and while site differences in ASV and OTU richness do not seem to reflect differences in sampling area, more uniform sampling would be preferable. For each site, AMF communities were more completely characterized in the OTU dataset than they were in the ASV dataset. Because ASV richness represents diversity at a sub-species or sub-population level, while OTUs are used as a proxy for species (Blaxter *et al*. 2005), it was more important that the OTU rarefaction curves indicated sufficient sampling at each site (Figure 1.10). Sites for which an asymptote was not reached were not sampled enough to represent true AMF richness. Based on these rarefaction curves, I avoided making conclusions about rarer taxa, since they may have been undersampled.

In this field study, soil P availability was important for plant performance, since *G. aristata plants* in soils with higher P availability were larger and had greater P concentration in their aboveground tissues than plants in lower soil P availability. However, soil P availability was not associated with changes in the amount of extraradical hyphae or root length colonized by AMF. Spatial structuring of AMF communities associated with *G. aristata* was observed, with communities becoming more different the father apart they were spatially across the Northern Tier. AMF communities were also structured by environmental variables like soil P availability, precipitation, temperature, and elevation. *Glomus* was the dominant genus at all sites, especially at sites in North Dakota and Minnesota.

While the twelve field sites were approximately at the same latitude, they varied in myriad ways. Different longitudes, soil chemistry and mineralogy, topography, plant communities, and climates resulted in different environments for *G. aristata* and associated AMF communities. It is valuable to explore the range of conditions in which these plant and fungal partners interact, but these varying contexts made it challenging to isolate the effects of any one driver of AMF community composition or plant performance. To more clearly understand these relationships, I conducted a greenhouse experiment as described in Chapter 2, which allowed me to manipulate soil P availability and mycorrhizal status while controlling for other environmental variables.

1.6. References

Allen, E. B., Allen, M. F., Helm, D. J., Trappe, J. M., Molina, R., & Rincon, E. Patterns and regulation of mycorrhizal plant and fungal diversity. *Plant Soil* **170**, 47–62 (1995).

Allen, M. F. Linking water and nutrients through the vadose zone: a fungal interface between the soil and plant systems: Linking water and nutrients through the vadose zone: a fungal interface between the soil and plant systems. *Journal of Arid Land* **3**, 155–163 (2011).

Anderson, M. J. A new method for non-parametric multivariate analysis of variance: Non-parametric MANOVA for ecology. *Austral Ecology* **26**, 32–46 (2001).

Augé, R. M. Water relations, drought and vesicular-arbuscular mycorrhizal symbiosis. *Mycorrhiza* **11**, 3–42 (2001).

Baker, K. F. & Cook, R. J. *Biological control of plant pathogens*. (W. H. Freeman, 1974).

Bazzaz, F. A., Chiariello, N. R., Coley, P. D. & Pitelka, L. F. Allocating Resources to Reproduction and Defense. *BioScience* **37**, 58–67 (1987).

Bengtsson-Palme, J., Ryberg, M., Hartmann, M., Branco, S., Wang, Z., Godhe, A., De Wit, P., Sáchez-García, M., Ebersberger, I., de Sousa, F., Amend, A., Jumpponen, A., Unterseher, M., Kristiansson, E., Abarenkov, K., Bertrand, Y. J. K., Sanli, K., Eriksson, K. M., Vik, U., Veldre, V., & R. H. Nilsson. Improved software detection and extraction of ITS1 and ITS2 from ribosomal ITS sequences of fungi and other eukaryotes for analysis of environmental sequencing data. *Methods in Ecology and Evolution* (2013).

Beule, L. & Karlovsky, P. Improved normalization of species count data in ecology by scaling with ranked subsampling (SRS): application to microbial communities. *PeerJ* **8**, e9593 (2020).

Bever, J. D. Host-specificity of AM fungal population growth rates can generate feedback on plant growth. *Plant and Soil* **244**, 281–290 (2002).

Bieleski, R. L. Phosphate Pools, Phosphate Transport, and Phosphate Availability. *Annual Review of Plant Physiology* **24**, 225–252 (1973).

Blaxter, M., Mann, J., Chapman, T., Thomas, F., Whitton, C., Floyd, R., & Abebe, E. Defining operational taxonomic units using DNA barcode data. *Philosophical Transactions of the Royal Society B: Biological Sciences* **360**, 1935–1943 (2005).

Bokulich, N. A., Kaehler, B. D., Ram Rideout, J., Dillon, M., Bolyen, E., Knight, R., Huttley, G. A., & Caporaso, J. G. Optimizing taxonomic classification of marker-gene amplicon sequences with QIIME 2's q2-feature-classifier plugin. *Microbiome* **6**, 90 (2018).

Bolyen, E. *et al.* Reproducible, interactive, scalable and extensible microbiome data science using QIIME 2. *Nature Biotechnology* **37**, 852–857 (2019).

Buttigieg, P. L. & Ramette, A. A guide to statistical analysis in microbial ecology: a community-focused, living review of multivariate data analyses. *FEMS Microbiology Ecology* **90**, 543–550 (2014).

Callahan, B. J. *et al.* DADA2: High-resolution sample inference from Illumina amplicon data. *Nature Methods* **13**, 581–583 (2016).

Camacho, C. *et al.* BLAST+: architecture and applications. *BMC Bioinformatics* **10**, 421 (2009).

Cavalier-Smith, T. A revised six-kingdom system of life. *Biological Reviews* **73**, 203–266 (2007).

Chatzistathis, T. & Therios, I. How soil nutrient availability influences plant biomass and how biomass stimulation alleviates heavy metal toxicity in soils: The cases of nutrient use efficient genotypes and phytoremediators, respectively. In *Biomass Now - Cultivation and Utilization* (ed. Matovic, M. D.) (InTech, 2013).

Chaudhary, V. B., O'Dell, T. E., Rillig, M. C. & Johnson, N. C. Multiscale patterns of arbuscular mycorrhizal fungal abundance and diversity in semiarid shrublands. *Fungal Ecology* **12**, 32–43 (2014).

Davison, J. *et al.* Global assessment of arbuscular mycorrhizal fungus diversity reveals very low endemism. *Science* **349**, 970–973 (2015).

Deshpande, V. *et al.* Fungal identification using a Bayesian classifier and the Warcup training set of internal transcribed spacer sequences. *Mycologia* **108**, 1–5 (2016).

Dumbrell, A. J. *et al.* Distinct seasonal assemblages of arbuscular mycorrhizal fungi revealed by massively parallel pyrosequencing. *New Phytologist* **190**, 794–804 (2011).

Epstein, E. *Mineral nutrition of plants: principles and perspectives.* (1972).

Friese, C. F. & Koske, R. E. The spatial dispersion of spores of vesicular-arbuscular mycorrhizal fungi in a sand dune: microscale patterns associated with the root architecture of American beachgrass. *Mycological Research* **95**, 952–957 (1991).

Grace, C. & Stribley, D. P. A safer procedure for routine staining of vesicular-arbuscular mycorrhizal fungi. *Mycological Research* **95**, 1160–1162 (1991).

Grime, J. P. Competitive exclusion in herbaceous vegetation. *Nature* **242**, 344–347 (1973).

Gweon, H. S. *et al.* PIPITS : an automated pipeline for analyses of fungal internal transcribed spacer sequences from the llumina sequencing platform. *Methods in Ecology and Evolution* **6**, 973–980 (2015).

Harper, J. L. & White, J. The Demography of Plants. *Annual Review of Ecological Systems* **5**, 419–463 (1974).

Hart, M. M. & Reader, R. J. Taxonomic basis for variation in the colonization strategy of arbuscular mycorrhizal fungi. *New Phytologist* **153**, 335–344 (2002).

Hazard, C. *et al.* The role of local environment and geographical distance in determining community composition of arbuscular mycorrhizal fungi at the landscape scale. *ISME J* **7**, 498–508 (2013).

Herms, D. & Mattson, W. The Dilemma of Plants: To Grow or Defend. *The Quarterly Review of Biology* **67**, 283–335 (1992).

Horn, S., Hempel, S., Verbruggen, E., Rillig, M. C. & Caruso, T. Linking the community structure of arbuscular mycorrhizal fungi and plants: a story of interdependence? *ISME J* **11**, 1400–1411 (2017).

Ihrmark, K. *et al.* New primers to amplify the fungal ITS2 region - evaluation by 454-sequencing of artificial and natural communities. *FEMS Microbiology Ecology* **82**, 666–677 (2012).

Jakobsen, I., Abbott, L. K. & Robson, A. D. External hyphae of vesicular-arbuscular mycorrhizal fungi associated with Trifolium subterraneum L. 2. Hyphal transport of 32P over defined distances. *New Phytologist* **120**, 509–516 (1992).

Jiang, Y. *et al.* Plants transfer lipids to sustain colonization by mutualistic mycorrhizal and parasitic fungi. *Science* **356**, 1172–1175 (2017).

Johnson, N. C., Graham, J. H. & Smith, F. A. Functioning of mycorrhizal associations along the mutualism-parasitism continuum. *New Phytologist* **135**, 575–585 (1997).

Joner, E. J., Briones, R. & Leyval, C. Metal-binding capacity of arbuscular mycorrhizal mycelium. *Plant and Soil* **226**, 227–234 (2000).

Jones, M. D. & Smith, S. E. Exploring functional definitions of mycorrhizas: Are mycorrhizas always mutualisms? *Canadian Journal of Botany* **82**, 1089–1109 (2004).

Katoh, K. & Standley, D. M. MAFFT Multiple Sequence Alignment Software Version 7: Improvements in Performance and Usability. *Molecular Biology and Evolution* **30**, 772–780 (2013).

Kivlin, S. N., Hawkes, C. V. & Treseder, K. K. Global diversity and distribution of arbuscular mycorrhizal fungi. *Soil Biology and Biochemistry* **43**, 2294–2303 (2011).

Kivlin, S. N., Winston, G. C., Goulden, M. L., & Treseder, K. K. Environmental filtering affects soil fungal community composition more than dispersal limitation at regional scales. *Fungal Ecology* **12**, 14-25 (2014).

Klironomos, J. N. Host-specificity and functional diversity among arbuscular mycorrhizal fungi. *Microbial biosystems: new frontiers. Proceedings of the 8th International Symposium on Microbial ecology*. Atlantic Canada Society for Microbial Ecology, Halifax, Canada, 845–851 (2000).

Klironomos, J. N., McCune, J. & Moutoglis, P. Species of arbuscular mycorrhizal fungi affect mycorrhizal responses to simulated herbivory. *Applied Soil Ecology* **26**, 133–141 (2004).

Klironomos, J. N. Variation in plant response to native and exotic arbuscular mycorrhizal fungi. *Ecology* **84**, 2292–2301 (2003).

Koch, A. M. *et al*. High genetic variability and low local diversity in a population of arbuscular mycorrhizal fungi. *Proceedings of the National Academy of Sciences of the United States of America* **101**, 2369 (2004).

Kohout, P. *et al.* Comparison of commonly used primer sets for evaluating arbuscular mycorrhizal fungal communities: Is there a universal solution? *Soil Biology and Biochemistry* **68**, 482–493 (2014).

Koide, R. T. & Kabir, Z. Extraradical hyphae of the mycorrhizal fungus *Glomus intraradices* can hydrolyse organic phosphate. *New Phytologist* **148**, 511–517 (2000).

Koning, R. E. The natural species and cultivars of the genus *Gaillardia*. Handbook of Flowering: Volume V (2018): 118. CRC Press. Ed. Abraham H. Halevy.

Lee, J., Lee, S. & Young, J. P. W. Improved PCR primers for the detection and identification of arbuscular mycorrhizal fungi: PCR primers for arbuscular mycorrhizal fungi. *FEMS Microbiology Ecology* **65**, 339–349 (2008).

Lekberg, Y., Gibbons, S. M., Rosendahl, S. & Ramsey, P. W. Severe plant invasions can increase mycorrhizal fungal abundance and diversity. *The ISME Journal* **7**, 1424-1433 (2013).

Lekberg, Y., Koide, R. T., Rohr, J. R., Aldrich-Wolfe, L. & Morton, J. B. Role of niche restrictions and dispersal in the composition of arbuscular mycorrhizal fungal communities. *Journal of Ecology* **95**, 95–105 (2007).

Lekberg, Y. *et al.* More bang for the buck? Can arbuscular mycorrhizal fungal communities be characterized adequately alongside other fungi using general fungal primers? *New Phytologist* **220**, 971–976 (2018).

Luginbuehl, L. H. *et al.* Fatty acids in arbuscular mycorrhizal fungi are synthesized by the host plant. *Science* **356**, 1175–1178 (2017).

Lutgen, E. R., Muir-Clairmont, D., Graham, J. & Rillig, M. C. Seasonality of arbuscular mycorrhizal hyphae and glomalin in a western Montana grassland. *Plant and Soil* **257**, 71–83 (2003).

MacArthur, R. H. & Wilson, E. O. *The theory of island biogeography*. (Princeton University Press, 1967).

Martínez-García, L. B., Richardson, S. J., Tylianakis, J. M., Peltzer, D. A. & Dickie, I. A. Host identity is a dominant driver of mycorrhizal fungal community composition during ecosystem development. *New Phytologist* **205**, 1565–1576 (2015).

McCune, B. & Mefford, M. J. PC-ORD. Multivariate Analysis of Ecological Data*. Wild Blueberry Media* (2018).

McDonald, D. *et al.* Striped UniFrac: enabling microbiome analysis at unprecedented scale. *Nature Methods* **15**, 847–848 (2018).

McGonigle, T. P., Miller, M. H., Evans, D. G., Fairchild, G. L. & Swan, J. A. A new method which gives an objective measure of colonization of roots by vesicular-arbuscular mycorrhizal fungi. *New Phytologist* **115**, 495–501 (1990).

McMurdie, P. J. & Holmes, S. Waste not, want not: Why rarefying microbiome data is inadmissible. *PLoS Computational Biology* **10**, e1003531 (2014).

Minnesota Department of Natural Resources. Rare Species Guide: *Gaillardia aristata*. https://www.dnr.state.mn.us/rsg/profile.html?/rsg/profile.html?action=elementDetail&selectedElement=PDAST3Y030.

Newsham, K. K., Fitter, A. H. & Watkinson, A. R. Arbuscular mycorrhiza protect an annual grass from root pathogenic fungi in the field. *The Journal of Ecology* **83**, 991 (1995).

Newsham, K. K., Fitter, A. H. & Watkinson, A. R. Multi-functionality and biodiversity in arbuscular mycorrhizas. *Trends in Ecology & Evolution* **10**, 407–411 (1995).

Nguyen, N. H. *et al.* FUNGuild: An open annotation tool for parsing fungal community datasets by ecological guild. *Fungal Ecology* **20**, 241–248 (2016).

Nilsson, R. H. *et al.* The UNITE database for molecular identification of fungi: handling dark taxa and parallel taxonomic classifications. *Nucleic Acids Research* **47**, D259–D264 (2019).

Oksanen, J. *et al.* vegan: Community Ecology Package. (2020).

Öpik, M. *et al.* The online database MaarjAM reveals global and ecosystemic distribution patterns in arbuscular mycorrhizal fungi (Glomeromycota). *New Phytologist* **188**, 223–241 (2010).

Öpik, M., Davison, J., Moora, M. & Zobel, M. DNA-based detection and identification of Glomeromycota: the virtual taxonomy of environmental sequences. *Botany* **92**, 135–147 (2014).

Owusu-Bennoah, E. & Wild, A. Autoradiography of the depletion zone of phosphate around onion roots in the presence of vesicular-arbuscular mycorrhiza. *New Phytologist* **82**, 133–140 (1979).

Paz, C., Öpik, M., Bulascoschi, L., Guillermo Bueno, C., & Galetti, M. Dispersal of Arbuscular Mycorrhizal Fungi: Evidence and Insights for Ecological Studies. *Microbial Ecology* **81**, 283-292 (2021).

Pearson, J. N. & Jakobsen, I. The relative contribution of hyphae and roots to phosphorus uptake by arbuscular mycorrhizal plants, measured by dual labelling with 32P and 33P. *New Phytologist* **124**, 489–494 (1993).

Pfeffer, P. E., Douds, D. D., Bécard, G. & Shachar-Hill, Y. Carbon Uptake and the Metabolism and Transport of Lipids in an Arbuscular Mycorrhiza. *Plant Physiology* **120**, 587–598 (1999).

Porcel, R., Aroca, R. & Ruiz-Lozano, J. M. Salinity stress alleviation using arbuscular mycorrhizal fungi. A review. *Agronomy for Sustainable Development* **32**, 181–200 (2012).

Pozo, M. J. & Azcón-Aguilar, C. Unraveling mycorrhiza-induced resistance. *Current Opinion in Plant Biology* **10**, 393–398 (2007).

Price, M. N., Dehal, P. S. & Arkin, A. P. FastTree 2 – Approximately Maximum-Likelihood Trees for Large Alignments. *PLoS ONE* **5**, e9490 (2010).

Rasmussen, P. U. *et al.* Multiscale patterns and drivers of arbuscular mycorrhizal fungal communities in the roots and root-associated soil of a wild perennial herb. *New Phytologist* **220**, 1248–1261 (2018).

Rognes, T., Flouri, T., Nichols, B., Quince, C. & Mahé, F. VSEARCH: a versatile open source tool for metagenomics. *PeerJ* **4**, e2584 (2016).

Rovira, A. D. Plant root exudates. *The Botanical Review* **35**, 35–57 (1969).

Schachtman, D. P., Reid, R. J. & Ayling, S. M. Phosphorus uptake by plants: From soil to cell. *Plant Physiology* **116**, 447–453 (1998).

Soil Survey Staff, Natural Resources Conservation Service, United States Department of Agriculture. Web Soil Survey. http://websoilsurvey.sc.egov.usda.gov/. Accessed [4/14/2021].

Smith, S. E. & Read, D. J. INTRODUCTION. in *Mycorrhizal Symbiosis* 1–8 (Academic Press Ltd., 2008).

Smith, S. E., Jakobsen, I., Grønlund, M. & Smith, F. A. Roles of arbuscular mycorrhizas in plant phosphorus nutrition: Interactions between pathways of phosphorus uptake in arbuscular mycorrhizal roots have important implications for understanding and manipulating plant phosphorus acquisition. *Plant Physiology* **156**, 1050–1057 (2011).

Smith, S. E. & Smith, F. A. Roles of arbuscular mycorrhizas in plant nutrition and growth: New paradigms from cellular to ecosystem scales. *Annual Review of Plant Biology* **62**, 227–250 (2011).

Smith, S. E., Smith, F. A. & Jakobsen, I. Mycorrhizal fungi can dominate phosphate supply to plants irrespective of growth responses. *Plant Physiology* **133**, 16–20 (2003).

Teste, F. P. Restoring grasslands with arbuscular mycorrhizal fungi around remnant patches. *Applied Vegetation Science* **19**, 3–4 (2016).

Theodorou, M. E. & Plaxton, W. C. Metabolic adaptations of plant respiration to nutritional phosphate deprivation. *Plant Physiology* **101**, 339–344 (1993).

Turenne, C. Y., Sanche, S. E., Hoban, D. J., Karlowsky, J. A. & Kabani, A. M. Rapid identification of fungi by using the ITS2 genetic region and an automated fluorescent capillary electrophoresis system. *Journal of Clinical Microbiology* **38**, 944–944 (2000).

USDA NRCS Plants Database. *Gaillardia aristata*. https://plants.usda.gov/home/plantProfile?symbol=gaar.

USNVC (United States National Vegetation Classification) Database. Federal Geographic Data Committee, Vegetation Subcommittee. Washington D.C. 12 April 2021.

Wallander, H., Johansson, U., Sterkenburg, E., Brandström Durling, M. & Lindahl, B. D. Production of ectomycorrhizal mycelium peaks during canopy closure in Norway spruce forests. *New Phytologist* **187**, 1124–1134 (2010).

Wang, Q., Garrity, G. M., Tiedje, J. M. & Cole, J. R. Naïve Bayesian classifier for rapid assignment of rRNA sequences into the new bacterial taxonomy. *AEM* **73**, 5261–5267 (2007).

Wang, T., Hamann, A., Spittlehouse, D. & Carroll, C. Locally downscaled and spatially customizable climate data for historical and future periods for North America. *PLoS ONE* **11**, e0156720 (2016).

White, T. J., Bruns, T., Lee, S. & Taylor, J. Amplification and direct sequencing of fungal ribosomal RNA genes for phylogenetics. in *PCR Protocols* 315–322 (Elsevier, 1990).

Wright, D. P., Read, D. J. & Scholes, J. D. Mycorrhizal sink strength influences whole plant carbon balance of *Trifolium repens* L. *Plant, Cell & Environment* **21**, 881–891 (1998).

Younginger, B. S., Sirová, D., Cruzan, M. B. & Ballhorn, D. J. Is biomass a reliable estimate of plant fitness? *Applications in Plant Sciences* **5**, 1600094 (2017).

Zhang, J., Kobert, K., Flouri, T. & Stamatakis, A. PEAR: a fast and accurate Illumina Paired-End reAd mergeR. *Bioinformatics* **30**, 614–620 (2014).

CHAPTER 2. THE IMPORTANCE OF PHOSPHORUS AVAILABILITY AND SOIL LEGACIES FOR COMMUNITY COMPOSITION AND NUTRIENT PROVISIONING OF ARBUSCULAR MYCORRHIZAL FUNGI ASSOCIATED WITH *GAILLARDIA ARISTATA*

2.1. Abstract

Mycorrhizas are a widespread symbiosis formed when arbuscular mycorrhizal fungi (AMF) colonize roots and provide nutrients like phosphorus (P) and services to their hosts in exchange for photosynthate. To investigate the importance of P availability and soil legacies, I grew the grassland forb *Gaillardia aristata* in the greenhouse with and without mycorrhizas and fertilized with or without P. Each plant in the mycorrhizal treatment was inoculated with field soil from one of 12 sites which ranged in mean soil P availability from 2 to 38 ppm, to test the hypothesis that AMF from sites varying in soil P availability would vary in their effectiveness at providing P to their host. I hypothesized that AMF communities from soils low in P availability would be more effective at scavenging and provisioning P than communities from soils high in P availability. If there was no difference in P provisioning between the two groups, I expected similar provisioning capacity to be due to shifts in AMF community composition, where taxa more important for P would become more prevalent. To characterize AMF communities, I identified AMF species present in the field soil inocula and in roots of *G. aristata* grown in the greenhouse using next-generation DNA sequencing. Mycorrhizas were important for plant growth and P status. Overall, community composition of AMF in the roots reflected the composition in the inoculum, but differences in composition did not result in differences in P status or growth. P fertilization did not shift AMF community composition or lead to greater *G. aristata* biomass when mycorrhizal but did result in better plant P status than plants fertilized without P. Acid phosphatase activity was highest when AMF were sourced from soils low in P availability but this was the only evidence that suggested a soil legacy for nutrient provisioning by AMF.

2.2. Introduction

Mycorrhizas are an ancient association between arbuscular mycorrhizal fungi (AMF) and plants that allowed the latter to colonize land about 450 million years ago (Redecker *et al*. 2000). AMF, which are obligate biotrophs, cannot survive without their hosts but have also proven indispensable to many plants; this mutualism has remained evolutionarily stable for hundreds of millions of years and is seen today in 80% of plant species (Smith & Read 2008). However, the mechanism for this stability is uncertain, especially since the roots of a single plant are often simultaneously colonized by more than one AMF species (Maherali & Klironomos 2012) and each of these fungal partners is likely associating with multiple hosts (Selosse *et al*. 2006).

As discussed in the first chapter, AMF are vital for plant P uptake. Their role in acquiring free inorganic phosphate (P_i) from the soil and provisioning it to plants is perhaps the most important function they provide to their hosts (Smith & Read 2008). Extraradical hyphae may also be capable of exploiting organic phosphate (P_o): Glomeromycetes secrete acid phosphatases from their extraradical hyphae which diffuse through the soil solution to mineralize P_o to P_i (St. John *et al*. 1983; Koide & Kabir 2000; Sato *et al*. 2015; but see also Joner & Johansen 2000). In particular, Sato *et al*. (2019) found that the AMF species *Rhizophagus clarus* secreted acid phosphatases in low P conditions. However, plants can also obtain P directly from the soil via root uptake and secrete their own acid phosphatases (Smith & Read 2008; Koide & Kabir 2000).

Legacy effects have been defined as effects that endure after the interaction that caused the effect ceases (Wurst & Ohgushi 2015). In the literature, these are usually discussed as plant-mediated phenomena. For example, invasion by an exotic plant species may shift the soil microbial community in ways that linger even after eradication of the invasive (Corbin & D'Antonio 2012), or early successional plant species can influence the soil microbial community in ways that affect later plant communities after the original species are gone (Kardol *et al*. 2007). Here, I was interested in whether AMF communities

may adapt to the local soil conditions in which they occur and whether those changes in the community will subsequently influence plant performance. As discussed in Chapter 1, AMF communities are shaped by their surroundings, including but not limited to physical, chemical, and biological soil properties, climatic variables, land use histories, plant community composition, and spatial distance.

I also sought to explore how an AMF community's history of environmental conditions would affect partnership with and provisioning to a plant host, which would consequently influence plant performance. Communities of soil microbes can shape the relative abundance and total productivity of species in plant communities (Bauer *et al*. 2020). Furthermore, soil microbes, especially AMF, can play a key role in plant response to local soil environment and mediation of plant response to environmental stressors (Johnson *et al*. 2010). Because AMF have important implications for plant performance, and because local soil conditions have important implications for AMF community composition, I sought to examine whether the P availability of a soil structures its AMF community in ways that persist even in a different soil P environment. I also wanted to know if this structuring of AMF community composition would have effects on the performance of associated plants.

Through a pot experiment in the greenhouse, I investigated whether AMF communities from soils of differing P availability had similar capacity to provide P to their hosts, or if they were influenced by the soil environment in which they were assembled. I also examined whether shifts in community composition were important for explaining provisioning capacity. I endeavored to answer:

1. Are mycorrhizas important for performance and P status in *G. aristata*?
2. Do AMF communities from soils of differing P availability have different capacity to provide P to their hosts?
3. Will AMF community composition shift when placed in soils of contrasting P availability? How will the resultant communities differ from each other and from their source communities?

I hypothesized that plants would benefit from being mycorrhizal and would perform better with than without AMF. I expected to see mycorrhizas benefit plants more in low soil P availability, since plants would be more likely to provision sufficient P on their own in soils with high soil P availability. I predicted that if mycorrhizas are important for a plant species, then mycorrhizal plants will have greater biomass and P than non-mycorrhizal plants.

I hypothesized that if history of environmental conditions structures fungal communities and services, then AMF communities should differ in their ability to provision P. AMF communities from soil with low P availability should be more efficient in obtaining P from soil and therefore have greater capacity to provide P to their hosts, resulting in greater plant biomass and higher plant P than plants with AMF communities sourced from high P soils. I also predicted that these advantages would be associated with more hyphal length in the soil and greater phosphatase activity in the soil. In high P soils, I expected that AMF communities from soils low in P availability would be too expensive and that plants hosting these communities would accumulate less biomass and have less P in their tissues than those hosting communities from high P soils. If plants preferentially associated with the best fungal partners, then I expected to see shifts in AMF community composition indicating which species may be more important for plant P acquisition. AMF that were more cooperative and provisioned more P should predominate in low but not high P availability.

2.3. Methods

2.3.1. Experimental design

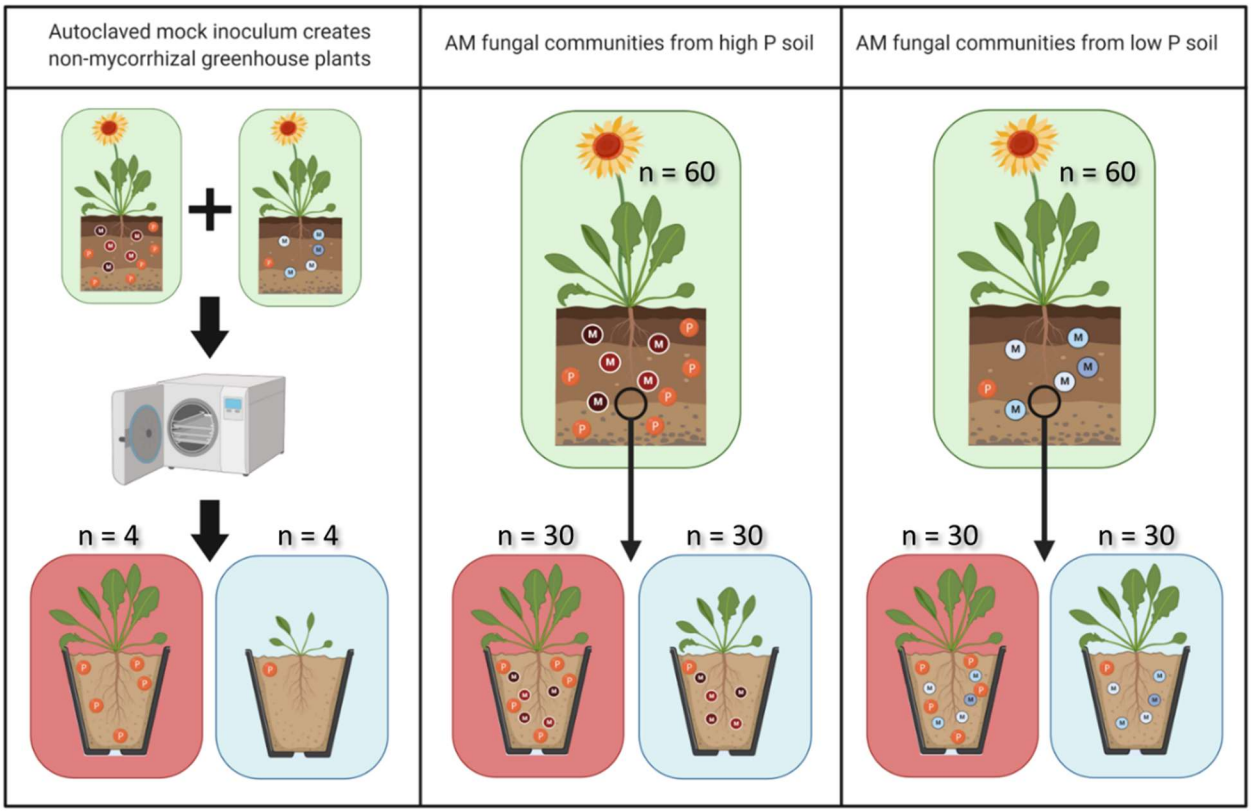

Figure 2.1. Representation of AMF inoculum origin and P fertilization treatments.
Note: Visual representation of the experimental design, where the top row of images (green background) depicts the source of the field soil used as AMF inoculum and the bottom row depicts the P fertilization treatment. Greenhouse *G. aristata* plants were either fertilized with (red background) or without (blue background) P. Phosphorus is represented by "P" icons, with more icons indicating higher soil P availability. AMF taxa are represented by "M" icons and differences in AMF community composition are represented by the different shades of these icons. Non-mycorrhizal plants (far left) were created by autoclaving field soil to remove microbes. After autoclaving, all greenhouse soils received the same microbial wash to establish similar microbial communities (minus AMF) in all treatments. The predicted performance of plants in each treatment is indicated by the size of the plants in the bottom row of the figure.

The greenhouse experiment consisted of two factors (Figure 2.1). The first factor was soil P availability, which I manipulated via fertilization. The second factor was the type of AMF community used to inoculate *G. aristata*. Plants were inoculated with soils containing AMF from field sites categorized as either high or low in P availability based on soil nutrient analysis described in Chapter 1 (Table 2.1).

Each pot in the experiment contained 1.5 L of 1:1 100-mesh quartzite sand (Granusil #2040, Sterling Supply, Minneapolis, Minnesota, USA) and background soil taken from a site near Bicentennial Prairie (47.0513941, -96.4305344; Mehlich III phosphorus level = 10 ppm). Background soil and sand were placed in autoclave trays filled to 10-cm depth and autoclaved for at least 60 min at 121 °C (with dry time set to zero) to ensure that the temperature of the material was above 80 °C for at least 30 min. This procedure has been shown to effectively kill microbial life (Wolf & Skipper, 1994), so that the background soil was free of AMF and the only fungi present during the experiment would be from the field soil inoculum. Autoclaved materials were stored in sterile bleached containers with lids to prevent contamination by airborne AMF and homogenized before being separated for fertilization treatments.

From each field site described in Chapter 1, ten soil samples were used to inoculate ten *G. aristata* in the greenhouse with each plant receiving inoculum collected under a different plant in the field. Each of the 10 replicates from each site was randomly assigned to either the high or ambient P treatment. The ambient P treatment remained at the P level of the background soil (10 ppm) aside from initial P fertilization to aid seedling establishment. The high P treatment soil was fertilized with 139.5 mg $Ca(H_2PO_4)_2$ per L of soil prior to adding soil to pots.

2.3.2. Inocula and microbial wash

AMF inocula were collected in June 2018 while conducting the field study described in Chapter 1. From the rhizosphere of each *G. aristata* plant sampled in the field, 50 mL of soil was stored at -20 °C until it was added to a greenhouse pot to establish a source AMF community. Since the inoculum only accounted for 3% of the total soil volume in each pot, its P level did not greatly affect that of the pot. Each pot was considered an independent replicate of the given factors: 1) Soil treatment, either fertilized with or without P and 2) AMF inoculum sourced from soils either high or low in soil P availability (Table 2.1).

Table 2.1. Mean P availability ± SE of soils used to inoculate *Gaillardia aristata* plants in the greenhouse.

Site	Mean soil P ± SE (ppm)	Tukey HSD
Sheep Camp	**20 ± 3**	**bc**
Lone Ponderosa	**38 ± 2**	**a**
Mt. Sentinel	**29 ± 3**	**ab**
Clearwater New	**21 ± 1**	**abc**
Clearwater	7 ± 1	d
Kleinschmidt	**15 ± 4**	**c**
Blackfoot	**24 ± 5**	**bc**
Beckman WMA	4 ± 0	de
Central Grasslands	3 ± 0	e
Delbert Berntson	3 ± 1	e
B-B Ranch	3 ± 0	e
Bicentennial Prairie	3 ± 0	e

Note: Mean and standard error for soil P availability (Mehlich III) in ppm beneath *G. aristata* at field sites. These soils were used to provide AMF community inocula to plants in greenhouse experiment. Sites are listed in order from west to east (n = 120) and sites with the same letter are not statistically different in soil P availability according to Tukey's HSD at $\alpha = 0.05$. AMF community inoculum from sites in bold were classified as originating from soil high in P availability, while the remainder were classified as low P.

To evaluate the effects of the mycorrhizal fungi, five pots from each of the two P fertilization treatments were randomly assigned to the non-mycorrhizal treatment and received an autoclaved mock inoculum. To make the mock inoculum as similar to the live inocula as possible, subsamples of soil were taken from five samples from each field site. These subsamples were pooled so that each non-mycorrhizal control pot would receive a mock inoculum representative of all sites. The pooled soil sample was autoclaved at 121 °C for 60 min to kill all AMF (thus creating a non-mycorrhizal control) then divided into 50 mL subsamples to be added to pots.

To control for the effect of microbial community, a microbial wash was applied to the soil in each pot (Koide & Li, 1989). All equipment was sterilized prior to creating the wash. Ultra-pure water was autoclaved for 20 min at 121 °C (liquids cycle) to ensure sterility. Wash bottle and tools were sterilized via a 30-minute soak in 10% bleach. Subsamples of 5 g from approximately 80 of the 120 soil samples (6 to 10 samples per site) were pooled and filtered through a 35-µm sieve using sterilized water, which should have retained all hyphal

and plant material but allowed microbes to pass. Seven milliliters of this microbial wash was added to each pot so that all pots would have a uniform microbial community representative of all sites. This process minimized any differences in the microbial community among mycorrhizal treatments other than the composition of AMF.

2.3.3. Experiment set-up

Seeds of *Gaillardia aristata* (provenance: Colorado; Wind River Seed Company, Manderson, WY, USA) were germinated in covered trays filled with a 1:1 ratio of Sunshine Mix #1 (Sun Gro Horticulture, Agawam, MA, USA; autoclaved in the manner described above) and 100-mesh quartzite sand (Granusil #2040, Sterling Supply, Minneapolis, Minnesota, USA). Seeds were added and then covered with 0.6 to 1.25 cm of soil that was misted daily with distilled water to maintain moisture.

A hyphal in-growth core was buried in the soil of each pot because I originally planned to place radioactively labeled P in the core to quantify its movement by AM hyphae but was unable to do so. Ultimately, soil inside each core was used for phosphatase assays, since phosphatases found there were less likely to be produced by roots. The cores were built from nylon mesh with openings of 25 μm, a size which hyphae can penetrate but roots cannot. Thus, only fungal hyphae should have been able to access the soil within the core (Figure 2.2). For each core, a strip of plastic was used to create a ring with diameter of 6.35 cm around which a 20 × 23 cm piece of mesh was glued (Gorilla Glue Company, Cincinnati, OH, USA), ensuring that all seams were thoroughly sealed to avoid invasion of the core by plant roots.

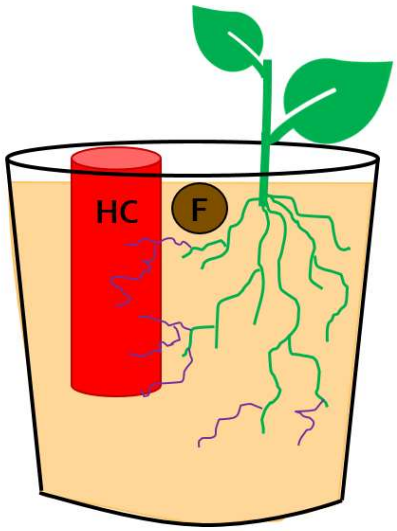

Figure 2.2. Set-up of pots for greenhouse experiment.
Note: Each pot contained one *Gaillardia aristata* plant (green) in a soil/sand mixture (tan), a hyphal in-growth core (HC) which hyphae but not roots could enter, and fungi (purple) sourced from field soil inocula (F) that were either high or low in soil P availability.

Pots were assembled at the beginning of August 2018. First, a hyphal in-growth core was positioned near the edge of a 16-cm diameter pot with the seam facing away from the plant. The pot and in-growth core were filled with either high or ambient P soil/sand mixture (as described above). Fifty milliliters of inoculum was placed in a depression in the center of the mixture. The mycorrhizal replicates received live soil inoculum from the field and the non-mycorrhizal controls received autoclaved mock inoculum. Two 12-d-old seedlings were transplanted from the germination tray to the pot with their roots directly in the inoculum. A 2.5-cm cap of soil/sand mixture was added above the inoculum to prevent cross-contamination of fungal spores, bringing the total volume of soil/sand mixture to 1.5 L. Each pot was later thinned to one seedling.

2.3.4. Greenhouse conditions

Pots were placed at random on greenhouse benches and their positions on the bench were re-randomized every 3 weeks to avoid effects of bench placement. Seedlings were misted until they were large enough to withstand watering and were shaded until they reached 4 weeks of age. Subsequently, they were exposed to ambient light plus greenhouse

high pressure sodium lighting with 600-watt bulbs which were automatically shut off when ambient light was greater than 200 W. Greenhouse lights were programmed to be on between 12 and 16 h d^{-1} unless ambient light was sufficient. A LI-COR Line Quantum Sensor (Lincoln, Nebraska, USA) measured 190 (morning) to 930 (afternoon) μmol $m^{-2}s^{-1}$ in August without supplemental lighting depending on weather conditions. A temperature range between 21 and 24 °C was maintained and relative humidity was set to 50%. Thrips were managed by wiping the pests off leaves with a 50% isopropyl alcohol solution.

2.3.5. Fertilization

Plants were fertilized with a modified Hoagland solution (Arnon & Hoagland 1940), which included a micronutrient solution (Appendix C). The solutions for the two fertilization treatments differed only in calcium dihydrogen phosphate content, which was the source of the phosphorus in the high P treatment. Plants in the high P treatment were fertilized with a solution that included 1 mL 1 M $Ca(H_2PO_4)_2$, while plants in the ambient P treatment were fertilized with a solution that contained an extra milliliter of deionized water. I chose calcium dihydrogen phosphate as a P fertilizer because the background soil was high in calcium (2726 ppm) so the difference between the two treatments was negligible, therefore minimizing the chance that differences in performance were due to increased calcium.

Plants were first fertilized 3 weeks after transplanting with 10 mL of full-strength fertilizer and then fertilized approximately every two weeks. The second fertilization of plants in the high P treatment consisted of 10 mL full strength fertilizer. Plants in the ambient P treatment received 1/8 strength solution at this time to help them establish successfully. The third fertilization was with 10 mL half strength Hoagland's solution (ambient P pots received no P) and subsequent fertilizations were with 20 mL of ¼ strength solution for plants in high P treatment only. The total amount of $Ca(H_2PO_4)_2$ applied to the soil of plants in the P fertilization treatment over the course of the experiment was 14.628 mg per pot.

2.3.6. Harvest and sample processing

After 418 d, plants were harvested. The aboveground biomass of each plant was clipped at the soil surface and dried at 60 °C to constant mass. Ten milliliters of soil was taken from the center of each in-growth core and stored at -20 °C until analyzed for phosphatase activity. At a distance of 2.5 cm from the in-growth core and from the plant, 100 mL of soil was taken from the center of the pot and air dried in a paper bag at room temperature before being used to estimate hyphal length in the soil. The root ball was removed from each pot and soil was gently loosened from roots, which were rinsed and patted dry. A total of 100 mg of root tissue was sampled from 3 random points on the root system and stored at -20 °C until DNA extraction. A root sample of 50 mg was taken from each plant and stored in 1% KOH (*w*/*v*) at 4 °C before being cleared and stained for root colonization quantification. The remainder of each root system was dried at 60 °C to constant mass and weighed. Dried roots and shoots were sent to Ward Laboratories (Kearney, Nebraska, USA) for analysis of P concentration. Plant tissue P was obtained by digesting a tissue sample with nitric acid, hydrochloric acid, and hydrogen peroxide and analyzed using ThermoFisher Scientific iCAP Inductively Coupled Plasma-Optical Emission Spectrometry (ICP-OES; Waltham, MA, USA). I used biomass and P concentration data to calculate P content. Assessments of root colonization and extraradical hyphae in soil were performed as described in Chapter 1.

2.3.7. Phosphatase assays

To compare the amount of phosphatase activity among treatments, assays modified from Dick *et al*. (1996) were performed. From each soil sample, 1 g was incubated at 37 °C for 1 hour with 0.2 mL of toluene, 4 mL of modified universal buffer (MUB), and 1 mL *p*-nitrophenyl phosphate (PNP) solution. The MUB was titrated to pH 6.5 for acid phosphatase and pH 11 for alkaline phosphatase. The 0.05 M PNP solution consisted of 0.840 g of disodium *p*-nitrophenyl phosphate tetrahydrate and 50 mL of MUB. After incubation, 4 mL of 0.5 M NaOH and 1 mL of $CaCl_2$ were added to each sample before filtering through

Whatman Grade 2 Filter Paper (Cytiva, Marlborough, MA, USA). The resulting liquid was diluted with distilled water to 2:5 and a subsample of approximately 1 mL was analyzed colorimetrically by spectrophotometer. The absorbance was recorded to determine the amount of *p*-nitrophenol produced by phosphatases from PNP. The same procedure was performed on controls to which the PNP solution was not added until after the $CaCl_2$ and NaOH and immediately before filtration, therefore preventing its hydrolysis to *p*-nitrophenol. Standards were used to calculate a calibration curve. Soil moisture for each sample, determined by weighing a subsample before and after drying, was used to calculate the dry weight of the sample. Phosphatase activity was determined via the equation:

$$\text{p-Nitrophenol } (\mu g\ g^{-1}\ dwt\ h^{-1}) = \frac{C \times v}{dwt \times SW \times t}$$

where *C* is the measured concentration of *p*-nitrophenol (μg mL^{-1} filtrate), *dwt* is the dry weight of 1 g moist soil, *v* is the total volume of the soil suspension in mL, *SW* is the weight of soil sample used (1 g), and *t* is the incubation time in hours. This equation corrects for the control and calculates the *p*-nitrophenol per mL of the filtrate by reference to the calibration curve.

2.3.8. Molecular analyses

Frozen root samples were ground and DNA was extracted as described in Chapter 1. Frozen soil samples collected during fieldwork and used as inoculum were homogenized dry for 10 min at 25 Hz on a TissueLyser II (QIAGEN, Germantown, Maryland, USA) according to manufacturer's instructions prior to DNA extraction. DNA was isolated from soils with the DNeasy PowerSoil Pro Kit (QIAGEN, Germantown, Maryland, USA) and was eluted once with 75 μL of TE buffer (10 mM Tris·Cl, 0.5 mM EDTA, pH 9.0). All eluates were stored at -20 °C until shipment on dry ice to MPG Ranch, where template DNA from soil and root samples, along with extraction negative controls, were amplified via polymerase chain reaction (PCR). Greenhouse root DNA extracts were amplified, sequenced, and processed with bioinformatics as described for field root and soil samples in Chapter 1.

A greenhouse root sample from the no P fertilization treatment group (GRCN-078) was omitted from further analysis due to having only two ITS2 sequences. For the ASV dataset, a field soil sample from the Kleinschmidt site (FSKL-062) was omitted from further analysis because it contained only 11 sequences.

Two non-mycorrhizal plants were removed from further analyses. One fertilized without P (GRNM-156) died during the experiment and was not replaced. A non-mycorrhizal plant fertilized with P (GRNM-152) became colonized by AMF; this plant was larger than others in its group, and I observed 5,004 sequences assigned to AMF in its roots.

2.3.9. Statistical analyses

Because two-way ANOVA showed there were no differences between *G. aristata* roots and shoots in biomass allocation among soil inoculum and P fertilization treatments ($F_{5,122} = 1.58$, $p = 0.17$), above- and belowground data were combined for statistical analyses. Differences in plant and fungal performance among treatments were tested by two-way ANOVA followed by Tukey's HSD (JMP®, Version Pro 15. SAS Institute Inc., Cary, NC, USA) on data that were transformed to meet assumptions of normality and homoscedasticity. Hyphal extent in the soil, plant P concentration and content were square root transformed. Acid phosphatase activity was $\log_{10}$-transformed. OTU richness was cube root transformed while OTU evenness was arcsine square root transformed. Plant biomass, AMF root colonization, alkaline phosphatase activity, and ASV evenness required no transformations to meet model assumptions.

A reduced model that included scorer showed an observer effect for the length of hyphae in the soil, so a single observer observed enough samples that I was able to run the analysis with only those data, although the results with that reduced sample size did not differ from those with the full dataset. On average, mycorrhizal plants had approximately five times more extraradical hyphae in the soil than non-mycorrhizal plants ($F_{2,33} = 9.23$, $p = 0.0007$). Non-mycorrhizal plants were excluded from the final model since I was

interested in differences among mycorrhizal plants in the inoculum origin and P fertilization treatments.

For root colonization, I ran a two-way ANOVA (JMP®, Version Pro 15. SAS Institute Inc., Cary, NC, USA) with a reduced model that included fertilization treatment, inoculum type, and their interaction, with observer as a blocking term. There was a significant observer effect, with some of the six observers counting more AMF structures across treatments than others ($F_{5,114} = 9.20$, $p < 0.0001$), but each observer scored samples from all treatments in equal numbers. One observer scored only a single sample and that observer and their observation were omitted from the analysis. Mycorrhizal *G. aristata* plants had roots that were more heavily colonized by AMF than those of non-mycorrhizal plants, which generally did not contain AMF structures ($F_{2,114} = 60.48$, $p < 0.0001$; Appendix E). Mean proportion of root length colonized for mycorrhizal plants was approximately 0.6; for non-mycorrhizal plants, only 0.03 of root length was colonized on average. Because I was interested in testing differences among mycorrhizal plants in the proportion of their root length colonized by AMF, non-mycorrhizal plants were excluded from the final model.

A chi square test (JMP®, Version Pro 15. SAS Institute Inc., Cary, NC, USA) was used to determine if taxonomic distribution of ASVs differed between treatments. Because I was constrained by the absence of a fertilization treatment in the field, I used a one-way ANOVA. A statistically significant test was followed by calculation of adjusted standardized residuals (Sharpe 2015) to identify which taxa differed between treatments.

Nonmetric multidimensional scaling (NMS) was performed in PC-ORD 7.08 (Wild Blueberry Media, Corvallis, OR, USA) to visualize AMF community composition across treatments. Ordinations were performed using the Sorenson distance measure, a random starting configuration, and 500 runs each with randomized and real data. ASV abundances were Hellinger-transformed in PC-ORD to downweight low-abundance sequences (Buttigieg & Ramette 2014). The optimal solution had three dimensions and a stress of 20.76. A one-way PERMANOVA was performed (PC-ORD 7.08, Wild Blueberry Media, Corvallis, OR, USA)

with communities from field soil inocula and greenhouse roots to determine how AMF communities changed from field inoculum to greenhouse and with and without P fertilization. A balanced design was achieved by randomly excluding half of the field soil communities from each field site. To assess the effects of inoculum origin and P fertilization in the greenhouse, a two-way PERMANOVA was performed (PC-ORD 7.08, Wild Blueberry Media, Corvallis, OR, USA) only with communities sampled from *G. aristata* roots grown in the greenhouse. The optimal three-dimensional solution for the corresponding NMS had a final stress of 20.28.

Diversity analyses were performed as described in Chapter 1. When analyzing ASV richness with field soil and greenhouse root samples, I was constrained by the absence of a fertilization treatment in the field, so I used a one-way ANOVA. Because ASV richness data did not meet assumptions about equal variance, a nonparametric Kruskal-Wallis test was performed followed by post hoc analysis with the Dunn test. I also performed two-way ANOVA that included only the soil inoculum and P fertilization treatments in the greenhouse.

2.4. Results

2.4.1. Effects of soil inoculum and P fertilization on growth and P status

Average biomass of *G. aristata* was affected by soil inoculum type ($F_{2,122}$ = 15.95, p < 0.0001) and fertilization treatment ($F_{1,122}$ = 27.30, p < 0.0001) and their interaction ($F_{2,122}$ = 9.96, p < 0.0001; Appendix E). Mean total biomass of mycorrhizal plants that were not fertilized with P did not differ statistically from mean total biomass of mycorrhizal and non-mycorrhizal plants that were fertilized with P (Figure 2.3A). Non-mycorrhizal plants that were fertilized without P were nearly 10 times smaller than plants in the other groups, which weighed over 10 g on average (Figure 2.3A). AMF communities from soils with high and low P availability resulted in plants that were the same size regardless of whether they were P fertilized or not. P fertilization only affected biomass for non-mycorrhizal plants, which were significantly smaller when they did not have access to additional P.

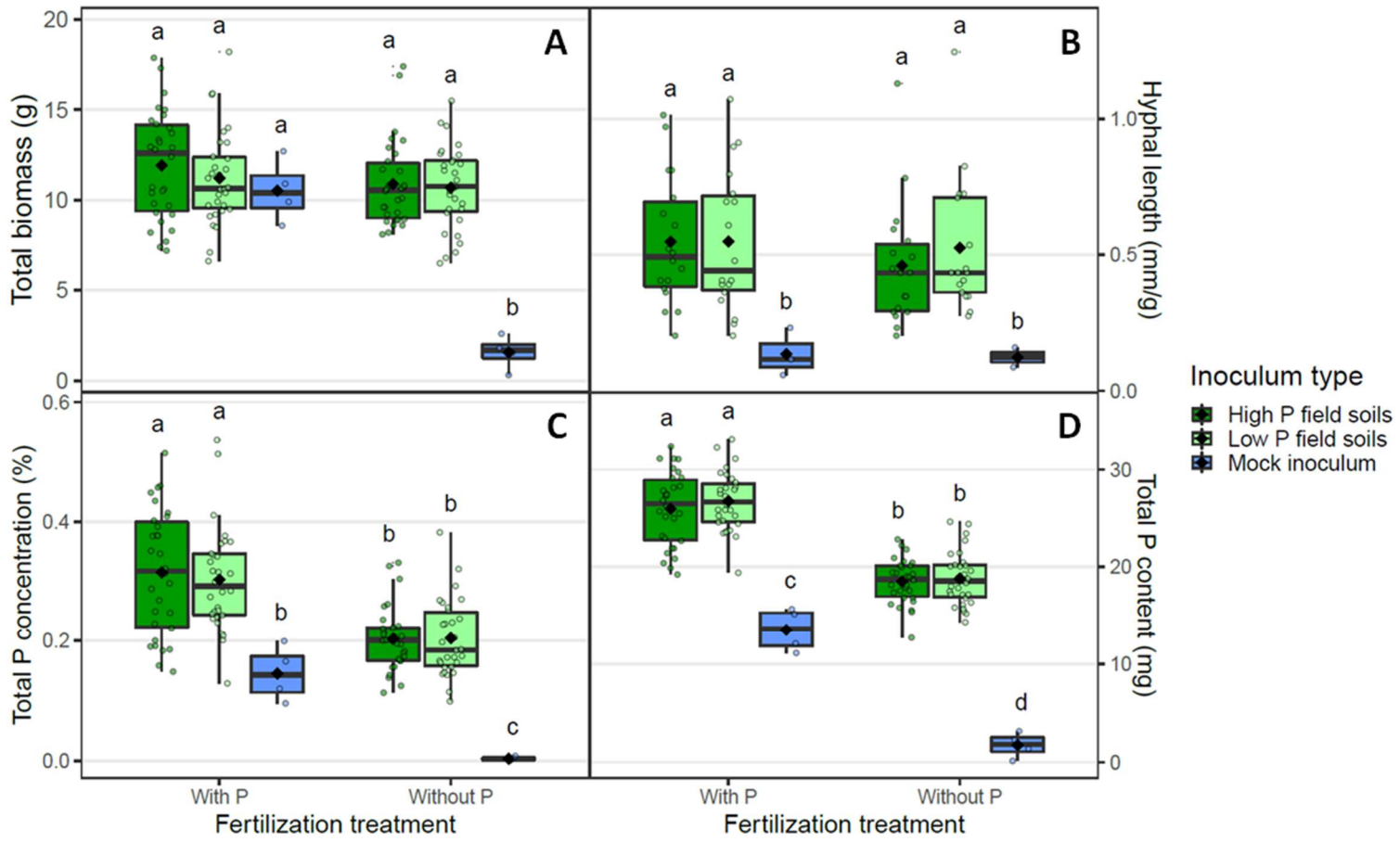

Figure 2.3. Total biomass (A), length of extraradical hyphae in soil (B), plant P concentration (C), and P content (D) for *Gaillardia aristata* plants.

Note: Seeds from Colorado were grown in the greenhouse in North Dakota, USA with or without P fertilization and without mycorrhizas (mock inoculum) or with mycorrhizas sourced from low or high P soils. Each point represents an observation, with n = 30 for each treatment, except for mock inoculum, where n = 4. The box and whisker plots display the median (center horizontal line) flanked by the 25th and 75th percentiles. The upper whisker extends from the 75th percentile line to the largest value no more than 1.5 * IQR from the 75th percentile (where IQR is the inter-quartile range, or distance between the first and third quartiles). The lower whisker extends from the 25th percentile line to the smallest value at most 1.5 * IQR. Black diamonds represent means. Means with the same letter were not statistically different by Tukey HSD.

Even though *G. aristata* plants in different fertilization and inoculum treatments had the same biomass, on average, plants fertilized with P had greater P concentration ($F_{1,122}$ = 77.76, $p < 0.0001$; Figure 2.3C) and P content ($F_{1,122}$ = 249.97, $p < 0.0001$; Figure 2.3D) on average than plants in ambient P regardless of whether their mycorrhizas were sourced from high or low P soils. Non-mycorrhizal plants fertilized with P achieved the same P concentration in their roots and shoots as mycorrhizal plants fertilized without P. P content in plants without mycorrhizas that received P fertilization was lower than mycorrhizal plants regardless of inoculum source and P fertilization treatment. Non-mycorrhizal plants that received no P fertilization had much less P in their tissues than plants in all other treatments.

Among mycorrhizal plants, the origin of the soil inoculum did not affect the extent of hyphae in the soil ($F_{1,31}$ = 0.009, p = 0.9259; Figure 2.3B). *G. aristata* inoculated with fungal communities from soils low in P availability did not differ in extent of hyphae present at the end of the experiment from those inoculated with communities from high P soils. Likewise, fertilization with P did not affect the length of hyphae associated with mycorrhizal plants ($F_{1,31}$ = 0.55, p = 0.4641; Figure 2.3B). On average, *G. aristata* plants fertilized with and without P had mycorrhizal partners that produced similar amounts of extraradical hyphae in the soil.

Origin of the soil inoculum did not influence the proportion of the root length colonized by AMF in mycorrhizal plants ($F_{1,113}$ = 0.09, p =0.7673; Appendix E). Similar levels of colonization were observed in plants inoculated with communities sourced from soils low and high in P. The roots of mycorrhizal *G. aristata* plants were similarly colonized by AMF regardless of P fertilization treatment ($F_{1,113}$ = 0.72, p = 0.3965; Appendix E). Fertilization with P did not change the proportion of the root length colonized by AMF. Soil inoculum had an effect on acid phosphatase activity ($F_{2,100}$ = 3.30, p = 0.04102; Appendix E). Acid phosphatase activity was higher in samples inoculated with soils low in P availability

than in non-mycorrhizal samples. Samples inoculated with soils high in P availability did not differ in acid phosphatase activity from the other two groups.

2.4.2. Greenhouse AMF communities differed from their field soil inocula

According to MaarjAM taxonomic assignment, three orders in the Glomeromycetes were represented in the dataset of 667 ASVs observed in greenhouse root communities (Table 2.2). For the four families represented, only one genus was observed in each family. Of the ASVs observed in the roots of *G. aristata*, 562 were assigned to *Glomus*, 49 to *Claroideoglomus*, seven to *Paraglomus*, six to *Diversispora*, and 43 were unknown Glomeromycetes. Rarefaction curves of ASV accumulation versus sample size did not approach an asymptote for either the field soil used to inoculate *G. aristata* in the greenhouse or the communities in the plants' roots, indicating that both groups were undersampled (Figure 2.5). Of the 667 AMF ASVs detected in roots of *G. aristata* in the greenhouse, 380 were also detected in the soil inoculum (Appendix E). There were 654 ASVs found in the inoculum but not observed in the roots, while 288 ASVs were only detected in the roots.

Table 2.2. Summary of ASVs observed in field soil inocula and greenhouse roots.

	Field soil inocula	Greenhouse root
Total sequences	318,890	400,868
Total ASVs	1,034	667
Mean # sequences per sample ± se	2,680 ± 79	3,397 ± 86
Orders represented	4	3
Families represented	9	4
ASVs assigned to species (including VTs)	537	372
ASVs only assigned to genus	442	253
ASVs only assigned to Glomeromycota	53	43

Note: Summary of AMF molecular datasets for field soil inocula and the *G. aristata* roots they were used to inoculate in the greenhouse. The MaarjAM database was used to assign taxonomy. Mean number of sequences per sample is reported with standard error.

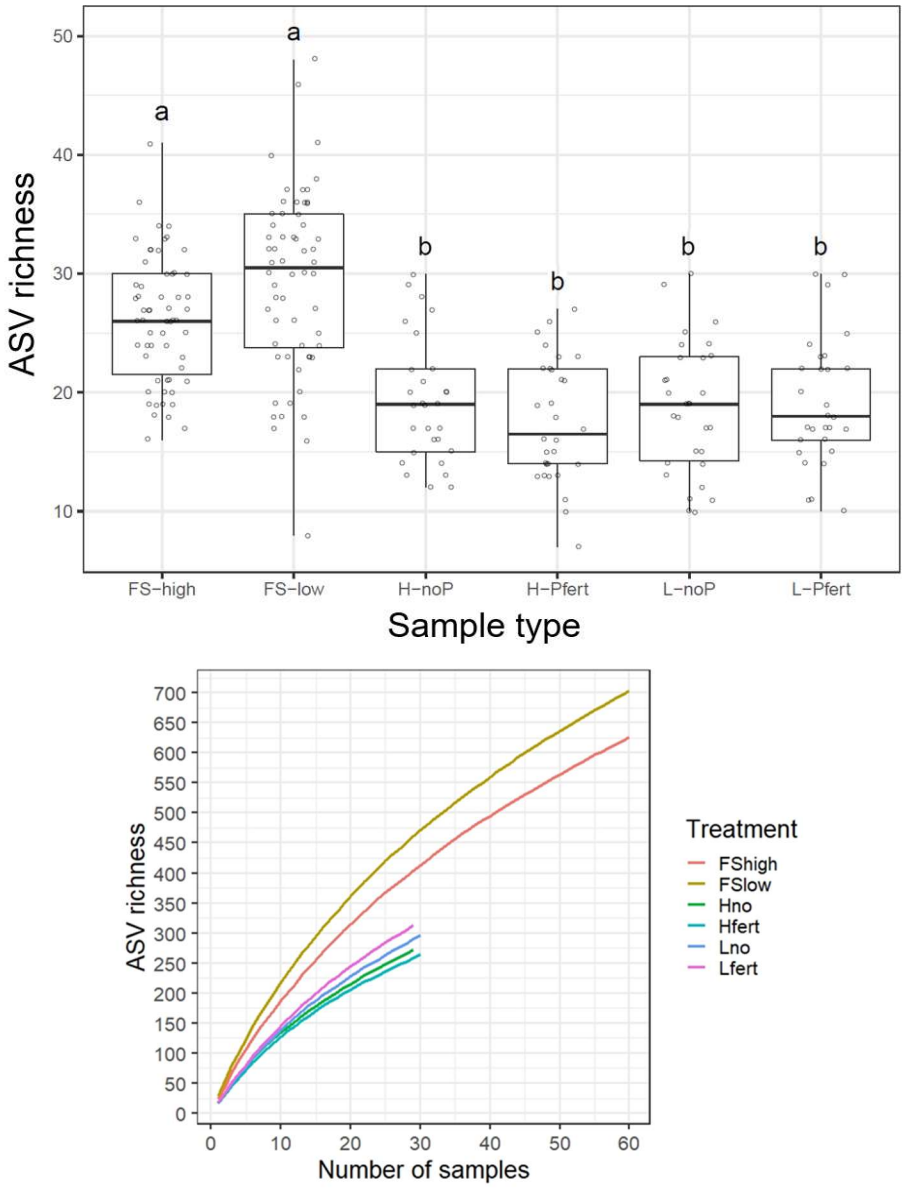

Figure 2.4. ASV richness of AMF communities by sample type (A) and randomized accumulation curves of samples at each site (B).
Note: (A) AMF communities were sampled from field soils (FS) that were either high (FS-high) or low (FS-low) in P availability and from roots of *G. aristata* grown in the greenhouse and inoculated with fungal communities from sites low (L) or high (H) in soil P availability and fertilized with (Pfert) or without (noP). Each point represents the number of ASVs observed in one sample, with n = 60 for field soil groups and n = 30 for greenhouse treatments. The box and whisker plots display the median (center horizontal line) flanked by the 25th and 75th percentiles. The upper whisker extends from the 75th percentile line to the largest value no greater than 1.5 * IQR from the 75th percentile (where IQR is the inter-quartile range, or distance between the first and third quartiles). The lower whisker extends from the 25th percentile line to the smallest value at most 1.5 * IQR. Groups with the same letter were not statistically different by Tukey HSD. (B) Each curve represents the cumulative ASV richness of AMF taxa observed based on the number of samples.

There was an effect of sample type on ASV richness (Figure 2.4A). Field soil inocula had greater richness of mycorrhizal fungi than greenhouse communities at the end of the experiment ($H_{5,231} = 93.26$, $p < 0.0001$). Phosphorus fertilization ($F_{1,114} = 0.40$, $p = 0.5278$) and soil P availability of the inoculum origin ($F_{1,114} = 0.28$, $p = 0.5989$) did not affect how many ASVs were found in each greenhouse AMF community (Figure 2.4A). Evenness did not differ by sample type ($F_{5,231} = 29.33$, $p = 0.6883$; Appendix E). While there was variation within groups, the mean evenness of all groups, both greenhouse AMF communities and the field soil communities with which they were inoculated, was approximately 0.65 according to Pielou's index. Like those of ASVs, rarefaction curves of OTU accumulation versus sample size did not reach an asymptote, indicating undersampling (Appendix E).

2.4.3. Soil inoculum origin, but not P fertilization, shifted AMF community composition in the greenhouse

AMF communities from soils low and high in P availability differed, and communities of AMF associated with the roots of *G. aristata* in the greenhouse were different from their field soil inocula ($F_{5,168} = 3.59$, $p = 0.0002$; Table 2.3). Greenhouse root communities in all four treatments shifted away from field communities sourced from high P soils along Axis 1 and also shifted away from all field soil communities along Axis 2.

Table 2.3. Pairwise comparisons of AMF community composition from PERMANOVA.

Level 1	Level 2	t	p
FS-low	FS-high	2.2736	0.000200 *
FS-low	L-noP	1.8966	0.000200 *
FS-low	L-Pfert	1.8922	0.000200 *
FS-low	H-Pfert	1.9348	0.000200 *
FS-low	H-noP	2.2206	0.000200 *
FS-high	L-noP	2.4636	0.000200 *
FS-high	L-Pfert	2.5101	0.000200 *
FS-high	H-Pfert	2.2444	0.000200 *
FS-high	H-noP	2.4408	0.000200 *
L-noP	L-Pfert	0.89127	0.778000
L-noP	H-Pfert	1.3172	0.012400 *
L-noP	H-noP	1.3588	0.007200 *
L-Pfert	H-Pfert	1.5307	0.000200 *
L-Pfert	H-noP	1.6201	0.000200 *
H-Pfert	H-noP	1.0144	0.418800

Note: PERMANOVA test comparing AMF communities sampled from field soils low (FS-low) or high (FS-high) in P availability and from roots of *Gaillardia aristata* grown in the greenhouse and inoculated with fungal communities from sites low (L) or high (H) in soil P availability and fertilized with (Pfert) or without (noP) P. Pairwise comparisons made between Level 1 and Level 2 in each row of the table. Rows marked with an asterisk display levels with statistically different AMF community compositions.

The origin of the soil inoculum affected the composition of AMF communities associated with *G. aristata* in the greenhouse ($F_{1,112} = 3.44$, $p = 0.0002$; Figure 2.5). There was no effect of P fertilization on AMF community composition ($F_{1,112} = 1.04$, $p = 0.39920$; Figure 2.5). AMF communities present in the field soil inocula differed based on whether they came from soils high or low in soil P availability. When *G. aristata* was inoculated with these communities in the greenhouse, P fertilization failed to cause them to converge and after 14 months, greenhouse communities still differed based on the origin of their soil inocula. Overall, differences observed in the field were retained in the greenhouse regardless of fertilization, with the origin of the AMF inoculum proving to be more for structuring greenhouse AMF communities than whether those communities were fertilized with or without P.

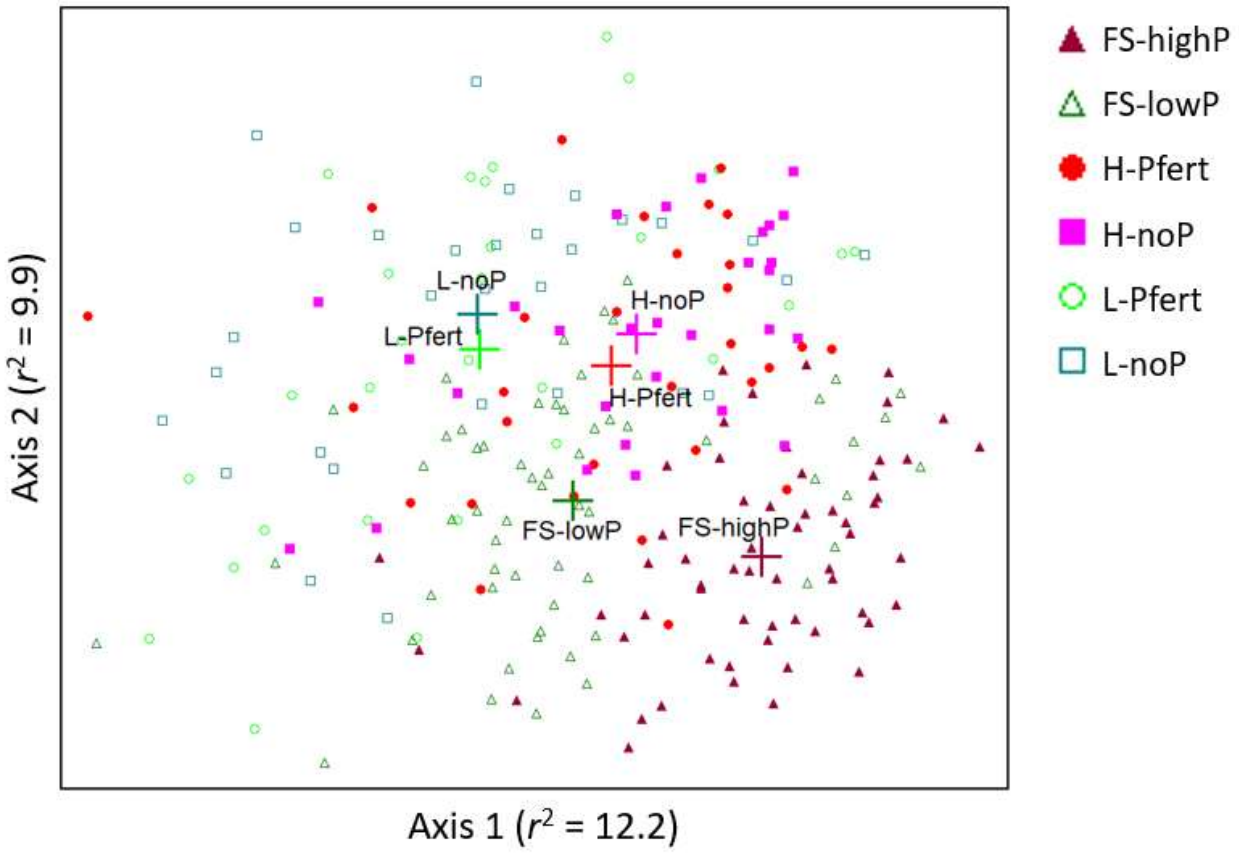

Figure 2.5. NMS visualization of field soil and greenhouse root AMF communities.
Note: AMF communities were sampled from field soils (FS) that were either high (FS-high) or low (FS-low) in P availability and from roots of *G. aristata* grown in the greenhouse and inoculated with fungal communities from sites low (L) or high (H) in soil P availability and fertilized with (Pfert) or without (noP) P. Each point represents one community, with more similar communities appearing more closely together. Ordination was performed on Hellinger-transformed ASV abundance table. R-square values on axes represent percentage of the variation in the original dataset was captured by the ordination. The optimal solution had three dimensions and a stress of 20.76.

Glomus taxa were the most prevalent in both field soil and greenhouse root communities (Figure 2.6). In the field soil inocula, the relative abundance of *Glomus* taxa in AMF communities from soils with high P availability was under 50%. After these communities formed mycorrhizas with *G. aristata* roots in the greenhouse, *Glomus* species accounted for approximately 90% of the community when soils were fertilized with P and 92% when fertilized without P. Likewise, AMF communities in inocula from soils with low P availability were composed of over 75% *Glomus* taxa, while in greenhouse roots of *G.*

aristata the relative abundance of *Glomus* was about 98% and 97% when fertilized with and without P, respectively.

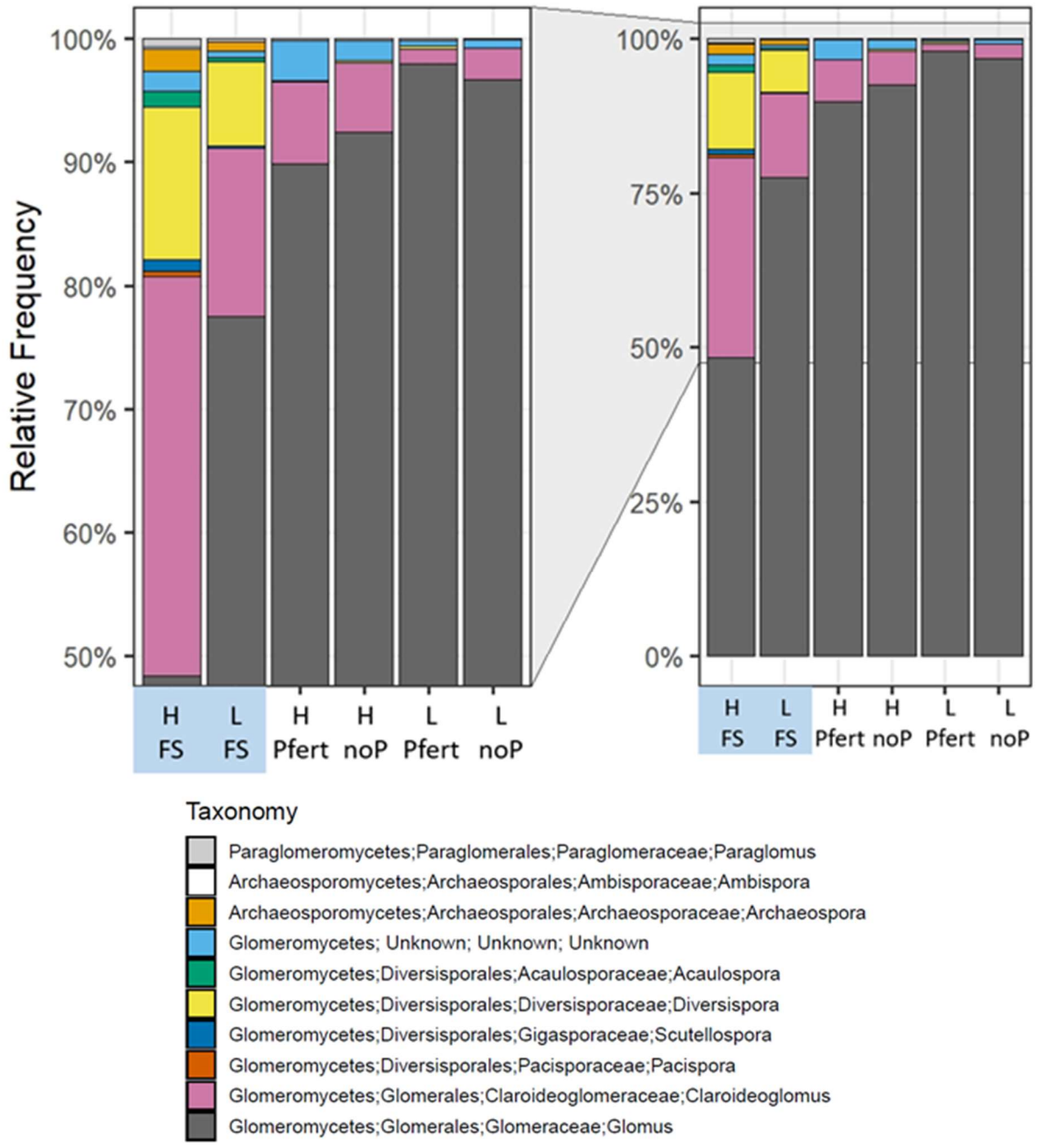

Figure 2.6. Summary of taxonomic distribution of AMF ASVs by inoculum origin and P fertilization treatment.
Note: Taxonomic distribution of ASVs, with the graphic on the left excluding the lower half of the bar plots which are uniformly *Glomus* in the right-hand plot. Bars labeled in blue (n = 60) are field soil communities (originating from soils either high (H) or low (L) in P) used as inocula for *G. aristata* in the greenhouse, whose root communities were fertilized with (Pfert) or without (noP) P (n = 30). ASVs were assigned to taxonomy using the MaarjAM database.

The relative frequency of ASVs varied by setting and treatment (χ^2 = 170507.7, *df* = 45, $p < 0.0001$). *Diversispora* was underrepresented in *G. aristata* roots in the greenhouse relative to the field soil inocula. AMF communities in inocula from field sites with high P availability and the greenhouse root communities that originated from them had a higher proportion of *Claroideoglomus* taxa than AMF communities from low P field soils and the greenhouse root communities that were inoculated with the field communities from low P soils. While *Ambispora*, *Archaeospora*, *Acaulospora*, *Scutellospora*, and *Pacispora* were present in the soil inocula at the start of the experiment, none of the ASVs detected in roots at the end of the experiment were assigned to these genera (Figure 2.6).

2.5. Discussion

Conducting a greenhouse experiment allowed me to examine the importance of AMF for *G. aristata* and the influence of P availability on AMF community composition and performance of plants with and without AMF. Being mycorrhizal improved plant performance in low P soil availability and improved plant P status. AMF communities were able to provision P similarly, regardless of whether they originated from soils low or high in P availability. P fertilization did not shape AMF community composition in the greenhouse but did allow non-mycorrhizal plants to achieve similar biomass to mycorrhizal plants.

2.5.1. Mycorrhizas were important for performance of *G. aristata* in low soil P availability

Mycorrhizas enabled plants fertilized without P to grow as large as P fertilized plants. Because P is an essential plant nutrient, it would be reasonable to predict that all plants fertilized with P would be larger than those fertilized without P. I did observe that effect for non-mycorrhizal plants: those fertilized without P were barely able to grow at all, while non-mycorrhizal plants fertilized with P were the same size as mycorrhizal plants, which suggests that P limitation is responsible for this difference in growth. However, when plants were mycorrhizal, those fertilized without P were the same size as plants that received additional P in their fertilizer, suggesting that mycorrhizas allowed *G. aristata* to

compensate for differences in soil P availability. I expected that plants with access to more P would grow larger, although there is evidence that this growth response does not always occur (Smith 2003).

Plants with inocula from soils high or low in P availability were able to obtain P to the same extent when associating with these communities. However, even though these plants were similar in size, mycorrhizal plants that were fertilized with P had better P status than mycorrhizal plants fertilized without P. This means that even though these plants appeared to be performing the same based on biomass, their P status shows that greater soil P availability leads to better P status for *G. aristata*. Interestingly, non-mycorrhizal plants fertilized with P had similar P concentration as mycorrhizal plants that didn't have access to additional P, which provides clear evidence for importance of mycorrhizas in alleviating P limitation in this plant species. These results provide strong evidence that AMF are important for P uptake in this plant. In addition to the benefits of being mycorrhizal, however, they also illustrate the costs. Under the same growing conditions, the mycorrhizal plants took up more P than their non-mycorrhizal counterparts, while achieving identical biomass. The additional photosynthesis they achieved as a result of increased P uptake was likely used for fungal biomass, as demonstrated by greater extent of extraradical hyphae, instead of their own biomass. In this way, the mycorrhizal plant benefitted from improved P uptake but also had less carbon to allocate to its own growth.

In the field, P content increased with *G. aristata* biomass while P concentration was fixed, but I was comparing plants with unknown histories and different environments. In contrast to the patterns seen in the field, when growing seeds from the same source under the same greenhouse conditions, I observed differences in P concentration. Based on those differences, I would have expected biomass to be greater in plants with better P status but the absence of this effect may be due to carbon costs, as described in the previous paragraph.

Greater hyphal length in the soil has been linked to greater plant growth (Jakobsen *et al*. 1992; Sawers *et al*. 2017). Mycorrhizal plants had approximately five times more hyphae in the soil than non-mycorrhizal plants. However, contrary to my prediction, *G. aristata* individuals inoculated with fungal communities from soils low in P availability did not have greater length of hyphae present at the end of the experiment than individuals inoculated with communities from soils high in P availability. In contrast, Antunes *et al*. (2012) did observe greater extraradical hyphae produced by communities structured under low nutrient conditions.

If the primary role of AMF hyphae in the soil is to acquire and transport P to the host, I would have expected fertilization with P to reduce hyphal length. However, fertilization with P, like soil inoculum origin, did not affect the length of hyphae present. It is possible that all plants were P limited in the greenhouse and therefore all plants were investing sufficiently in their mycorrhizas that those mycorrhizas produced similar levels of hyphae to scavenge the soil for P. However, extraradical hyphae have functions other than providing P and may have been growing to find others hosts. Similar levels of root colonization by AMF across all mycorrhizal treatments (Appendix E) provides additional evidence that these plants were investing equally in their mycorrhizas.

For many plant species, the extent to which they benefit from mycorrhizas is unclear, and conflicting evidence in the literature can be found for *G. aristata*. Maron *et al*. (2011) reported a mean mycorrhizal responsiveness of -7%, indicating that this species grew less well when colonized. Porter (2014) reported that AMF inoculation did not affect the growth of *G. aristata* raised for restoration. Conversely, this species has been observed to display high mycorrhizal responsiveness (Ylva Lekberg, unpublished research) which my results in the greenhouse support. These conflicting findings may be due to differing soil P availabilities or other environmental conditions. Further, AMF can provide benefits other than P provisioning to plants, such as pathogen protection, and these may not always result in greater biomass (Newsham *et al*. 1995; Pozo & Azcón-Aguilar 2007).

Mean phosphatase activity reported in the literature is 617 mg *p*-nitrophenol kg^{-1} soil h^{-1} for acid phosphatases and 122 mg *p*-nitrophenol kg^{-1} soil h^{-1} for alkaline phosphatases (Dick 1994). While the mean values I observed for alkaline phosphatase activity, ranging from 70 to 95 mg *p*-nitrophenol kg^{-1} soil h^{-1}, were close to those reported in the literature, the mean acid phosphatase activity here was approximately 10 times lower than that seen in the literature. Acid phosphatase activity inside hyphal in-growth cores did not differ between soils fertilized with or without P. Addition of phosphate fertilizer has been shown to suppress phosphatase activity (Dick 1994), so I expected to observe differences between soils fertilized with and without P. Specifically, I expected to observe lower phosphatase activity in soils fertilized with P than in those fertilized without P. However, the P-fixing nature of the background soil could explain the lack of this phenomenon. When calcium dihydrogen phosphate was added to a soil sample, Mehlich III P availability was similar to that of a sample that received no P fertilizer.

I intended for the plants in the P fertilization treatment to receive sufficient P to alleviate any P limitation, but because the background soil used in the greenhouse was highly P-fixing, it is possible that I was unable to achieve this goal. However, I have some evidence that P fertilization was effective, such as biomass differences between non-mycorrhizal plants fertilized with and without P, differences in P status between plants fertilized with and without P, and the equal biomass achieved by fertilized non-mycorrhizal and fertilized mycorrhizal plants.

Better P status in mycorrhizal *G. aristata* without increases in biomass may be interpreted as luxury P consumption (Chapin 1980). *Gaillardia aristata* is a perennial plant (USDA PLANTS Database https://plants.sc.egov.usda.gov/home/plantProfile?symbol=GAAR), and the absorption and storage of excess P would be advantageous for future seasons of growth. However, the pattern I observed could also be attributed to the carbon cost of being mycorrhizal. Biological market theory, which seeks to explain biotic interactions in economic terms, may

be a useful lens through which to understand the AM symbiosis. The theory states that the exchange of resources between partners in a mutualism can be explained by a cost/benefit framework in which partners compete, invest and trade strategically (Noë & Hammerstein 1995). In this view, plants and fungi must navigate a varying exchange rate that depends on supply and demand of the resources being traded (Noë & Hammerstein 1995). From a biological market perspective, the cost of paying a plant's fungal partners for P would result in less carbon to allocate towards biomass, which also concurs with the effect I observed.

2.5.2. Little evidence for an effect of inoculum origin on P provisioning

Acid phosphatase activity inside hyphal in-growth cores was higher than non-mycorrhizal controls when AMF communities were sourced from soils low in P availability. Because a microbial wash was applied to all samples, microbial communities should be similar across treatments, so this effect is likely attributable to AMF and suggests that AMF communities sourced from soils low in P availability produce were better at producing phosphatases. This was the only evidence I found in support of a legacy effect of inoculum origin.

For mycorrhizal plants, origin of inoculum did not affect biomass. Plants associating with AMF from soils low or high in P availability were able to obtain P to the same extent. This shows that regardless of P history, AMF can be efficient at taking up P when this nutrient is limiting. If legacy effects were important, I would have expected plants inoculated with AMF from soils low in P availability to grow larger or have a higher concentration of P than plants inoculated with AMF from soils high in P availability. I did not observe this effect and therefore found no evidence for a soil P legacy. Antunes *et al.* (2012) also found no evidence that nutrient-deficient soil conditions selected for increased capacity of AMF to provision that nutrient to their host.

On average, plant P concentration was higher in plants fertilized with P than in plants fertilized without P, regardless of the soil P availability of their soil inoculum origin, which suggests that the two inoculum types are equally effective at provisioning P and are not

constrained by the environment from which they originated. Because Glomus was the predominant taxon associating with G. aristata across soil inoculum and P fertilization treatments, it was perhaps not surprising that there was no inoculum effect observed.

Under legacy effects, I would have expected plants with AMF from soils of low P availability to have more P in their tissues than those from high P since their fungal partners would be more efficient at obtaining P, which I did not find. Interestingly, non-mycorrhizal *G. aristata* fertilized with P had the same mean P concentration as mycorrhizal plants fertilized without P, but these plants had lower mean P concentration than mycorrhizal plants fertilized with P, indicating the importance of P fertilization for P status. Even though non-mycorrhizal plants fertilized with P were the same size as mycorrhizal plants, which by appearance would indicate successful alleviation of P limitation, they had lower concentration and content of this essential plant nutrient. In fact, despite similar sizes, mycorrhizal plants have better P status than non-mycorrhizal plants.

In contrast to what I observed, some previous studies on soil P legacies found that AMF from soils of low P availability were associated with greater P uptake than those from high P soils (Louis & Lim 1988; Boerner 1990). However, these studies focused on isolates of a single AMF species instead of an assemblage of species. Similar patterns of legacy effects have been reported for drought stress, again using isolates of AMF (Stahl & Smith 1984). Paymaneh *et al*. (2019) investigated whether AMF from soils of varying salinities would improve seedling tolerance to salinity or drought when these conditions were manipulated in the greenhouse. Similar to my findings, they saw no evidence of a legacy effect in terms of ability to improve plant nutrient status and found no relationship between degree of mycorrhiza formation (in the form of root colonization) and amount of stress tolerance conferred (in the form of plant nutrient uptake).

Johnson *et al*. (2010) grew ecotypes of *Andropogon gerardii* from P-limited and N-limited prairies in combinations of local and distant soils and AMF communities from whole soil inocula. Contrary to what I observed, they found that AMF differed in function and that

communities from low N environments were better at sourcing N. AMF community composition was not characterized so it is unknown whether functional differences were due to shifts in community composition.

2.5.3. AMF community composition differed by inoculum origin but not P fertilization

Greenhouse communities of AMF associated with *G. aristata* roots were less diverse than the soil inocula. Not only was there lower ASV richness, but there were also fewer orders and families represented in *G. aristata* roots. Because the only AMF species present in the roots could be those that were introduced via the inoculum, and because it is unlikely all AMF species present in the soil would thrive in *G. aristata* roots and the greenhouse environment due to environmental filtering of AMF communities, it makes sense for less diversity to be observed in greenhouse root communities. However, greater OTU richness was observed in these samples than in the field soil inocula.

When categorized by their soil P availability, communities sampled from field soils and used as inocula were distinct from each other in their composition, and those patterns persisted in the greenhouse – AMF communities present in *G. aristata* roots in the greenhouse were also distinct based on the origin of their inocula. It is not surprising that AMF communities in *G. aristata* roots at the end of the experiment reflected the origin of their inoculum, since the AMF species that colonized roots in the greenhouse should be a subset of the species that were in the inocula.

Root communities of *G. aristata* in the greenhouse shifted from those in their inocula. This may have been due to a greenhouse effect, where the environmental conditions in the greenhouse shape community composition. Because all communities shifted in a similar direction along Axis 2 of the NMS in Figure 2.6, this explanation seems likely. If P availability influences AMF communities, then I should have observed shifts in community composition between those fertilized with and without P. However, while P fertilization affected plant P status, this effect does not seem attributable to a shift in AMF

community composition While other studies have observed shifts in AMF community composition with addition of P fertilizer (Dueñas *et al*. 2020), I saw no such effect. Composition of AMF communities fertilized with and without P was very similar and these communities grew similar amounts of extraradical hyphae and resulted in plants of similar size but communities that received additional P provisioned more P to their hosts, resulting in plants with better P status than those that received no additional P via fertilization.

Glomus was the most abundant AMF taxon in both field soils and *G. aristata* root communities sampled in the greenhouse. In temperate work, it is typical for AMF communities to be dominated by this genus (Zhao *et al*. 2017) but the reason for this phenomenon is unclear. It is possible species belonging to this taxon are the most beneficial to their plant hosts. For example, perhaps they are more cooperative (Kiers *et al*. 2011). Alternatively, they may be the most successful generalists, adapting to a range of environmental conditions (Bever *et al*. 2009). It may also be the case that *Glomus* has more nuclei per unit of hyphal length and so is most easy to detect using PCR on DNA (Corradi *et al*. 2007).

When examining the taxonomic distribution of AMF communities, the clearest differences were between field soil inocula and root communities in the greenhouse. Notably, *Glomus* species became more dominant after field soil communities formed mycorrhizas with *G. aristata*, regardless of P fertilization or field soil P availability. After these communities formed mycorrhizas with *G. aristata* roots in the greenhouse, *Glomus* species accounted for approximately 90% of the community when soils were fertilized with P and 92% when fertilized without P. Perhaps *G. aristata* preferentially associates with *Glomus*, or maybe the other sequences detected in the inocula were from fungi that were dormant or dead. Given the dominance of *Glomus* in *G. aristata* roots sampled in the field, the latter explanation is unlikely.

2.5.4. Limitations and future directions

A few limitations impacted this work. Species accumulation curves indicated that I may not have reached sufficient sampling depths for all treatments. Treatments where an asymptote was not reached may not have been sampled enough to adequately represent AMF diversity, which limited the conclusions I could draw about rare taxa. Consequently, I restricted my discussion to the most frequently detected taxa. More importantly, sampling effort was similar across treatments in the greenhouse experiment which allowed me to make comparisons across treatments.

The annealing temperature used for PCR was not high enough to be specific for AMF, which allowed primers to bind nonspecifically to the template, and I had many *G. aristata* sequences in the bioinformatics pipeline products. When primers anneal to plant and non-AM fungal sequences in early steps of amplification, there are fewer primers available for AMF sequences to bind and those non-target sequences will multiply exponentially over the course of PCR. However, using a low annealing temperature allows fungi which don't match the primers to be detected, perhaps resulting in a more complete representation of the AMF community.

Harvesting the plants sooner may have prevented them from becoming pot bound, with roots filling the pot and having no space for further growth. The dense masses of roots that encircled the insides of greenhouse pots with little soil to be seen indicated that belowground resources may have been limited which could alter interactions within the mutualism. It also may have limited the extent to which plants could grow aboveground, which may have implications for relationships in biomass among plants in different treatments. All non-mycorrhizal plants were smaller than those with mycorrhizas at the beginning of the experiment (Appendix E), and this pattern may have persisted if space had not been an issue.

An earlier harvest may have resulted in more obvious differences between sample types. For example, at the beginning of the experiment, all non-mycorrhizal plants were

smaller than those with mycorrhizas regardless of P fertilization (Appendix E). On the other hand, when a perennial plant is harvested after only a few months of growth, an even smaller portion of its life is being examined than the portion I observed. A related limitation is that AMF communities were characterized at the end of the experiment and changes in community composition over time were not captured.

Future work should seek to replicate these results using seed from multiple *G. aristata* populations and with soils of contrasting P availability from Montana and Minnesota. Conducting a common garden experiment with seed and soil, not just AMF, from multiple sites that vary in nutrient availability and growing them in all combinations of local and distant would allow for exploration of legacy effects and local adaptation for plants and AMF. Using isotope labeling to more precisely quantify P, C, and N uptake and exchange within mycorrhizas should provide deeper insights into exchange rates, costs and benefits to being mycorrhizal, and the legitimacy of biological market theory in soil ecosystems.

2.5.5. Conclusions

This experiment demonstrated that mycorrhizas and P are crucial to the performance of *G. aristata*. Mutualism with AMF improved plant P status and enhanced plant growth in low soil P availability. When grown without mycorrhizas, P fertilization alleviated P limitation and allowed plants to obtain biomass similar to plants in mycorrhizal treatments. Similarly, when fertilized without P, being mycorrhizal alleviated P limitation and enabled plants to grow to the same size as plants fertilized with P. While P fertilization was important for biomass accumulation (when non-mycorrhizal), P content, and P concentration in *G. aristata*, it did not shape AMF community composition. Instead, plants associated with communities of similar composition in different soil P environments differed in their ability to accumulate biomass.

Overall, differences in AMF community composition observed in the field were retained in the greenhouse regardless of fertilization, with the origin of AMF inocula proving to be more important for structuring greenhouse AMF communities than whether those

communities were fertilized with or without P. Origin of inocula did not affect biomass accumulation or P status in *G. aristata* or the extent of extraradical hyphae associated with the plant but did have effects on root community composition. As shown in Chapter 1, environmental conditions structure AMF communities but when those communities are exposed to foreign soil environments, these legacies seem not to constrain the functioning of AMF and may not be as important for mycorrhizas and performance as the new context in which the communities are placed.

2.6. References

Antunes, P. M., Lehmann, A., Hart, M. M., Baumecker, M. & Rillig, M. C. Long-term effects of soil nutrient deficiency on arbuscular mycorrhizal communities. *Functional Ecology* **26**, 532-540 (2012).

Argüello, A., O'Brien, M. J., van der Heijden, M. G., Wiemken, A., Schmid, B., & Niklaus, P. A. Options of partners improve carbon for phosphorus trade in the arbuscular mycorrhizal mutualism. *Ecology Letters* **19**, 648-656 (2016).

Arnon, D. I., & Hoagland, D. R. Crop production in artificial culture solutions and in soils with special reference to factors influencing yields and absorption of inorganic nutrients. *Soil Science* **50**, 463-485 (1940).

Bauer, J. T., Koziol, L., & Bever, J. D. Local adaptation of mycorrhizae communities changes plant community composition and increases aboveground productivity. *Oecologia* **192**, 735-744 (2020).

Beule, L. & Karlovsky, P. Improved normalization of species count data in ecology by scaling with ranked subsampling (SRS): application to microbial communities. *PeerJ* **8**, e9593 (2020).

Bever, J. D., Richardson, S. C., Lawrence, B. M., Holmes, J., & Watson, M. Preferential allocation to beneficial symbiont with spatial structure maintains mycorrhizal mutualism. *Ecol Lett* **12**, 13–21 (2009).

Boerner, R. E. J. Role of mycorrhizal fungus origin in growth and nutrient uptake by *Geranium robertianum*. *American Journal of Botany* **77**, 483–489 (1990).

Chapin, F.S. III (1980) The mineral nutrition of wild plants. *Annual Review of Ecology and Systematics*, **11**, 233–260.

Corbin, J. D. & D'Antonio, C. M. Gone but not forgotten? Invasive plants' legacies on community and ecosystem properties. *Invasive Plant Science Management* **5**, 117–124 (2012).

Corradi, N., Croll, D., Colard, A., Kuhn, G., Ehinger, M., & Sanders, I. R. Gene copy number polymorphisms in an arbuscular mycorrhizal fungal population. *Applied and environmental microbiology* **73**, 366–369 (2007).

Dick, R. P. Soil Enzyme Activities as Indicators of Soil Quality. in *SSSA Special Publications* (eds. Doran, J. W., Coleman, D. C., Bezdicek, D. F. & Stewart, B. A.) 107–124 (Soil Science Society of America and American Society of Agronomy, 1994).

Dick, R. P., Breakwell, D. P. & Turco, R. F. Soil Enzyme Activities and Biodiversity Measurements as Integrative Microbiological Indicators. in *SSSA Special Publications* (eds. Doran, J. W. & Jones, A. J.) 247–271 (Soil Science Society of America, 1996).

Dueñas, J. F., Camenzind, T., Roy, J., Hempel, S., Homeier, J., Pablo Suárez, J. & Rillig, M.C. Moderate phosphorus additions consistently affect community composition of arbuscular mycorrhizal fungi in tropical montane forests in southern Ecuador. *New Phytologist* **227**, 1505-1518 (2020).

Jakobsen, I., Abbott, L. K. & Robson, A. D. External hyphae of vesicular-arbuscular mycorrhizal fungi associated with *Trifolium subterraneum* L. 2. Hyphal transport of 32P over defined distances. *New Phytologist* **120**, 509–516 (1992).

Ji, B. & Bever, J. D. Plant preferential allocation and fungal reward decline with soil phosphorus: implications for mycorrhizal mutualism. *Ecosphere* **7**, e01256 (2016).

Johnson, N. C. Can fertilization of soil select less mutualistic mycorrhizae? *Ecological Applications* **3**, 749–757 (1993).

Johnson, N. C., Wilson, G. W. T., Bowker, M. A., Wilson, J. A. & Miller, R. M. Resource limitation is a driver of local adaptation in mycorrhizal symbioses. *Proceedings of the National Academy of Sciences* **107**, 2093-2098 (2010).

Joner, E. J. & Johansen, A. Phosphatase activity of external hyphae of two arbuscular mycorrhizal fungi. *Mycological Research* **104**, 81–86 (2000).

Kardol, P., Cornips, N. J., van Kempen, M. M. L., Bakx-Schotman, J. M. T. & van der Putten, W. H. Microbe-mediated plant-soil feedback causes historical contingency effects in plant community assembly. *Ecological Monographs* **77**, 147–162 (2007).

Kiers, E. T., Duhamel, M., Beesetty, Y., Mensah, J. A., Franken, O., Verbruggen, E., Fellbaum, C. R., Kowalchuk, G. A., Hart, M. M., Bago, A., Palmer, T. M., West, S. A., Vandenkoornhuyse, P., Jansa, J., & Bücking, H. Reciprocal rewards stabilize cooperation in the mycorrhizal symbiosis. *Science* **333**, 880–882 (2011).

Koide, R. T. & Kabir, Z. Extraradical hyphae of the mycorrhizal fungus *Glomus intraradices* can hydrolyse organic phosphate. *New Phytologist* **148**, 511–517 (2000).

Koide, R. T. & Li, M. Appropriate controls for vesicular-arbuscular mycorrhiza research. *New Phytologist* **111**, 35–44 (1989).

Lekberg, Y. *et al.* More bang for the buck? Can arbuscular mycorrhizal fungal communities be characterized adequately alongside other fungi using general fungal primers? *New Phytologist* **220**, 971–976 (2018).

Louis, I. & Lim, G. Differential response in growth and mycorrhizal colonisation of soybean to inoculation with two isolates of *Glomus clarum* in soils of different P availability. *Plant and Soil* **112**, 37–43 (1988).

Maherali, H. & Klironomos, J. N. Phylogenetic and trait-based assembly of arbuscular mycorrhizal fungal communities. *PLoS ONE* **7**, e36695 (2012).

Noë, R. & Hammerstein, P. Biological markets. *Trends in Ecology & Evolution* **10**, 336–339 (1995).

Noë, R. & Kiers, E. T. Mycorrhizal markets, firms, and co-ops. *Trends in Ecology & Evolution* **33**, 777-789 (2018).

Öpik, M., Davison, J., Moora, M. & Zobel, M. DNA-based detection and identification of Glomeromycota: the virtual taxonomy of environmental sequences. *Botany* **92**, 135–147 (2014).

Paymaneh, Z., Sarcheshmehpour, M., Bukovská, P. & Jansa, J. Could indigenous arbuscular mycorrhizal communities be used to improve tolerance of pistachio to salinity and/or drought? *Symbiosis* **79**, 269–283 (2019).

Redecker, D. Glomalean Fungi from the Ordovician. *Science* **289**, 1920–1921 (2000).

Sato, T., Ezawa, T., Cheng, W. & Tawaraya, K. Release of acid phosphatase from extraradical hyphae of arbuscular mycorrhizal fungus *Rhizophagus clarus*. *Soil Science and Plant Nutrition* **61**, 269–274 (2015).

Sato, T. *et al.* Secretion of acid phosphatase from extraradical hyphae of the arbuscular mycorrhizal fungus *Rhizophagus clarus* is regulated in response to phosphate availability. *Mycorrhiza* **29**, 599–605 (2019).

Sawers, R. J. H. *et al.* Phosphorus acquisition efficiency in arbuscular mycorrhizal maize is correlated with the abundance of root-external hyphae and the accumulation of transcripts encoding PHT1 phosphate transporters. *New Phytologist* **214**, 632–643 (2017).

Selosse, M.-A., Richard, F., He, X. & Simard, S. W. Mycorrhizal networks: des liaisons dangereuses? *Trends in Ecology & Evolution* **21**, 621–628 (2006).

Sharpe, D. Chi-square test is statistically significant: now what? *Practical Assessment, Research, and Evaluation* **20**, 8 (2015).

Smith, S. E. Mycorrhizal fungi can dominate phosphate supply to plants irrespective of growth responses. *Plant Physiology* **133**, 16–20 (2003).

Smith, S. E. & Read, D. J. in *Mycorrhizal Symbiosis* 1–8 (Academic Press Ltd., 2008).

St. John, T. V., Coleman, D. C. & Reid, C. P. P. Association of vesicular-arbuscular mycorrhizal hyphae with soil organic particles. *Ecology* **64**, 957–959 (1983).

Stahl, P. D. & Smith, W. K. Effects of different geographic isolates of *Glomus* on the water relations of *Agropyron Smithii*. *Mycologia* **76**, 261–267 (1984).

Verbruggen, E., El Mouden, C., Jansa, J., Akkermans, G., Bücking, H., West, S. A., & Kiers, E. T. Spatial structure and interspecific cooperation: theory and an empirical test using the mycorrhizal mutualism. *The American Naturalist* **179**, E133-E146 (2012).

Werner, G. & and Kiers, E. T. Partner selection in the mycorrhizal mutualism. *New Phytologist* **205**, 1437-1442 (2015).

Wolf, D. C. & Skipper, H. D. Soil Sterilization. in *SSSA Book Series* (eds. Weaver, R. W. *et al*.) 41–51 (Soil Science Society of America, 1994).

Wurst, S. & Ohgushi, T. Do plant- and soil-mediated legacy effects impact future biotic interactions? *Functional Ecology* **29**, 1373–1382 (2015).

Zhao, H., Li, X., Zhang, Z., Zhao, Y., Yang, J., & Zhu, Y. Species diversity and drivers of arbuscular mycorrhizal fungal communities in a semi-arid mountain in China. *PeerJ* **5** e4155 (2017).

APPENDIX A. METHODS FOR PLANT AND SOIL NUTRIENT ANALYSIS

All plant and soil analyses were conducted by Ward Laboratories, Inc. (Kearney, Nebraska, USA). Plant tissue mineral content (Ca, Mg, K, Zn, Fe, Mn, Cu, P, S, Na, Mo, B) was obtained by digesting a tissue sample with nitric acid, hydrochloric acid, and hydrogen peroxide and analyzed using ThermoFisher Scientific iCAP Inductively Coupled Plasma-Optical Emission Spectrometry (ICP-OES; Waltham, MA, USA). Plant N was quantified via combustion with a Leco TruMac Nitrogen/Carbon Analyzer (Saint Joseph, MI, USA). Soil mineral content (Ca, Mg, K, Na, Zn, Fe, Mn, Cu, and S) was analyzed on an ICP-OES. Soil P availability was quantified colorimetrically using the Mehlich III method. Soil pH was measured with a Ross Sure-Flow (Waltham, MA, USA) reference electrode in a 1:1 soil:water ratio method, while an electrical conductivity electrode measured soluble salts in a 1:1 soil:water solution. Soil samples were dried and ashed to obtain loss-on-ignition values for organic matter content. Ammonium-nitrogen (NH4-N) and nitrate-nitrogen (NO3-N) were extracted from soil with potassium chloride (KCl) via flow injection analysis. Soil cation exchange capacity (CEC) was calculated by summing cations in milliequivalents per 100 grams of soil after extracting cations with ammonium acetate.

APPENDIX B. PCR PRIMERS AND BARCODES

Table B1. Illumina barcodes attached to samples in PCR.

Sample ID	Reverse Barcode	Forward Barcode	Combined Barcode
FRBB-130	GTCGTGAT	TAAGACAC	GTCGTGATTAAGACAC
FRBB-131	GTCGTGAT	GGCTCTGA	GTCGTGATGGCTCTGA
FRBB-132	CAGCCTCG	GTAAGGAG	CAGCCTCGGTAAGGAG
FRBB-133	CAGCCTCG	CTAATCGA	CAGCCTCGCTAATCGA
FRBB-134	CAGCCTCG	AGGCGAAG	CAGCCTCGAGGCGAAG
FRBB-135	TGCCTCTT	GTAAGGAG	TGCCTCTTGTAAGGAG
FRBB-136	TGCCTCTT	CTAATCGA	TGCCTCTTCTAATCGA
FRBB-137	TGCCTCTT	AGGCGAAG	TGCCTCTTAGGCGAAG
FRBB-138	TCCTCTAC	GTAAGGAG	TCCTCTACGTAAGGAG
FRBB-139	TCCTCTAC	CTAATCGA	TCCTCTACCTAATCGA
FRBF-050	CCGTTTGT	ATAGAGGC	CCGTTTGTATAGAGGC
FRBF-051	TGCTGGGT	CTCTCTAT	TGCTGGGTCTCTCTAT
FRBF-052	TGCTGGGT	TGCTAAGT	TGCTGGGTTGCTAAGT
FRBF-053	TGCTGGGT	ATAGAGGC	TGCTGGGTATAGAGGC
FRBF-054	ACCACTGT	TATCCTCT	ACCACTGTTATCCTCT
FRBF-055	ACCACTGT	TGTTCTCT	ACCACTGTTGTTCTCT
FRBF-056	ACCACTGT	CCTATCCT	ACCACTGTCCTATCCT
FRBF-057	TGGATCTG	TATCCTCT	TGGATCTGTATCCTCT
FRBF-058	TGGATCTG	TGTTCTCT	TGGATCTGTGTTCTCT
FRBF-059	TGGATCTG	CCTATCCT	TGGATCTGCCTATCCT
FRBI-120	CAGCCTCG	AGAGTAGA	CAGCCTCGAGAGTAGA
FRBI-121	CAGCCTCG	TAAGACAC	CAGCCTCGTAAGACAC
FRBI-122	CAGCCTCG	GGCTCTGA	CAGCCTCGGGCTCTGA
FRBI-123	TGCCTCTT	AGAGTAGA	TGCCTCTTAGAGTAGA
FRBI-124	TGCCTCTT	TAAGACAC	TGCCTCTTTAAGACAC
FRBI-125	TGCCTCTT	GGCTCTGA	TGCCTCTTGGCTCTGA
FRBI-126	TCCTCTAC	AGAGTAGA	TCCTCTACAGAGTAGA
FRBI-127	TCCTCTAC	TAAGACAC	TCCTCTACTAAGACAC
FRBI-128	TCCTCTAC	GGCTCTGA	TCCTCTACGGCTCTGA
FRBI-129	GTCGTGAT	AGAGTAGA	GTCGTGATAGAGTAGA
FRBW-100	TGCTGGGT	CTAGAACA	TGCTGGGTCTAGAACA
FRBW-101	TGCTGGGT	TAATCTTA	TGCTGGGTTAATCTTA
FRBW-102	ACCACTGT	AAGGAGTA	ACCACTGTAAGGAGTA
FRBW-103	ACCACTGT	TAAGTTCC	ACCACTGTTAAGTTCC
FRBW-104	ACCACTGT	CAGGACGT	ACCACTGTCAGGACGT
FRBW-105	TGGATCTG	AAGGAGTA	TGGATCTGAAGGAGTA
FRBW-106	TGGATCTG	TAAGTTCC	TGGATCTGTAAGTTCC
FRBW-107	TGGATCTG	CAGGACGT	TGGATCTGCAGGACGT
FRBW-108	CCGTTTGT	AAGGAGTA	CCGTTTGTAAGGAGTA
FRBW-109	CCGTTTGT	TAAGTTCC	CCGTTTGTTAAGTTCC
FRCG-110	CCGTTTGT	CAGGACGT	CCGTTTGTCAGGACGT
FRCG-111	TGCTGGGT	AAGGAGTA	TGCTGGGTAAGGAGTA
FRCG-112	TGCTGGGT	TAAGTTCC	TGCTGGGTTAAGTTCC
FRCG-113	TGCTGGGT	CAGGACGT	TGCTGGGTCAGGACGT
FRCG-114	ACCACTGT	TAGACCTA	ACCACTGTTAGACCTA
FRCG-115	ACCACTGT	GTACTGAC	ACCACTGTGTACTGAC
FRCG-116	TGGATCTG	CTAAGCCT	TGGATCTGCTAAGCCT
FRCG-117	TGGATCTG	TAGACCTA	TGGATCTGTAGACCTA
FRCG-118	TGGATCTG	GTACTGAC	TGGATCTGGTACTGAC
FRCG-119	CCGTTTGT	CTAAGCCT	CCGTTTGTCTAAGCCT
FRCL-080	ACCACTGT	AGGCGAAG	ACCACTGTAGGCGAAG
FRCL-081	TGGATCTG	GTAAGGAG	TGGATCTGGTAAGGAG
FRCL-082	TGGATCTG	CTAATCGA	TGGATCTGCTAATCGA
FRCL-083	TGGATCTG	AGGCGAAG	TGGATCTGAGGCGAAG
FRCL-084	CCGTTTGT	GTAAGGAG	CCGTTTGTGTAAGGAG
FRCL-085	CCGTTTGT	CTAATCGA	CCGTTTGTCTAATCGA
FRCL-086	CCGTTTGT	AGGCGAAG	CCGTTTGTAGGCGAAG
FRCL-087	TGCTGGGT	GTAAGGAG	TGCTGGGTGTAAGGAG
FRCL-088	TGCTGGGT	CTAATCGA	TGCTGGGTCTAATCGA

Table B1. Illumina barcodes attached to samples in PCR (continued).

Sample ID	Reverse Barcode	Forward Barcode	Combined Barcode
FRCL-089	TGCTGGGT	AGGCGAAG	TGCTGGGTAGGCGAAG
FRCN-070	TGGATCTG	TAAGACAC	TGGATCTGTAAGACAC
FRCN-071	TGGATCTG	GGCTCTGA	TGGATCTGGGCTCTGA
FRCN-072	CCGTTTGT	AGAGTAGA	CCGTTTGTAGAGTAGA
FRCN-073	CCGTTTGT	TAAGACAC	CCGTTTGTTAAGACAC
FRCN-074	CCGTTTGT	GGCTCTGA	CCGTTTGTGGCTCTGA
FRCN-075	TGCTGGGT	AGAGTAGA	TGCTGGGTAGAGTAGA
FRCN-076	TGCTGGGT	TAAGACAC	TGCTGGGTTAAGACAC
FRCN-078	ACCACTGT	GTAAGGAG	ACCACTGTGTAAGGAG
FRCN-079	ACCACTGT	CTAATCGA	ACCACTGTCTAATCGA
FRCN-77	TGCTGGGT	GGCTCTGA	TGCTGGGTGGCTCTGA
FRDB-140	TCCTCTAC	AGGCGAAG	TCCTCTACAGGCGAAG
FRDB-141	GTCGTGAT	GTAAGGAG	GTCGTGATGTAAGGAG
FRDB-142	GTCGTGAT	CTAATCGA	GTCGTGATCTAATCGA
FRDB-143	GTCGTGAT	AGGCGAAG	GTCGTGATAGGCGAAG
FRDB-144	CAGCCTCG	ACTGCATA	CAGCCTCGACTGCATA
FRDB-145	CAGCCTCG	CTAGAACA	CAGCCTCGCTAGAACA
FRDB-146	CAGCCTCG	TAATCTTA	CAGCCTCGTAATCTTA
FRDB-147	TGCCTCTT	ACTGCATA	TGCCTCTTACTGCATA
FRDB-148	TGCCTCTT	CTAGAACA	TGCCTCTTCTAGAACA
FRDB-149	TGCCTCTT	TAATCTTA	TGCCTCTTTAATCTTA
FRKL-060	CCGTTTGT	TATCCTCT	CCGTTTGTTATCCTCT
FRKL-061	CCGTTTGT	TGTTCTCT	CCGTTTGTTGTTCTCT
FRKL-062	CCGTTTGT	CCTATCCT	CCGTTTGTCCTATCCT
FRKL-063	TGCTGGGT	TATCCTCT	TGCTGGGTTATCCTCT
FRKL-064	TGCTGGGT	TGTTCTCT	TGCTGGGTTGTTCTCT
FRKL-065	TGCTGGGT	CCTATCCT	TGCTGGGTCCTATCCT
FRKL-066	ACCACTGT	AGAGTAGA	ACCACTGTAGAGTAGA
FRKL-067	ACCACTGT	TAAGACAC	ACCACTGTTAAGACAC
FRKL-068	ACCACTGT	GGCTCTGA	ACCACTGTGGCTCTGA
FRKL-069	TGGATCTG	AGAGTAGA	TGGATCTGAGAGTAGA
FRLP-090	ACCACTGT	ACTGCATA	ACCACTGTACTGCATA
FRLP-091	ACCACTGT	CTAGAACA	ACCACTGTCTAGAACA
FRLP-092	ACCACTGT	TAATCTTA	ACCACTGTTAATCTTA
FRLP-093	TGGATCTG	ACTGCATA	TGGATCTGACTGCATA
FRLP-094	TGGATCTG	CTAGAACA	TGGATCTGCTAGAACA
FRLP-095	TGGATCTG	TAATCTTA	TGGATCTGTAATCTTA
FRLP-096	CCGTTTGT	ACTGCATA	CCGTTTGTACTGCATA
FRLP-097	CCGTTTGT	CTAGAACA	CCGTTTGTCTAGAACA
FRLP-098	CCGTTTGT	TAATCTTA	CCGTTTGTTAATCTTA
FRLP-099	TGCTGGGT	ACTGCATA	TGCTGGGTACTGCATA
FRMS-040	TGCTGGGT	TGAACCTT	TGCTGGGTTGAACCTT
FRMS-041	TGCTGGGT	TATAGCCT	TGCTGGGTTATAGCCT
FRMS-042	ACCACTGT	CTCTCTAT	ACCACTGTCTCTCTAT
FRMS-043	ACCACTGT	TGCTAAGT	ACCACTGTTGCTAAGT
FRMS-044	ACCACTGT	ATAGAGGC	ACCACTGTATAGAGGC
FRMS-045	TGGATCTG	CTCTCTAT	TGGATCTGCTCTCTAT
FRMS-046	TGGATCTG	TGCTAAGT	TGGATCTGTGCTAAGT
FRMS-047	TGGATCTG	ATAGAGGC	TGGATCTGATAGAGGC
FRMS-048	CCGTTTGT	CTCTCTAT	CCGTTTGTCTCTCTAT
FRMS-049	CCGTTTGT	TGCTAAGT	CCGTTTGTTGCTAAGT
FRNC-009	CAGCCTCG	AAGGAGTA	CAGCCTCGAAGGAGTA
FRNC-010	CAGCCTCG	TAAGTTCC	CAGCCTCGTAAGTTCC
FRNC-011	CAGCCTCG	CAGGACGT	CAGCCTCGCAGGACGT
FRNC-012	TGCCTCTT	AAGGAGTA	TGCCTCTTAAGGAGTA
FRNC-013	TGCCTCTT	TAAGTTCC	TGCCTCTTTAAGTTCC
FRNC-014	TGCCTCTT	CAGGACGT	TGCCTCTTCAGGACGT
FRSC-030	ACCACTGT	TAGATCGC	ACCACTGTTAGATCGC
FRSC-031	ACCACTGT	TGAACCTT	ACCACTGTTGAACCTT
FRSC-032	ACCACTGT	TATAGCCT	ACCACTGTTATAGCCT
FRSC-033	TGGATCTG	TAGATCGC	TGGATCTGTAGATCGC
FRSC-034	TGGATCTG	TGAACCTT	TGGATCTGTGAACCTT
FRSC-035	TGGATCTG	TATAGCCT	TGGATCTGTATAGCCT

Table B1. Illumina barcodes attached to samples in PCR (continued).

Sample ID	Reverse Barcode	Forward Barcode	Combined Barcode
FRSC-036	CCGTTTGT	TAGATCGC	CCGTTTGTTAGATCGC
FRSC-037	CCGTTTGT	TGAACCTT	CCGTTTGTTGAACCTT
FRSC-038	CCGTTTGT	TATAGCCT	CCGTTTGTTATAGCCT
FRSC-039	TGCTGGGT	TAGATCGC	TGCTGGGTTAGATCGC
FSBB-130	GTCGTGAT	TGAACCTT	GTCGTGATTGAACCTT
FSBB-131	GTCGTGAT	TATAGCCT	GTCGTGATTATAGCCT
FSBB-132	CAGCCTCG	CTCTCTAT	CAGCCTCGCTCTCTAT
FSBB-133	CAGCCTCG	TGCTAAGT	CAGCCTCGTGCTAAGT
FSBB-134	CAGCCTCG	ATAGAGGC	CAGCCTCGATAGAGGC
FSBB-135	TGCCTCTT	CTCTCTAT	TGCCTCTTCTCTCTAT
FSBB-136	TGCCTCTT	TGCTAAGT	TGCCTCTTTGCTAAGT
FSBB-137	TGCCTCTT	ATAGAGGC	TGCCTCTTATAGAGGC
FSBB-138	TCCTCTAC	CTCTCTAT	TCCTCTACCTCTCTAT
FSBB-139	TCCTCTAC	TGCTAAGT	TCCTCTACTGCTAAGT
FSBF-050	CCTCTCTG	ATAGAGGC	CCTCTCTGATAGAGGC
FSBF-051	AGCGTAGC	CTCTCTAT	AGCGTAGCCTCTCTAT
FSBF-052	AGCGTAGC	TGCTAAGT	AGCGTAGCTGCTAAGT
FSBF-053	AGCGTAGC	ATAGAGGC	AGCGTAGCATAGAGGC
FSBF-054	CATGCCTA	TATCCTCT	CATGCCTATATCCTCT
FSBF-055	CATGCCTA	TGTTCTCT	CATGCCTATGTTCTCT
FSBF-056	CATGCCTA	CCTATCCT	CATGCCTACCTATCCT
FSBF-057	GTAGAGAG	TATCCTCT	GTAGAGAGTATCCTCT
FSBF-058	GTAGAGAG	TGTTCTCT	GTAGAGAGTGTTCTCT
FSBF-059	GTAGAGAG	CCTATCCT	GTAGAGAGCCTATCCT
FSBI-120	CAGCCTCG	TAGATCGC	CAGCCTCGTAGATCGC
FSBI-121	CAGCCTCG	TGAACCTT	CAGCCTCGTGAACCTT
FSBI-122	CAGCCTCG	TATAGCCT	CAGCCTCGTATAGCCT
FSBI-123	TGCCTCTT	TAGATCGC	TGCCTCTTTAGATCGC
FSBI-124	TGCCTCTT	TGAACCTT	TGCCTCTTTGAACCTT
FSBI-125	TGCCTCTT	TATAGCCT	TGCCTCTTTATAGCCT
FSBI-126	TCCTCTAC	TAGATCGC	TCCTCTACTAGATCGC
FSBI-127	TCCTCTAC	TGAACCTT	TCCTCTACTGAACCTT
FSBI-128	TCCTCTAC	TATAGCCT	TCCTCTACTATAGCCT
FSBI-129	GTCGTGAT	TAGATCGC	GTCGTGATTAGATCGC
FSBW-100	AGCGTAGC	CTAGAACA	AGCGTAGCCTAGAACA
FSBW-101	AGCGTAGC	TAATCTTA	AGCGTAGCTAATCTTA
FSBW-102	CATGCCTA	AAGGAGTA	CATGCCTAAAGGAGTA
FSBW-103	CATGCCTA	TAAGTTCC	CATGCCTATAAGTTCC
FSBW-104	CATGCCTA	CAGGACGT	CATGCCTACAGGACGT
FSBW-105	GTAGAGAG	AAGGAGTA	GTAGAGAGAAGGAGTA
FSBW-106	GTAGAGAG	TAAGTTCC	GTAGAGAGTAAGTTCC
FSBW-107	GTAGAGAG	CAGGACGT	GTAGAGAGCAGGACGT
FSBW-108	CCTCTCTG	AAGGAGTA	CCTCTCTGAAGGAGTA
FSBW-109	CCTCTCTG	TAAGTTCC	CCTCTCTGTAAGTTCC
FSCG-110	CCTCTCTG	CAGGACGT	CCTCTCTGCAGGACGT
FSCG-111	AGCGTAGC	AAGGAGTA	AGCGTAGCAAGGAGTA
FSCG-112	AGCGTAGC	TAAGTTCC	AGCGTAGCTAAGTTCC
FSCG-113	AGCGTAGC	CAGGACGT	AGCGTAGCCAGGACGT
FSCG-114	CATGCCTA	CTAAGCCT	CATGCCTACTAAGCCT
FSCG-115	CATGCCTA	TAGACCTA	CATGCCTATAGACCTA
FSCG-116	CATGCCTA	GTACTGAC	CATGCCTAGTACTGAC
FSCG-117	GTAGAGAG	CTAAGCCT	GTAGAGAGCTAAGCCT
FSCG-118	GTAGAGAG	TAGACCTA	GTAGAGAGTAGACCTA
FSCG-119	GTAGAGAG	GTACTGAC	GTAGAGAGGTACTGAC
FSCL-080	CATGCCTA	AGGCGAAG	CATGCCTAAGGCGAAG
FSCL-081	GTAGAGAG	GTAAGGAG	GTAGAGAGGTAAGGAG
FSCL-082	GTAGAGAG	CTAATCGA	GTAGAGAGCTAATCGA
FSCL-083	GTAGAGAG	AGGCGAAG	GTAGAGAGAGGCGAAG
FSCL-084	CCTCTCTG	GTAAGGAG	CCTCTCTGGTAAGGAG
FSCL-085	CCTCTCTG	CTAATCGA	CCTCTCTGCTAATCGA
FSCL-086	CCTCTCTG	AGGCGAAG	CCTCTCTGAGGCGAAG
FSCL-087	AGCGTAGC	GTAAGGAG	AGCGTAGCGTAAGGAG
FSCL-088	AGCGTAGC	CTAATCGA	AGCGTAGCCTAATCGA

Table B1. Illumina barcodes attached to samples in PCR (continued).

Sample ID	Reverse Barcode	Forward Barcode	Combined Barcode
FSCL-089	AGCGTAGC	AGGCGAAG	AGCGTAGCAGGCGAAG
FSCN-070	GTAGAGAG	TAAGACAC	GTAGAGAGTAAGACAC
FSCN-071	GTAGAGAG	GGCTCTGA	GTAGAGAGGGCTCTGA
FSCN-072	CCTCTCTG	AGAGTAGA	CCTCTCTGAGAGTAGA
FSCN-073	CCTCTCTG	TAAGACAC	CCTCTCTGTAAGACAC
FSCN-074	CCTCTCTG	GGCTCTGA	CCTCTCTGGGCTCTGA
FSCN-075	AGCGTAGC	AGAGTAGA	AGCGTAGCAGAGTAGA
FSCN-076	AGCGTAGC	TAAGACAC	AGCGTAGCTAAGACAC
FSCN-078	CATGCCTA	GTAAGGAG	CATGCCTAGTAAGGAG
FSCN-079	CATGCCTA	CTAATCGA	CATGCCTACTAATCGA
FSCN-77	AGCGTAGC	GGCTCTGA	AGCGTAGCGGCTCTGA
FSDB-140	TCCTCTAC	ATAGAGGC	TCCTCTACATAGAGGC
FSDB-141	GTCGTGAT	CTCTCTAT	GTCGTGATCTCTCTAT
FSDB-142	GTCGTGAT	TGCTAAGT	GTCGTGATTGCTAAGT
FSDB-143	GTCGTGAT	ATAGAGGC	GTCGTGATATAGAGGC
FSDB-144	CAGCCTCG	TATCCTCT	CAGCCTCGTATCCTCT
FSDB-145	CAGCCTCG	TGTTCTCT	CAGCCTCGTGTTCTCT
FSDB-146	CAGCCTCG	CCTATCCT	CAGCCTCGCCTATCCT
FSDB-147	TGCCTCTT	TATCCTCT	TGCCTCTTTATCCTCT
FSDB-148	TGCCTCTT	TGTTCTCT	TGCCTCTTTGTTCTCT
FSDB-149	TGCCTCTT	CCTATCCT	TGCCTCTTCCTATCCT
FSKL-060	CCTCTCTG	TATCCTCT	CCTCTCTGTATCCTCT
FSKL-061	CCTCTCTG	TGTTCTCT	CCTCTCTGTGTTCTCT
FSKL-062	CCTCTCTG	CCTATCCT	CCTCTCTGCCTATCCT
FSKL-063	AGCGTAGC	TATCCTCT	AGCGTAGCTATCCTCT
FSKL-064	AGCGTAGC	TGTTCTCT	AGCGTAGCTGTTCTCT
FSKL-065	AGCGTAGC	CCTATCCT	AGCGTAGCCCTATCCT
FSKL-066	CATGCCTA	AGAGTAGA	CATGCCTAAGAGTAGA
FSKL-067	CATGCCTA	TAAGACAC	CATGCCTATAAGACAC
FSKL-068	CATGCCTA	GGCTCTGA	CATGCCTAGGCTCTGA
FSKL-069	GTAGAGAG	AGAGTAGA	GTAGAGAGAGAGTAGA
FSLP-090	CATGCCTA	ACTGCATA	CATGCCTAACTGCATA
FSLP-091	CATGCCTA	CTAGAACA	CATGCCTACTAGAACA
FSLP-092	CATGCCTA	TAATCTTA	CATGCCTATAATCTTA
FSLP-093	GTAGAGAG	ACTGCATA	GTAGAGAGACTGCATA
FSLP-094	GTAGAGAG	CTAGAACA	GTAGAGAGCTAGAACA
FSLP-095	GTAGAGAG	TAATCTTA	GTAGAGAGTAATCTTA
FSLP-096	CCTCTCTG	ACTGCATA	CCTCTCTGACTGCATA
FSLP-097	CCTCTCTG	CTAGAACA	CCTCTCTGCTAGAACA
FSLP-098	CCTCTCTG	TAATCTTA	CCTCTCTGTAATCTTA
FSLP-099	AGCGTAGC	ACTGCATA	AGCGTAGCACTGCATA
FSMS-040	AGCGTAGC	TGAACCTT	AGCGTAGCTGAACCTT
FSMS-041	AGCGTAGC	TATAGCCT	AGCGTAGCTATAGCCT
FSMS-042	CATGCCTA	CTCTCTAT	CATGCCTACTCTCTAT
FSMS-043	CATGCCTA	TGCTAAGT	CATGCCTATGCTAAGT
FSMS-044	CATGCCTA	ATAGAGGC	CATGCCTAATAGAGGC
FSMS-045	GTAGAGAG	CTCTCTAT	GTAGAGAGCTCTCTAT
FSMS-046	GTAGAGAG	TGCTAAGT	GTAGAGAGTGCTAAGT
FSMS-047	GTAGAGAG	ATAGAGGC	GTAGAGAGATAGAGGC
FSMS-048	CCTCTCTG	CTCTCTAT	CCTCTCTGCTCTCTAT
FSMS-049	CCTCTCTG	TGCTAAGT	CCTCTCTGTGCTAAGT
FSNC-020	GTCGTGAT	CAGGACGT	GTCGTGATCAGGACGT
FSNC-021	CAGCCTCG	CTAAGCCT	CAGCCTCGCTAAGCCT
FSNC-022	CAGCCTCG	TAGACCTA	CAGCCTCGTAGACCTA
FSNC-023	CAGCCTCG	GTACTGAC	CAGCCTCGGTACTGAC
FSNC-024	TGCCTCTT	CTAAGCCT	TGCCTCTTCTAAGCCT
FSNC-025	TCCTCTAC	CTAAGCCT	TCCTCTACCTAAGCCT
FSSC-030	CATGCCTA	TAGATCGC	CATGCCTATAGATCGC
FSSC-031	CATGCCTA	TGAACCTT	CATGCCTATGAACCTT
FSSC-032	CATGCCTA	TATAGCCT	CATGCCTATATAGCCT
FSSC-033	GTAGAGAG	TAGATCGC	GTAGAGAGTAGATCGC
FSSC-034	GTAGAGAG	TGAACCTT	GTAGAGAGTGAACCTT
FSSC-035	AGCGTAGC	GTACTGAC	AGCGTAGCGTACTGAC

Table B1. Illumina barcodes attached to samples in PCR (continued).

Sample ID	Reverse Barcode	Forward Barcode	Combined Barcode
FSSC-036	AGCGTAGC	TAGACCTA	AGCGTAGCTAGACCTA
FSSC-037	CCTCTCTG	GTACTGAC	CCTCTCTGGTACTGAC
FSSC-038	CCTCTCTG	TAGACCTA	CCTCTCTGTAGACCTA
FSSC-039	AGCGTAGC	TAGATCGC	AGCGTAGCTAGATCGC
GRBB-130	TTGACCCT	TGCTAAGT	TTGACCCTTGCTAAGT
GRBB-131	TTGACCCT	CTAATCGA	TTGACCCTCTAATCGA
GRBB-132	TGGTCACA	CTCTCTAT	TGGTCACACTCTCTAT
GRBB-133	TGGTCACA	ACTGCATA	TGGTCACAACTGCATA
GRBB-134	TGGTCACA	TGCTAAGT	TGGTCACATGCTAAGT
GRBB-135	TGGTCACA	CTAGAACA	TGGTCACACTAGAACA
GRBB-136	TGGTCACA	TATAGCCT	TGGTCACATATAGCCT
GRBB-137	TGGTCACA	GGCTCTGA	TGGTCACAGGCTCTGA
GRBB-138	TGGTCACA	CAGGACGT	TGGTCACACAGGACGT
GRBB-139	TTGACCCT	CTCTCTAT	TTGACCCTCTCTCTAT
GRBF-050	GTGTGGTG	ATAGAGGC	GTGTGGTGATAGAGGC
GRBF-051	TGGGTTTC	CTCTCTAT	TGGGTTTCCTCTCTAT
GRBF-052	TGGGTTTC	TGCTAAGT	TGGGTTTCTGCTAAGT
GRBF-053	TGGGTTTC	ATAGAGGC	TGGGTTTCATAGAGGC
GRBF-054	GAGGGGTT	TATCCTCT	GAGGGGTTTATCCTCT
GRBF-055	GAGGGGTT	TGTTCTCT	GAGGGGTTTGTTCTCT
GRBF-056	GAGGGGTT	CCTATCCT	GAGGGGTTCCTATCCT
GRBF-057	AGGTTGGG	TATCCTCT	AGGTTGGGTATCCTCT
GRBF-058	AGGTTGGG	TGTTCTCT	AGGTTGGGTGTTCTCT
GRBF-059	AGGTTGGG	CCTATCCT	AGGTTGGGCCTATCCT
GRBI-120	TGGTCACA	TAGATCGC	TGGTCACATAGATCGC
GRBI-121	TGGTCACA	GTAAGGAG	TGGTCACAGTAAGGAG
GRBI-122	TGGTCACA	TGAACCTT	TGGTCACATGAACCTT
GRBI-123	TGGTCACA	CTAATCGA	TGGTCACACTAATCGA
GRBI-124	TGGTCACA	TAGACCTA	TGGTCACATAGACCTA
GRBI-125	TGGTCACA	CCTATCCT	TGGTCACACCTATCCT
GRBI-126	TGGTCACA	TAATCTTA	TGGTCACATAATCTTA
GRBI-127	TTGACCCT	TAGATCGC	TTGACCCTTAGATCGC
GRBI-128	TTGACCCT	AGAGTAGA	TTGACCCTAGAGTAGA
GRBI-129	TTGACCCT	AAGGAGTA	TTGACCCTAAGGAGTA
GRBW-100	TGGGTTTC	CTAGAACA	TGGGTTTCCTAGAACA
GRBW-101	TGGGTTTC	TAATCTTA	TGGGTTTCTAATCTTA
GRBW-102	GAGGGGTT	AAGGAGTA	GAGGGGTTAAGGAGTA
GRBW-103	GAGGGGTT	TAAGTTCC	GAGGGGTTTAAGTTCC
GRBW-104	GAGGGGTT	CAGGACGT	GAGGGGTTCAGGACGT
GRBW-105	AGGTTGGG	AAGGAGTA	AGGTTGGGAAGGAGTA
GRBW-106	AGGTTGGG	TAAGTTCC	AGGTTGGGTAAGTTCC
GRBW-107	AGGTTGGG	CAGGACGT	AGGTTGGGCAGGACGT
GRBW-108	GTGTGGTG	AAGGAGTA	GTGTGGTGAAGGAGTA
GRBW-109	GTGTGGTG	TAAGTTCC	GTGTGGTGTAAGTTCC
GRCG-110	GTGTGGTG	CAGGACGT	GTGTGGTGCAGGACGT
GRCG-111	TGGGTTTC	AAGGAGTA	TGGGTTTCAAGGAGTA
GRCG-112	TGGGTTTC	TAAGTTCC	TGGGTTTCTAAGTTCC
GRCG-113	TGGGTTTC	CAGGACGT	TGGGTTTCCAGGACGT
GRCG-114	GAGGGGTT	GTACTGAC	GAGGGGTTGTACTGAC
GRCG-115	AGGTTGGG	CTAAGCCT	AGGTTGGGCTAAGCCT
GRCG-116	AGGTTGGG	TAGACCTA	AGGTTGGGTAGACCTA
GRCG-117	AGGTTGGG	GTACTGAC	AGGTTGGGGTACTGAC
GRCG-118	GTGTGGTG	CTAAGCCT	GTGTGGTGCTAAGCCT
GRCG-119	GTGTGGTG	TAGACCTA	GTGTGGTGTAGACCTA
GRCL-080	GAGGGGTT	AGGCGAAG	GAGGGGTTAGGCGAAG
GRCL-081	AGGTTGGG	GTAAGGAG	AGGTTGGGGTAAGGAG
GRCL-082	AGGTTGGG	CTAATCGA	AGGTTGGGCTAATCGA
GRCL-083	AGGTTGGG	AGGCGAAG	AGGTTGGGAGGCGAAG
GRCL-084	GTGTGGTG	GTAAGGAG	GTGTGGTGGTAAGGAG
GRCL-085	GTGTGGTG	CTAATCGA	GTGTGGTGCTAATCGA
GRCL-086	GTGTGGTG	AGGCGAAG	GTGTGGTGAGGCGAAG
GRCL-087	TGGGTTTC	GTAAGGAG	TGGGTTTCGTAAGGAG
GRCL-088	TGGGTTTC	CTAATCGA	TGGGTTTCCTAATCGA

Table B1. Illumina barcodes attached to samples in PCR (continued).

Sample ID	Reverse Barcode	Forward Barcode	Combined Barcode
GRCL-089	TGGGTTTC	AGGCGAAG	TGGGTTTCAGGCGAAG
GRCN-070	AGGTTGGG	TAAGACAC	AGGTTGGGTAAGACAC
GRCN-071	AGGTTGGG	GGCTCTGA	AGGTTGGGGGCTCTGA
GRCN-072	GTGTGGTG	AGAGTAGA	GTGTGGTGAGAGTAGA
GRCN-073	GTGTGGTG	TAAGACAC	GTGTGGTGTAAGACAC
GRCN-074	GTGTGGTG	GGCTCTGA	GTGTGGTGGGCTCTGA
GRCN-075	TGGGTTTC	AGAGTAGA	TGGGTTTCAGAGTAGA
GRCN-076	TGGGTTTC	TAAGACAC	TGGGTTTCTAAGACAC
GRCN-078	GAGGGGTT	GTAAGGAG	GAGGGGTTGTAAGGAG
GRCN-079	GAGGGGTT	CTAATCGA	GAGGGGTTCTAATCGA
GRCN-77	TGGGTTTC	GGCTCTGA	TGGGTTTCGGCTCTGA
GRDB-140	TTGACCCT	GTAAGGAG	TTGACCCTGTAAGGAG
GRDB-141	TTGACCCT	CTAAGCCT	TTGACCCTCTAAGCCT
GRDB-142	TTGACCCT	TGTTCTCT	TTGACCCTTGTTCTCT
GRDB-143	TTGACCCT	CTAGAACA	TTGACCCTCTAGAACA
GRDB-144	TGGTCACA	TATCCTCT	TGGTCACATATCCTCT
GRDB-145	TGGTCACA	AAGGAGTA	TGGTCACAAAGGAGTA
GRDB-146	TGGTCACA	TGTTCTCT	TGGTCACATGTTCTCT
GRDB-147	TGGTCACA	TAAGTTCC	TGGTCACATAAGTTCC
GRDB-148	TGGTCACA	ATAGAGGC	TGGTCACAATAGAGGC
GRDB-149	TGGTCACA	AGGCGAAG	TGGTCACAAGGCGAAG
GRKL-060	GTGTGGTG	TATCCTCT	GTGTGGTGTATCCTCT
GRKL-061	GTGTGGTG	TGTTCTCT	GTGTGGTGTGTTCTCT
GRKL-062	GTGTGGTG	CCTATCCT	GTGTGGTGCCTATCCT
GRKL-063	TGGGTTTC	TATCCTCT	TGGGTTTCTATCCTCT
GRKL-064	TGGGTTTC	TGTTCTCT	TGGGTTTCTGTTCTCT
GRKL-065	TGGGTTTC	CCTATCCT	TGGGTTTCCCTATCCT
GRKL-066	GAGGGGTT	AGAGTAGA	GAGGGGTTAGAGTAGA
GRKL-067	GAGGGGTT	TAAGACAC	GAGGGGTTTAAGACAC
GRKL-068	GAGGGGTT	GGCTCTGA	GAGGGGTTGGCTCTGA
GRKL-069	AGGTTGGG	AGAGTAGA	AGGTTGGGAGAGTAGA
GRLP-090	GAGGGGTT	ACTGCATA	GAGGGGTTACTGCATA
GRLP-091	GAGGGGTT	CTAGAACA	GAGGGGTTCTAGAACA
GRLP-092	GAGGGGTT	TAATCTTA	GAGGGGTTTAATCTTA
GRLP-093	AGGTTGGG	ACTGCATA	AGGTTGGGACTGCATA
GRLP-094	AGGTTGGG	CTAGAACA	AGGTTGGGCTAGAACA
GRLP-095	AGGTTGGG	TAATCTTA	AGGTTGGGTAATCTTA
GRLP-096	GTGTGGTG	ACTGCATA	GTGTGGTGACTGCATA
GRLP-097	GTGTGGTG	CTAGAACA	GTGTGGTGCTAGAACA
GRLP-098	GTGTGGTG	TAATCTTA	GTGTGGTGTAATCTTA
GRLP-099	TGGGTTTC	ACTGCATA	TGGGTTTCACTGCATA
GRMS-040	TGGGTTTC	TGAACCTT	TGGGTTTCTGAACCTT
GRMS-041	TGGGTTTC	TATAGCCT	TGGGTTTCTATAGCCT
GRMS-042	GAGGGGTT	CTCTCTAT	GAGGGGTTCTCTCTAT
GRMS-043	GAGGGGTT	TGCTAAGT	GAGGGGTTTGCTAAGT
GRMS-044	GAGGGGTT	ATAGAGGC	GAGGGGTTATAGAGGC
GRMS-045	AGGTTGGG	CTCTCTAT	AGGTTGGGCTCTCTAT
GRMS-046	AGGTTGGG	TGCTAAGT	AGGTTGGGTGCTAAGT
GRMS-047	AGGTTGGG	ATAGAGGC	AGGTTGGGATAGAGGC
GRMS-048	GTGTGGTG	CTCTCTAT	GTGTGGTGCTCTCTAT
GRMS-049	GTGTGGTG	TGCTAAGT	GTGTGGTGTGCTAAGT
GRNC-015	TCCTCTAC	AAGGAGTA	TCCTCTACAAGGAGTA
GRNC-016	TCCTCTAC	TAAGTTCC	TCCTCTACTAAGTTCC
GRNC-017	TCCTCTAC	CAGGACGT	TCCTCTACCAGGACGT
GRNC-018	GTCGTGAT	AAGGAGTA	GTCGTGATAAGGAGTA
GRNC-019	GTCGTGAT	TAAGTTCC	GTCGTGATTAAGTTCC
GRNM-150	TGGTCACA	GTACTGAC	TGGTCACAGTACTGAC
GRNM-151	TTGACCCT	TATCCTCT	TTGACCCTTATCCTCT
GRNM-152	TTGACCCT	ACTGCATA	TTGACCCTACTGCATA
GRNM-153	TTGACCCT	TGAACCTT	TTGACCCTTGAACCTT
GRNM-154	TTGACCCT	TAAGACAC	TTGACCCTTAAGACAC
GRNM-155	TTGACCCT	TAAGTTCC	TTGACCCTTAAGTTCC
GRNM-157	TGGTCACA	AGAGTAGA	TGGTCACAAGAGTAGA

Table B1. Illumina barcodes attached to samples in PCR (continued).

Sample ID	Reverse Barcode	Forward Barcode	Combined Barcode
GRNM-158	TGGTCACA	CTAAGCCT	TGGTCACACTAAGCCT
GRNM-159	TGGTCACA	TAAGACAC	TGGTCACATAAGACAC
GRSC-030	GAGGGGTT	TAGATCGC	GAGGGGTTTAGATCGC
GRSC-031	GAGGGGTT	TGAACCTT	GAGGGGTTTGAACCTT
GRSC-032	GAGGGGTT	TATAGCCT	GAGGGGTTTATAGCCT
GRSC-033	AGGTTGGG	TAGATCGC	AGGTTGGGTAGATCGC
GRSC-034	AGGTTGGG	TGAACCTT	AGGTTGGGTGAACCTT
GRSC-035	AGGTTGGG	TATAGCCT	AGGTTGGGTATAGCCT
GRSC-036	GTGTGGTG	TAGATCGC	GTGTGGTGTAGATCGC
GRSC-037	GTGTGGTG	TGAACCTT	GTGTGGTGTGAACCTT
GRSC-038	GTGTGGTG	TATAGCCT	GTGTGGTGTATAGCCT
GRSC-039	TGGGTTTC	TAGATCGC	TGGGTTTCTAGATCGC
PCR_PLATE_1	AGCGTAGC	CTAAGCCT	AGCGTAGCCTAAGCCT
PCR_PLATE_2	TCCTCTAC	TATCCTCT	TCCTCTACTATCCTCT
PCRNEG-1	ACCACTGT	CTAAGCCT	ACCACTGTCTAAGCCT
PCRNEG-2	GAGGGGTT	CTAAGCCT	GAGGGGTTCTAAGCCT
PCRNEG-3	TTGACCCT	TAGACCTA	TTGACCCTTAGACCTA

Table B2. PCR primers used during amplification.

Taxonomy Detection	Gene	Primer name	Direction	Sequence	Reference
Wide taxonomic coverage of fungi	ITS2	fITS7 ITS7o ITS4	Forward Forward Reverse	5′-GTG AAT CAT CGA ATC TTT G-3′ 5′-GTG AAT CAT CRA ATY TTT G-3′ 5′- TCC TCC GCT TAT TGA TAT GC-3′	Ihrmark *et al*. 2012 Kohout *et al*. 2014 White *et al*. 1990
Arbuscular Mycorrhizal Fungi (AMF)	18S	WANDA AML2	Forward Reverse	5′-CAG CCG CGG TAA TTC CAG CT-3′ 5′-GAA CCC AAA CAC TTT GGT TTC C-3′	Dumbrell *et al*. 2011 Lee *et al*. 2008

Note: Primers were used to amplify fungal DNA from soil and *G. aristata* root samples collected from field sites across Montana, North Dakota and Minnesota, as well as root samples of the same plant species grown in the greenhouse.

APPENDIX C. HOAGLAND'S SOLUTION FOR FERTILIZATION

Table C1. Nutrients per liter in Hoagland's solution used for fertilization.

High P fertilizer	No P fertilizer
6 mL 1 M KNO_3	6 mL 1 M KNO_3
4 mL 1 M $Ca(NO_3)_2 \bullet 4H_2O$	4 mL 1 M $Ca(NO_3)_2 \bullet 4H_2O$
2 mL 1 M $MgSO_4 \bullet 7H_2O$	2 mL 1 M $MgSO_4 \bullet 7H_2O$
1 mL 1 M $Ca(H_2PO_4)_2$	-
1 mL 6% iron chelate FeEDDHA	1 mL 6% iron chelate FeEDDHA
1 mL micronutrient solution	1 mL micronutrient solution
985 mL deionized water	986 mL deionized water

Table C2. Nutrients plus deionized water to 1 L in micronutrient solution.

Micronutrient solution
1.43 g H_3BO_3
0.905 g $MnCl_2 \bullet 4H_2O$
0.11 g $ZnSO_4 \bullet 7H_2O$
0.04 g $CuSO_4 \bullet 5H_2O$
0.0125 g $Na_2MoO_4 \bullet 2H_2O$ minimum 99.5%

Note: *Gaillardia aristata* plants in the greenhouse were fertilized with a modified Hoagland's solution (Table C1). The two fertilization treatments received the same fertilizer except that the high P treatment had $Ca(H_2PO_4)_2$ and the no P treatment did not. Each fertilizer solution included 1 mL of a micronutrient solution (Table C2).

APPENDIX D. ADDITIONAL RESULTS FOR CHAPTER 1

D.1. Spatial gradients lead to site differences in soil properties

Many soil chemical properties differed by site. Nitrate-nitrogen content was the highest at Bicentennial Prairie and differed significantly from soils at Central Grasslands, Clearwater, and Mt. Sentinel. Ammonium-nitrogen was the highest at Clearwater New and differed significantly from all of the sites in ND and MN except B-B Ranch. Beckman WMA had the lowest ammonium-nitrogen content. Soil K generally followed a longitudinal gradient; it was highest in western sites and lowest in eastern sites. Soil Ca was highest at Kleinschmidt, Delbert Berntson, and Bicentennial Prairie and lowest at Beckman WMA. Soil Mg generally followed a longitudinal gradient; it was highest in eastern sites and lowest in western sites. Soil Fe was highest at Blackfoot and lowest at Beckman WMA. Soil Mn was highest at Central Grasslands, followed by Mt. Sentinel, Lone Ponderosa, Blackfoot, Delbert Berntson, and Sheep Camp; it was lowest at Beckman WMA. Soil Cu was the highest at Lone Ponderosa and the lowest at Sheep Camp, Bicentennial Prairie, and Beckman WMA. Soil Zn was the highest at Clearwater New and the lowest at Beckman WMA. Delbert Berntson was the site with the highest soil Na content. Clearwater New had the highest soil sulfate level while Sheep Camp had the lowest. Soil pH was the most acidic at Blackfoot (pH = 6.18) and the most alkaline at Beckman WMA (pH = 7.82). Soil salts were highest at Bicentennial Prairie and lowest at Clearwater and Clearwater New. Bicentennial Prairie, Clearwater New, and Blackfoot had the highest soil organic matter while Beckman WMA had the lowest. Soil CEC was highest at Kleinschmidt and lowest at Sheep Camp and Beckman WMA.

Table D1. Soil chemical properties that differed among sites.

Site	2N KCl NO3-N (ppm)	KCl NH4-N (ppm)	P Melich III ppm	K (ppm)	Ca (ppm)	Mg (ppm)	Fe (ppm)	Mn (ppm)
Sheep Camp	1.77 ± 0.16 ab	3.80 ± 0.35 ab	20 ± 3 bc	348 ± 25 ab	1711 ± 115 bc	185 ± 4 de	24.8 ± 1.9 abc	12.8 ± 1.3 a
Lone Ponderosa	1.93 ± 0.30 ab	3.10 ± 0.36 abc	38 ± 2 a	399 ± 15 a	2456 ± 176 ab	182 ± 19 de	16.4 ± 2.5 cd	14.4 ± 1.1 a
Mt. Sentinel	1.06 ± 0.21 b	2.94 ± 0.61 abc	29 ± 3 ab	309 ± 31 ab	1701 ± 32 bc	199 ± 10 cde	35.5 ± 9.5 abc	14.8 ± 1.8 a
Clearwater New	1.46 ± 0.13 ab	4.75 ± 0.67 a	21 ± 1 abc	252 ± 16 b	2082 ± 72 abc	166 ± 11 e	48.8 ± 2.3 ab	10.3 ± 0.6 ab
Clearwater	1.06 ± 0.17 b	3.27 ± 0.35 abc	7 ± 1 d	248 ± 17 b	1753 ± 39 bc	226 ± 22 bcde	52.7 ± 5.7 ab	10.5 ± 0.4 ab
Kleinschmidt	1.78 ± 0.39 ab	3.31 ± 0.35 abc	15 ± 4 c	248 ± 47 b	3349 ± 460 a	241 ± 13 bcd	28.9 ± 12.1 bcd	10.8 ± 3.5 ab
Blackfoot	2.72 ± 1.21 ab	2.88 ± 0.40 abc	24 ± 5 bc	302 ± 36 ab	2104 ± 82 abc	271 ± 21 abc	62.9 ± 9.7 a	14.6 ± 1.9 a
Beckman WMA	1.76 ± 0.26 ab	1.64 ± 0.35 c	4 ± 0 de	88 ± 5 d	1771 ± 305 c	207 ± 10 cde	8.4 ± 0.4 d	4.1 ± 0.7 b
Central Grasslands	1.30 ± 0.12 b	2.60 ± 0.30 bc	3 ± 0 e	272 ± 28 ab	2288 ± 142 abc	361 ± 23 a	29.3 ± 9.3 abc	15.2 ± 2.6 a
Delbert Berntson	2.92 ± 1.00 ab	1.95 ± 0.14 bc	3 ± 1 e	225 ± 48 bc	3350 ± 520 a	410 ± 40 a	15.7 ± 3.5 cd	14.6 ± 3.5 a
B-B Ranch	1.82 ± 0.30 ab	3.35 ± 0.42 abc	3 ± 0 e	97 ± 23 cd	2006 ± 74 abc	303 ± 15 ab	30.4 ± 5.0 abc	10.5 ± 1.4 ab
Bicentennial Prairie	5.49 ± 0.78 a	1.97 ± 0.13 bc	3 ± 0 e	97 ± 8 cd	2774 ± 167 a	409 ± 46 a	15.7 ± 2.1 cd	7.3 ± 0.8 ab

Site	Cu (ppm)	Zn (ppm)	Na (ppm)	Sulfate (ppm)	pH (1:1)	Salts 1:1 (mmho/cm)	OM (LOI%)	CEC (me/100g)
Sheep Camp	0.49 ± 0.02 f	1.93 ± 0.23 bc	4 ± 1 ab	4.9 ± 0.3 c	6.8 ± 0.1 cde	0.10 ± 0.00 bcd	6.0 ± 0.2 ab	11.0 ± 0.6 e
Lone Ponderosa	5.23 ± 1.07 a	1.06 ± 0.12 cd	5 ± 1 a	6.4 ± 0.5 abc	7.0 ± 0.1 bcd	0.12 ± 0.01 abc	6.6 ± 0.5 ab	14.8 ± 0.8 bcde
Mt. Sentinel	1.05 ± 0.12 bc	2.01 ± 0.41 bc	4 ± 2 b	6.1 ± 0.4 abc	6.8 ± 0.1 cde	0.09 ± 0.00 cd	4.6 ± 0.2 bc	11.6 ± 0.4 de
Clearwater New	0.99 ± 0.12 bc	7.73 ± 1.47 a	5 ± 1 a	8.3 ± 1.1 a	6.3 ± 0.1 de	0.07 ± 0.00 d	8.4 ± 0.6 a	16.6 ± 0.6 abcd
Clearwater	0.88 ± 0.06 cd	3.02 ± 0.33 abc	4 ± 0 ab	6.1 ± 0.4 abc	6.3 ± 0.1 de	0.07 ± 0.01 d	7.4 ± 0.2 ab	14.2 ± 0.9 cde
Kleinschmidt	1.67 ± 0.13 b	3.14 ± 1.45 bc	5 ± 1 a	7.9 ± 2.0 abc	7.1 ± 0.4 bc	0.13 ± 0.01 abc	6.6 ± 1.5 ab	21.2 ± 1.4 a
Blackfoot	1.30 ± 0.18 bc	5.22 ± 1.34 ab	8 ± 5 ab	7.4 ± 0.7 ab	6.2 ± 0.2 e	0.10 ± 0.01 bcd	8.0 ± 0.6 a	18.2 ± 1.4 abc
Beckman WMA	0.49 ± 0.06 f	0.59 ± 0.18 d	7 ± 1 a	5.4 ± 0.2 abc	7.8 ± 0.1 a	0.12 ± 0.01 bc	2.7 ± 0.1 c	10.8 ± 1.6 e
Central Grasslands	0.54 ± 0.04 ef	2.13 ± 0.32 bc	4 ± 0 ab	6.8 ± 0.6 abc	7.0 ± 0.1 bcd	0.14 ± 0.01 ab	7.1 ± 0.8 ab	15.2 ± 0.6 abcde
Delbert Berntson	0.87 ± 0.16 cde	1.68 ± 0.73 cd	11 ± 1 a	6.5 ± 0.7 abc	7.6 ± 0.1 ab	0.14 ± 0.02 ab	4.6 ± 0.7 bc	20.8 ± 2.8 ab
B-B Ranch	0.56 ± 0.03 def	1.99 ± 0.44 bc	5 ± 1 a	5.0 ± 0.2 bc	6.9 ± 0.1 bcd	0.12 ± 0.01 abc	6.2 ± 0.4 ab	12.8 ± 0.5 cde
Bicentennial Prairie	0.48 ± 0.04 f	2.10 ± 0.27 bc	5 ± 0 a	5.9 ± 0.1 abc	7.2 ± 0.1 abc	0.17 ± 0.01 a	8.4 ± 0.7 a	17.5 ± 1.2 abc

Note: Soil chemical properties shown with means and SE. Soils around the roots of individual *G. aristata* plants (n = 10) were collected at 12 sites from Montana to Minnesota in June 2018. Sites are arranged from west to east. The box and whisker plots display the median (center horizontal line) flanked by the 25th and 75th percentiles. The upper whisker extends from the 75th percentile line to the largest value no further than 1.5 * IQR from the 75th percentile (where IQR is the inter-quartile range, or distance between the first and third quartiles). The lower whisker extends from the 25th percentile line to the smallest value at most 1.5 * IQR of the hinge. Black diamonds represent means. Following normalization on selected variables, one-way ANOVAs and Tukey's HSD multiple comparison tests were performed. Values followed by the same letter within each column are not statistically different (p < 0.05). Separated into two tables here for readability.

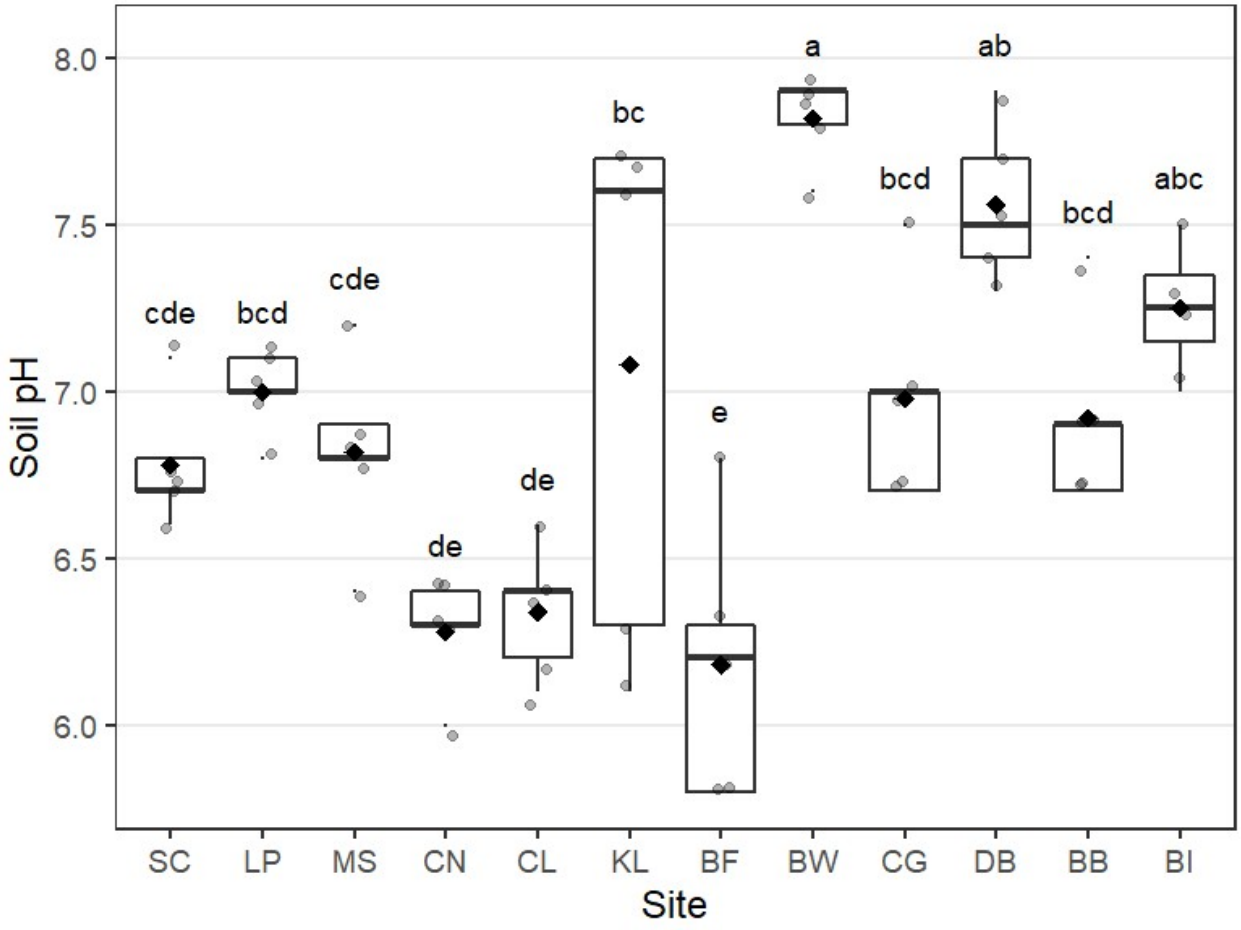

Figure D1. Field soil pH by site.
Note: Soils around the roots of individual *G. aristata* plants (n = 10) were collected at 12 sites from Montana to Minnesota in June 2018. Sites are arranged from west to east. The box and whisker plots display the median (center horizontal line) flanked by the 25th and 75th percentiles. The upper whisker extends from the 75th percentile line to the largest value no further than 1.5 * IQR from the 75th percentile (where IQR is the inter-quartile range, or distance between the first and third quartiles). The lower whisker extends from the 25th percentile line to the smallest value at most 1.5 * IQR of the hinge. Black diamonds represent means. One-way ANOVA and Tukey's HSD multiple comparison test were performed. Sites with the same letter are not statistically different (p < 0.05).

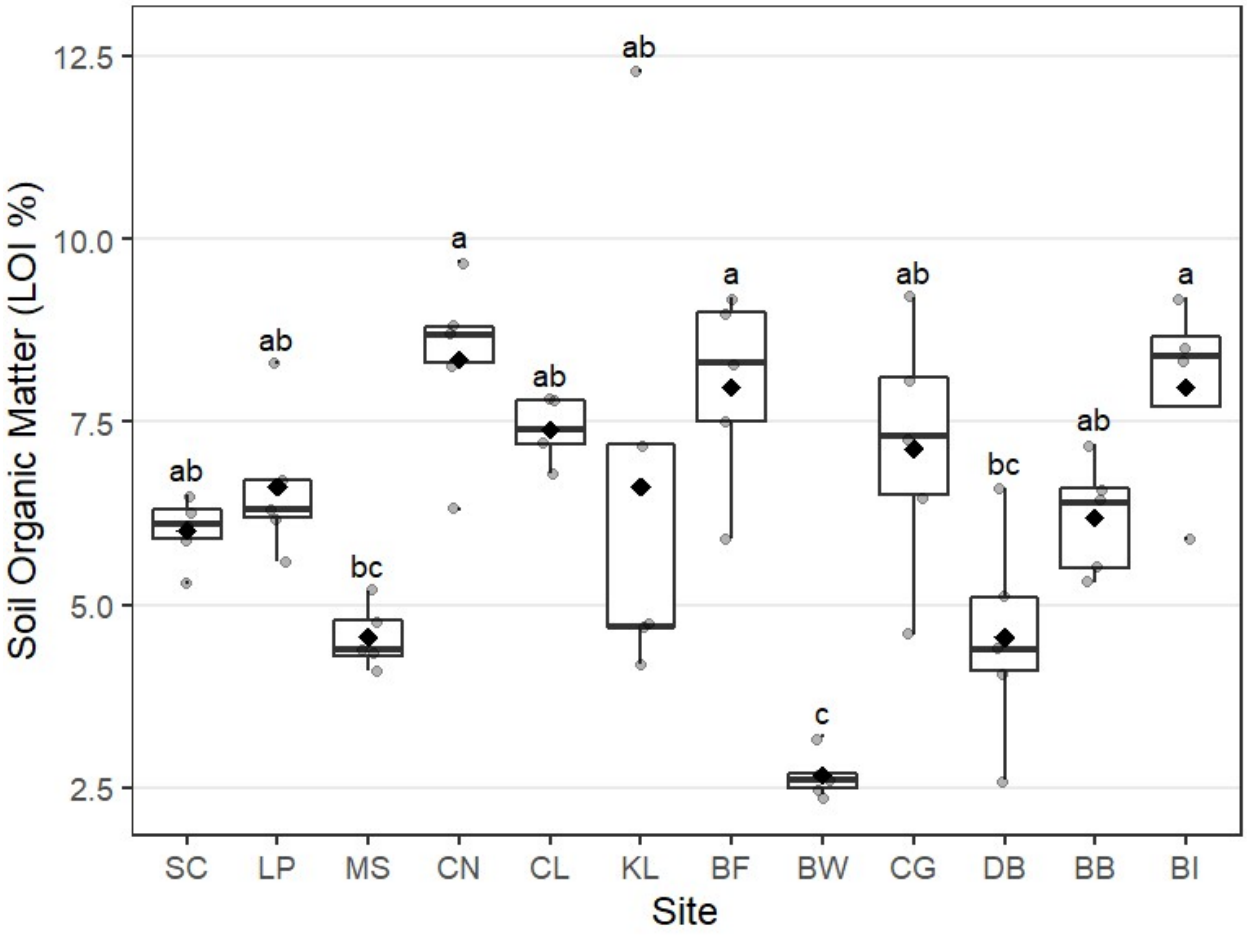

Figure D2. Field soil organic matter by site.
Note: Soils around the roots of individual *G. aristata* plants (n = 10) were collected at 12 sites from Montana to Minnesota in June 2018. Sites are arranged from west to east. The box and whisker plots display the median (center horizontal line) flanked by the 25th and 75th percentiles. The upper whisker extends from the 75th percentile line to the largest value no further than 1.5 * IQR from the 75th percentile (where IQR is the inter-quartile range, or distance between the first and third quartiles). The lower whisker extends from the 25th percentile line to the smallest value at most 1.5 * IQR of the hinge. Black diamonds represent means. One-way ANOVA and Tukey's HSD multiple comparison test were performed. Sites with the same letter are not statistically different (p < 0.05).

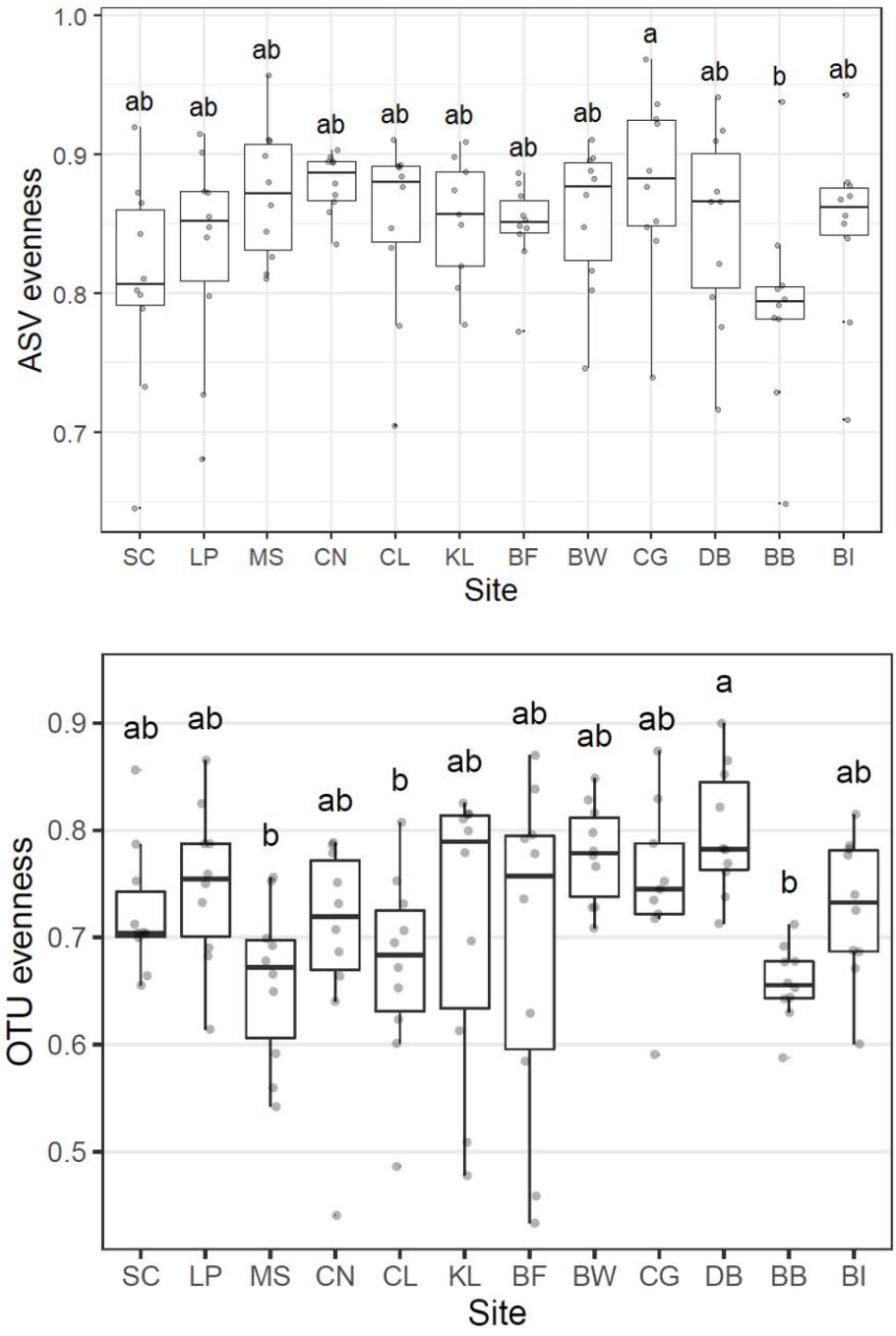

Figure D3. ASV and OTU evenness by site.
Note: *Gaillardia aristata* plants (n = 10) were collected at 12 sites from Montana to Minnesota in June 2018 and evenness of their root AMF communities were characterized with 18S and ITS2 data. Sites are arranged from west to east. The box and whisker plots display the median (center horizontal line) flanked by the 25th and 75th percentiles. Black diamonds represent means. One-way ANOVA and Tukey's HSD multiple comparison test were performed. Sites with the same letter are not statistically different ($p < 0.05$).

Table D2. Fungal OTUs observed at all 12 field sites.

Phylum	Subphylum	Class	Order	Family	Species	Conf	Possible guild	OTU	Seqs	Prop
Ascomycota	Pezizomycotina	Dothideomycetes	Pleosporales	Leptosphaeriaceae	Paraphoma chrysanthemicola	0.98	Leaf Saprotroph-Plant Pathogen-Undefined Saprotroph	7221	4168	0.63
Unknown						1	Unassigned	5784	3961	0.59
Ascomycota	Pezizomycotina	Leotiomycetes	Helotiales	Incertae sedis	Tetracladium furcatum	0.97	Undefined Saprotroph	6718	3109	0.54
Ascomycota	Pezizomycotina	Eurotiomycetes	Chaetothyriales	Herpotrichiellaceae	Exophiala sp.	1	Animal Pathogen-Undefined Saprotroph	2743	1617	0.42
Ascomycota	Pezizomycotina	Leotiomycetes	Helotiales	Unknown		0.97	Unassigned	6838	1467	0.81
Ascomycota	Pezizomycotina	Eurotiomycetes	Chaetothyriales	Herpotrichiellaceae	Phialophora mustea	0.98	Wood Saprotroph	6681	1244	0.68
Ascomycota	Pezizomycotina	Dothideomycetes	Pleosporales	Unknown		0.88	Unassigned	5147	936	0.26
Ascomycota	Pezizomycotina	Incertae sedis	Incertae sedis	Incertae sedis	Knufia sp.	0.96	Animal Pathogen-Plant Pathogen-Soil Saprotroph-Undefined Saprotroph	4697	653	0.32
Ascomycota	Pezizomycotina	Dothideomycetes	Pleosporales	Unknown		0.92	Unassigned	5376	640	0.25
Zygomycota	Mucoromycotina	Incertae sedis	Mortierellales	Mortierellaceae	Mortierella alpina	1	Endophyte-Litter Saprotroph-Soil Saprotroph-Undefined Saprotroph	343	310	0.38
Ascomycota	Pezizomycotina	Unknown				0.95	Unassigned	6209	305	0.23
Glomeromycota	Incertae sedis	Glomeromycetes	Glomerales	Glomeraceae	Unassigned	1	Arbuscular Mycorrhizal	2092	206	0.24

Note**:** Core OTUs observed in *G. aristata* roots collected at 12 sites from Montana to Minnesota in June 2018, arranged from most to least abundant. Guilds were assigned to ITS2 data by FUNGuild. Conf = confidence level (from 0 to 1) of assigned taxonomy. Seqs = number of sequences observed for each OTU. Prop = proportion of samples in which an OTU was observed.

Table D3. AMF ASVs observed at all 12 field sites.

Class	Order	Family	Genus	Species	VT	Sequence ID	Seqs	Prop
Glomeromycetes	Glomerales	Glomeraceae	Glomus			f2a0db7e6f2f94ff263adab6728e2069	18072	0.32
Glomeromycetes	Glomerales	Glomeraceae	Glomus			f6820be9a9f5975ba57757ba7df85722	14723	0.28
Glomeromycetes	Glomerales	Glomeraceae	Glomus			5502ee03250a5cf7ff4a00e8340ce921	11511	0.34
Glomeromycetes	Glomerales	Glomeraceae	Glomus			12b464a9aa2d0f9ea12c39382a958ddd	9426	0.27
Glomeromycetes	Glomerales	Glomeraceae	Glomus	Glomus sp.	VTX00177	ca2c2a9fa18cd5b42e59564fff7030e6	5729	0.2

Note: Core ASVs observed in *G. aristata* roots collected at 12 sites from Montana to Minnesota in June 2018, arranged from most to least abundant. Seqs = number of sequences observed for each ASV. Prop = proportion of samples in which an ASV was observed.

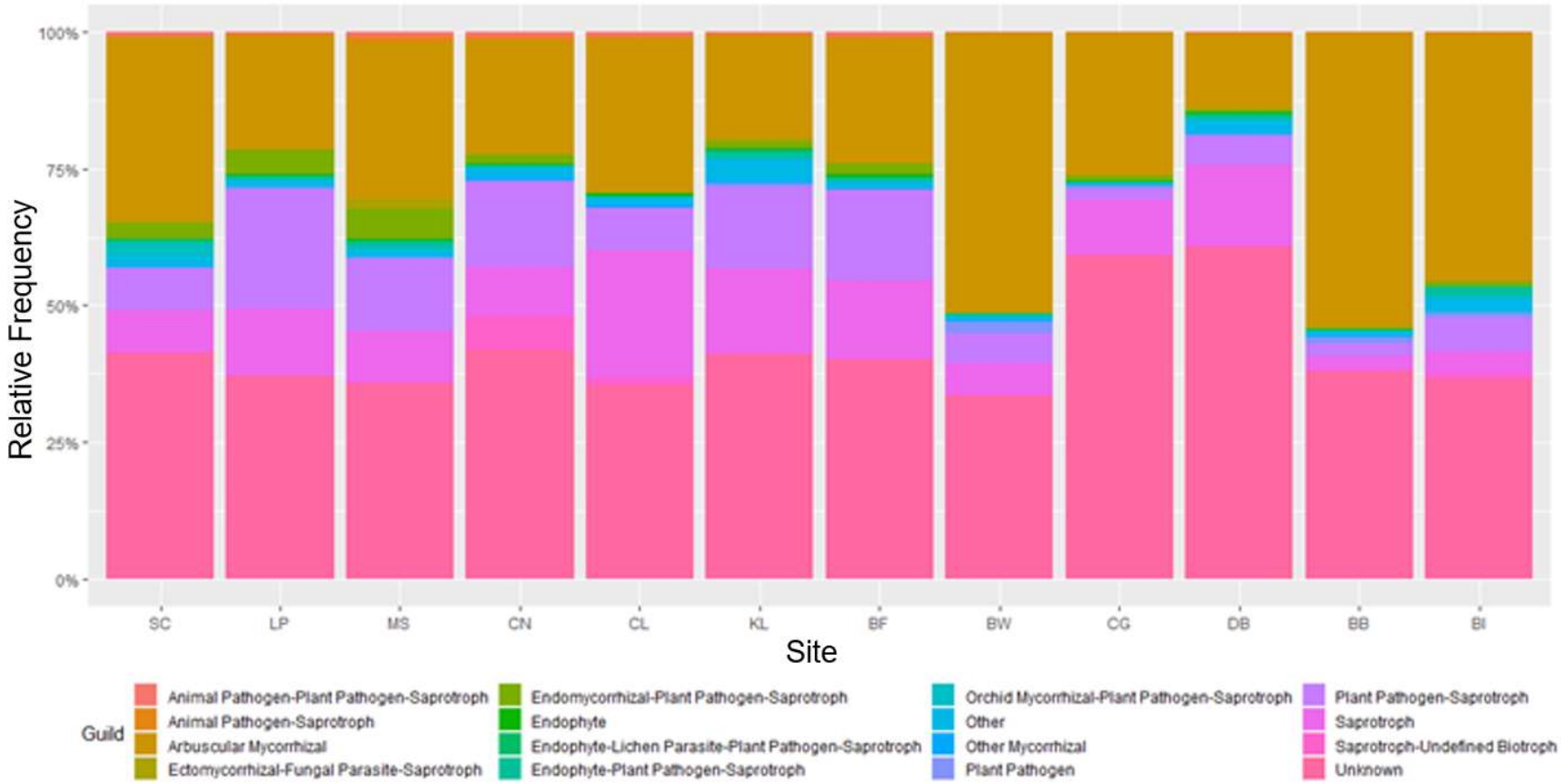

Figure D4. Summary of guild distribution of OTUs by site.
Note: Guild distribution of OTUs observed in *G. aristata* roots collected at 12 sites from Montana to Minnesota in June 2018.Guilds from FUNGuild were simplified and plotted by relative frequency. Sites are arranged from west to east.

Table D4. Adjusted standardized residuals for chi square test of AMF taxonomic distribution by site.

Site	*Ambispora*	*Archaeospora*	*Unknown*	*Acaulospora*	*Diversispora*	*Scutellospora*	*Pacispora*	*Claroideoglomus*	*Paraglomus*	*Glomus*
SC	-1	-1	8	16	37	2	-6	27	-5	-45
LP	-1	-6	53	-16	13	-5	0	20	-5	-35
MS	-1	8	-3	-1	14	-1	-4	-2	-5	-3
CN	8	-6	-12	20	21	11	33	14	-2	-25
CL	-1	34	4	46	19	-5	-2	48	26	-65
KL	-1	-6	-5	-15	-9	21	3	22	4	-9
BF	-1	4	8	23	5	1	-5	-4	4	-8
BW	-1	-7	-4	-17	-20	-6	-6	3	1	15
CG	-1	-6	-13	-14	-24	-5	-5	-34	-5	48
DB	-1	-5	-2	-13	-22	-4	2	-15	-4	27
BB	-1	-6	-18	-14	-26	-5	-5	-43	-5	58
BI	-1	-3	-19	-14	-10	-5	-5	-45	-5	52

Note: Adjusted standardized residuals for taxonomic distribution of AMF ASVs observed in *G. aristata* roots collected at 12 sites from Montana to Minnesota in June 2018. Sites are arranged from west (top) to east (bottom). Taxonomy is divided by AMF genus. Absolute values greater than 3 indicate lack of fit of H_0 for that cell, meaning that the observed relative frequency for that cell was greater (positive residuals) or less (negative residuals) than what would be expected due to chance.

Table D5. Adjusted standardized residuals for chi square test of AMF taxonomic distribution by soil P category.

Group	*Ambispora*	*Archaeospora*	*Unknown*	*Acaulospora*	*Diversispora*	*Scutellospora*	*Pacispora*	*Claroideoglomus*	*Paraglomus*	*Glomus*
High P	2	-4	28	14	44	16	13	42	-5	-24
Low P	-2	4	-28	-14	-44	-16	-13	-42	5	24

Note: Adjusted standardized residuals for taxonomic distribution of AMF ASVs observed in *G. aristata* roots collected at 12 sites from Montana to Minnesota in June 2018. Groups based on mean soil P availability of each site (Figure 1.2). Taxonomy is divided by AMF genus. Absolute values greater than 3 indicate lack of fit of H_0 for that cell, meaning that the observed relative frequency for that cell was greater (positive residuals) or less (negative residuals) than what would be expected due to chance.

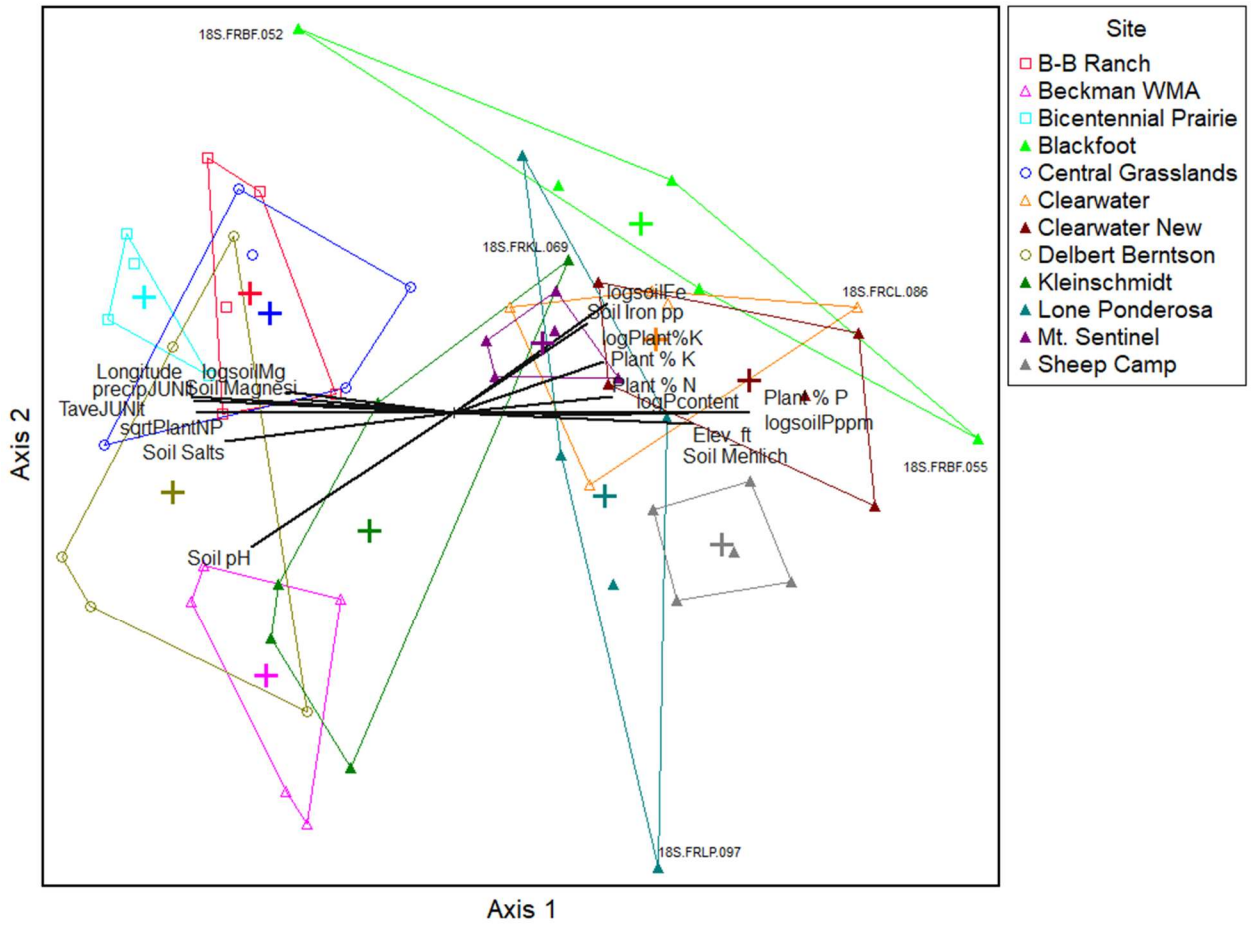

Figure D5. NMS of 18S AMF communities associated with *G. aristata* roots.
Note: *Gaillardia aristata* plants (*n* = 10) were collected at 12 sites from Montana to Minnesota in June 2018 and their root AMF communities were characterized by NMS. Each point represents the fungal community associated with a single plant's roots. Samples shown are those where plant and soil nutrient data was collected – half of the samples did not have this data and are not included in the ordination. Closed shapes represent sites high in soil P availability and open shapes representing low soil P sites. Black arrows represent environmental variables correlated with the axes of the ordination. Ordination was performed on Hellinger-transformed ASV abundance table.

APPENDIX E. ADDITIONAL RESULTS FOR CHAPTER 2

Table E1. Analysis of variance for differences in biomass of *G. aristata* among soil inoculum and P fertilization treatments.

	DF	*SS*	*MS*	*F*	*P*
Soil inoculum	2	203.66	101.83	15.95	< 0.0001
P fertilization	1	174.36	174.36	27.30	< 0.0001
Soil inoculum × P fertilization	2	127.25	63.63	9.96	< 0.0001
Error	122	779.15	6.39		
Total	127	1163.23			

Note: Seeds of *Gaillardia aristata* from Colorado were grown in the greenhouse in North Dakota, USA with or without P fertilization and without mycorrhizas (mock inoculum) or with mycorrhizas sourced from low or high P soils After approximately 14 months, plants were harvest and total biomass was analyzed by two-way analysis of variance for differences among soil inoculum and fertilization treatments and their interaction. DF, degrees of freedom; SS, sum of squares; MS, mean square; F, F statistic; P, p-value.

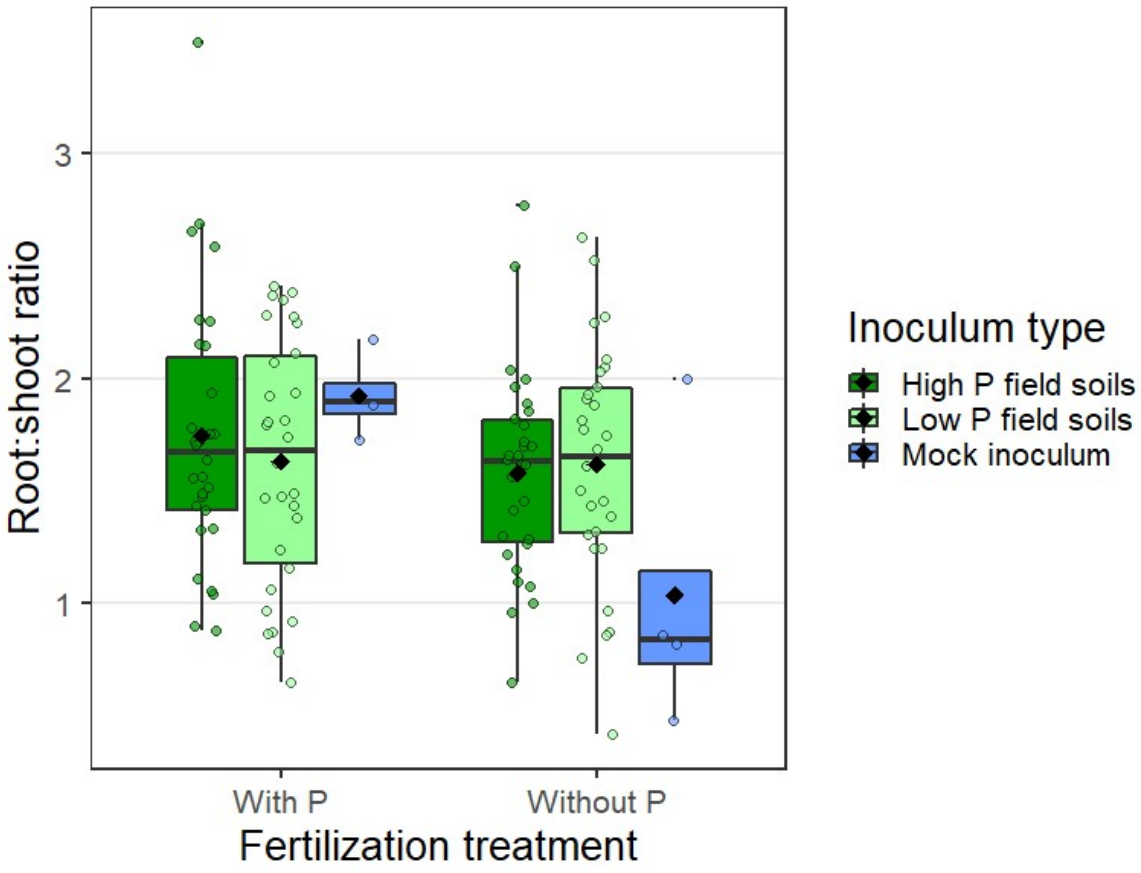

Figure E1. Root-to-shoot biomass ratios by soil inoculum and P fertilization treatments. Note: Data are for *Gaillardia aristata* plants. Seeds from Colorado were grown in the greenhouse in North Dakota, USA with or without P fertilization and without mycorrhizas (mock inoculum) or with mycorrhizas sourced from low or high P soils. Shoot biomass was divided by root biomass to obtain ratios. Each point is an observation. The box plots display the median (center horizontal line) flanked by the 25th and 75th percentiles. Black diamonds represent means.

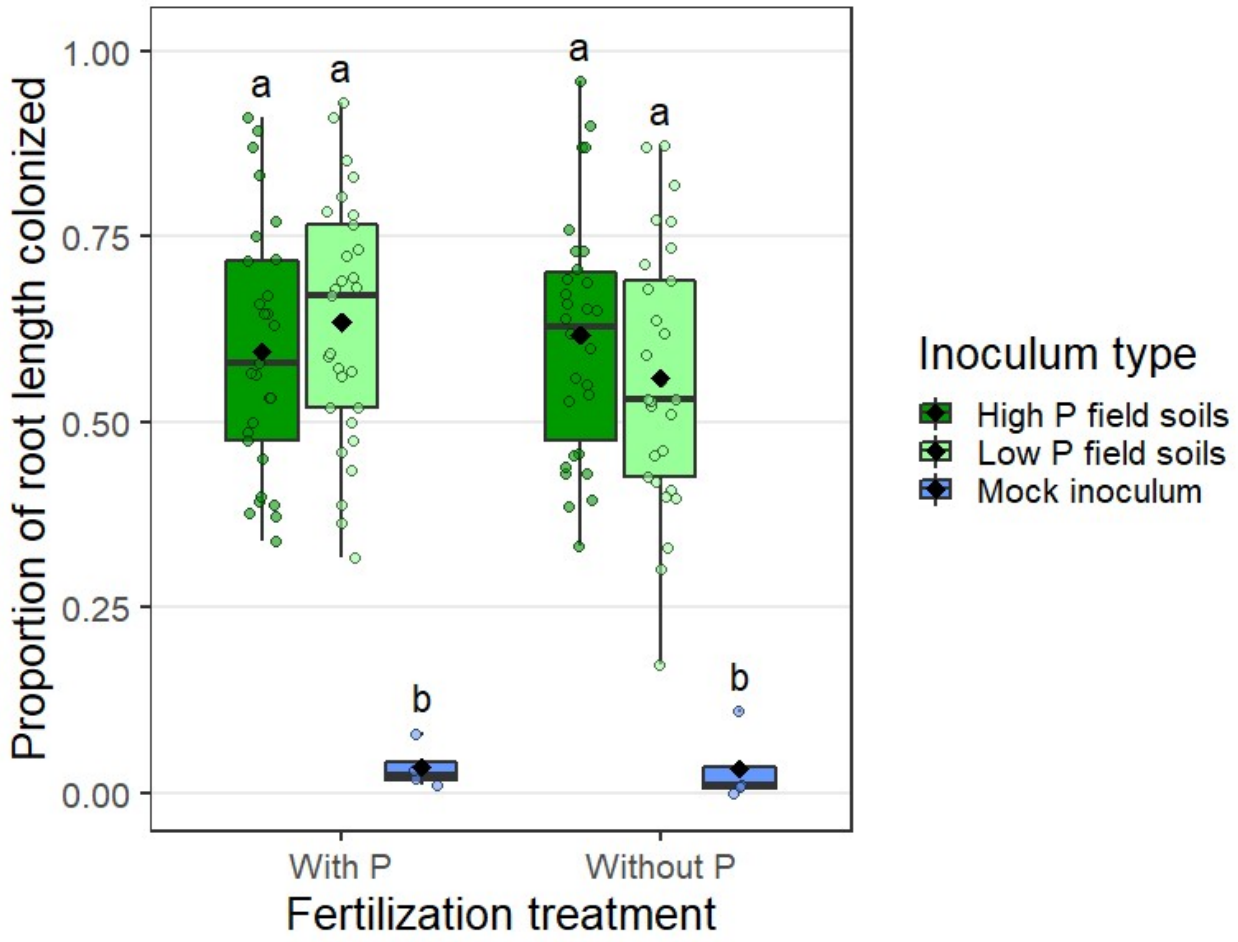

Figure E2. Proportion of root length colonized by AMF.
Note: Data are for *Gaillardia aristata* plants. Seeds from Colorado were grown in the greenhouse in North Dakota, USA with or without P fertilization and without mycorrhizas (mock inoculum) or with mycorrhizas sourced from low or high P soils. Each root sample was examined at 100 points for presence of AMF structures. Each point is an observation. The box and whisker plots display the median (center horizontal line) flanked by the 25th and 75th percentiles. The upper whisker extends from the 75th percentile line to the largest value no further than 1.5 * IQR from the 75th percentile (where IQR is the inter-quartile range, or distance between the first and third quartiles). The lower whisker extends from the 25th percentile line to the smallest value at most 1.5 * IQR of the hinge. Black diamonds represent means. Boxplots connected by the same letter were not significantly different per ANOVA and Tukey HSD.

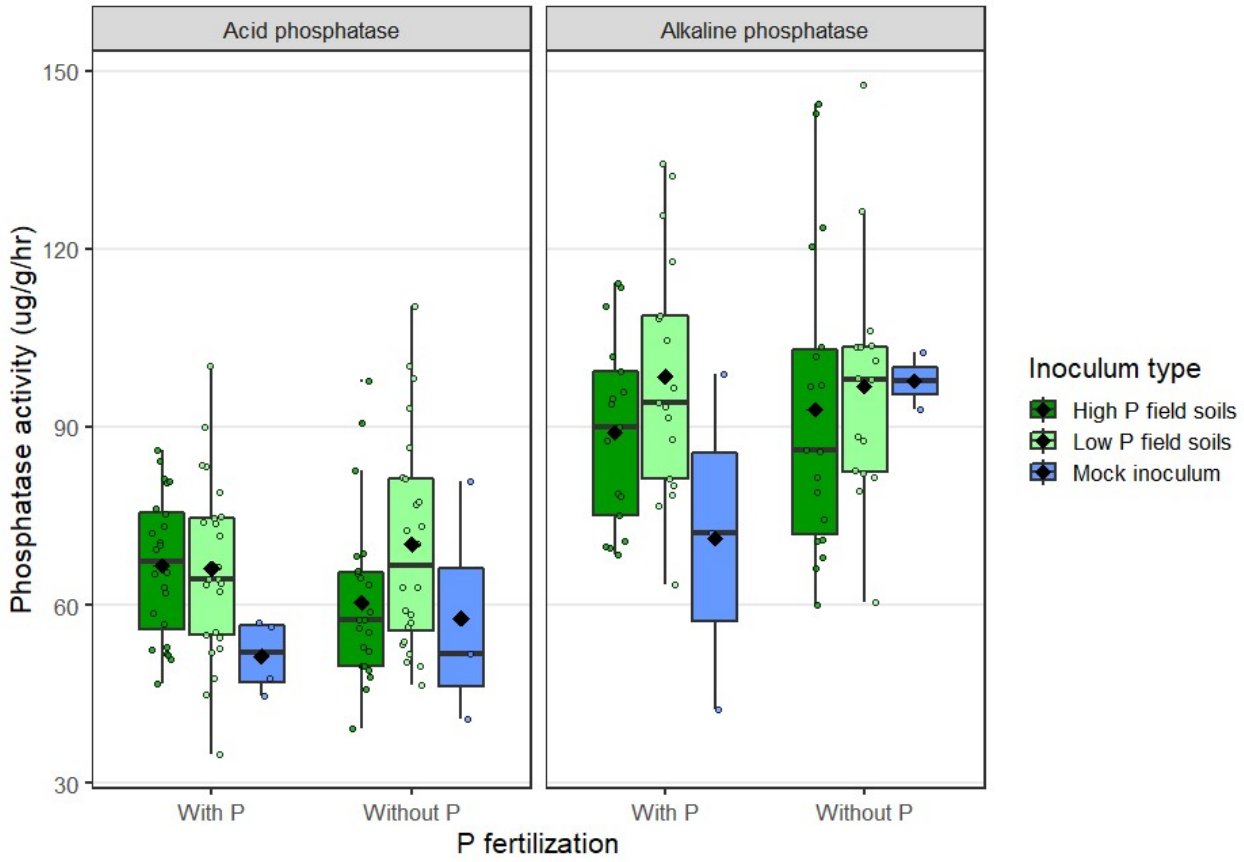

Figure E3. Acid and alkaline phosphatase activity in greenhouse soils.
Note: Phosphatase activity was measured from soil in hyphal in-growth core to exclude phosphatases excreted by *Gaillardia aristata* plants. Seeds from Colorado were grown in the greenhouse in North Dakota, USA with or without P fertilization and without mycorrhizas (mock inoculum) or with mycorrhizas sourced from low or high P soils. Each point is an observation. The box and whisker plots display the median (center horizontal line) flanked by the 25th and 75th percentiles. The upper whisker extends from the 75th percentile line to the largest value no further than 1.5 * IQR from the 75th percentile (where IQR is the inter-quartile range, or distance between the first and third quartiles). The lower whisker extends from the 25th percentile line to the smallest value at most 1.5 * IQR of the hinge. Black diamonds represent means.

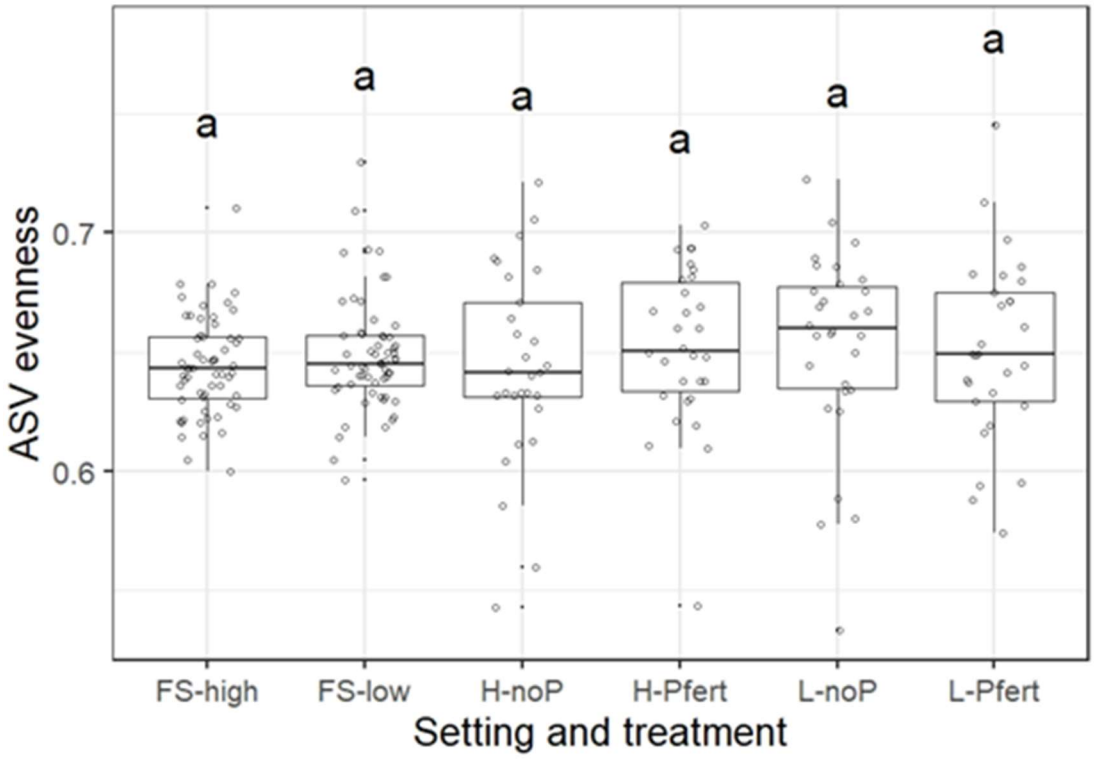

Figure E4. Evenness of ASVs by soil inoculum and P fertilization treatments.
Note: AMF communities were sampled from field soils (FS) and from roots of *G. aristata* grown in the greenhouse with (Pfert) or without (noP) P fertilization. Each point represents an observation, with n = 60 for field soil groups and n = 30 for greenhouse treatments. Evenness calculated using Pielou's index. The box and whisker plots display the median (center horizontal line) flanked by the 25th and 75th percentiles. The upper whisker extends from the 75th percentile line to the largest value no further than 1.5 * IQR from the 75th percentile (where IQR is the inter-quartile range, or distance between the first and third quartiles). The lower whisker extends from the 25th percentile line to the smallest value at most 1.5 * IQR of the hinge. Groups with the same letter were not statistically different per ANOVA and Tukey HSD.

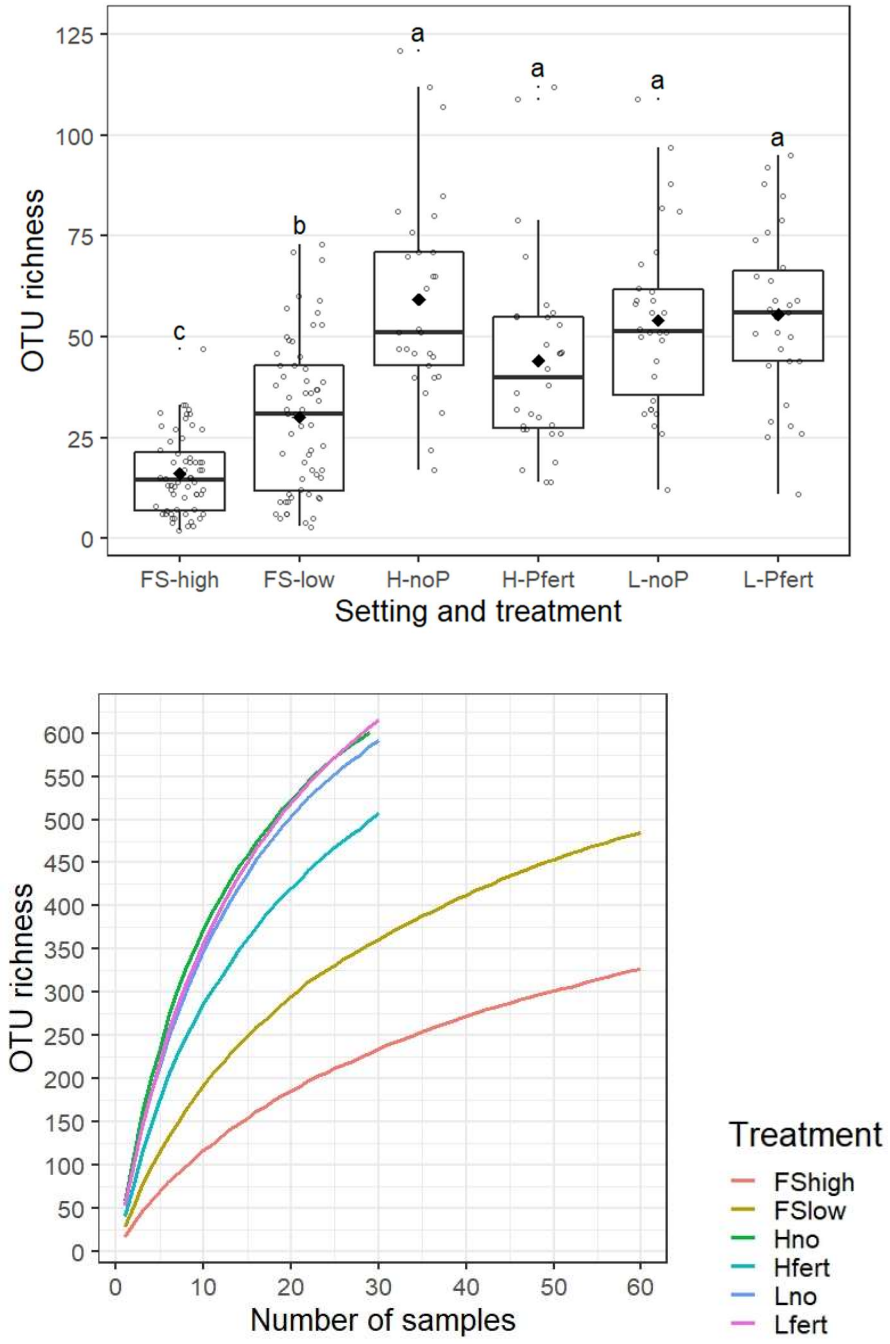

Figure E5. OTU richness by sample type and species accumulation curves.
Note: AMF communities were sampled from field soils (FS) and from roots of *G. aristata* grown in the greenhouse with (Pfert) or without (noP) P fertilization. Each point represents an observation, with n = 60 for field soil groups and n = 30 for greenhouse treatments. The box and whisker plots display the median (center horizontal line) flanked by the 25th and 75th percentiles. Groups with the same letter were not statistically different by Tukey HSD. Black diamonds indicate group means.

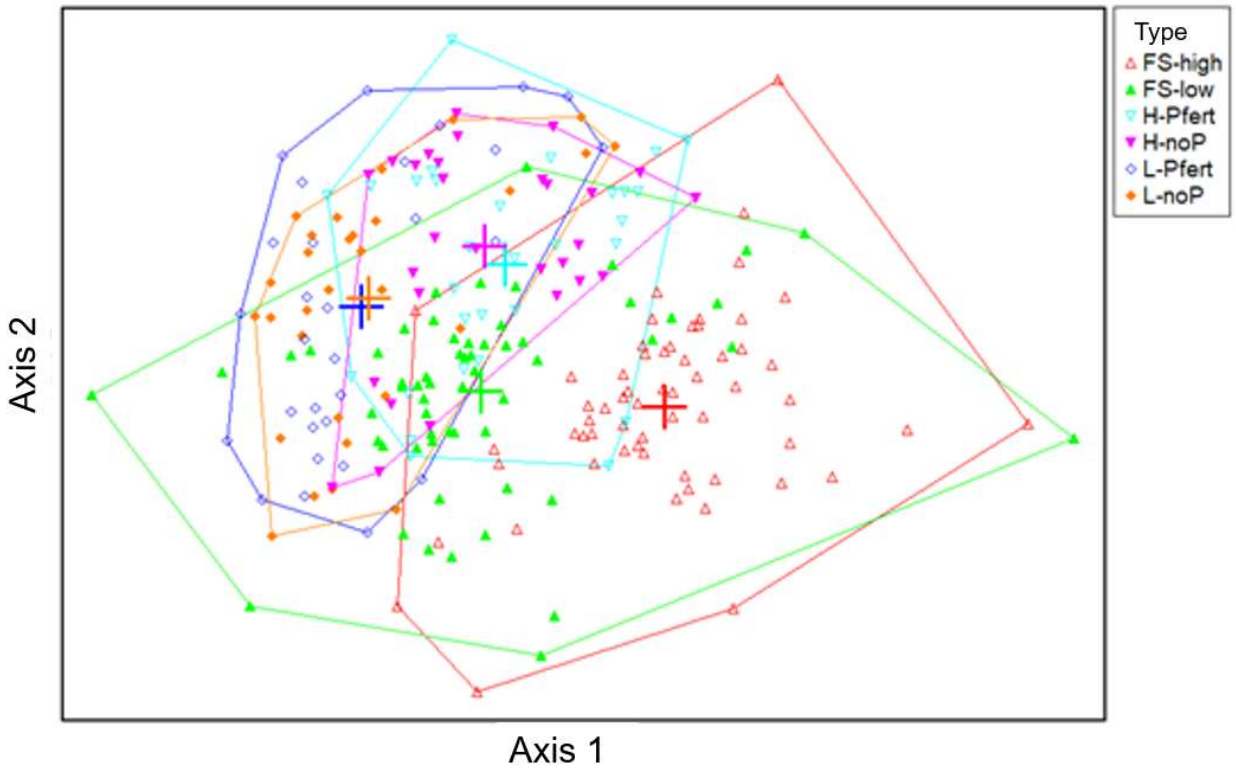

Figure E6. NMS visualization of ITS2 field soil and greenhouse root AMF communities. Note: AMF communities were sampled from field soils (FS) that were either high (H) or low (L) in P availability and from roots of *G. aristata* grown in the greenhouse with (Pfert) or without (noP) P fertilization. Each point represents one community, with more similar communities appearing more closely together. NMS was performed with Hellinger-transformed OTU abundance table.

Table E2. Adjusted standardized residuals for chi square test of AMF taxonomic distribution by soil inoculum and P fertilization treatments.

Treatment	*Ambispora*	*Archaeospora*	Unknown	*Acaulospora*	*Diversispora*	*Scutellospora*	*Pacispora*	*Claroideoglomus*	*Glomus*	*Paraglomus*
FS-high	19	74	14	65	177	62	47	271	-359	35
FS-low	-1	12	-34	4	58	-7	-10	18	-35	-5
High-noP	-5	-26	9	-21	-69	-17	-11	-70	103	-9
High-Pfert	-5	-26	60	-21	-73	-17	-11	-59	82	-9
Low-noP	-5	-25	-19	-20	-70	-16	-11	-99	136	-10
Low-Pfert	-5	-25	-27	-20	-67	-16	-11	-114	149	-8

Note: AMF communities were sampled from field soils (FS) either high or low in soil P availability and from roots of *G. aristata* grown in the greenhouse with (Pfert) or without (noP) P fertilization. Taxonomy is divided by AMF genus. Absolute values greater than 3 indicate lack of fit of H_0 for that cell, meaning that the observed relative frequency for that cell was greater (positive residuals) or less (negative residuals) than what would be expected due to chan

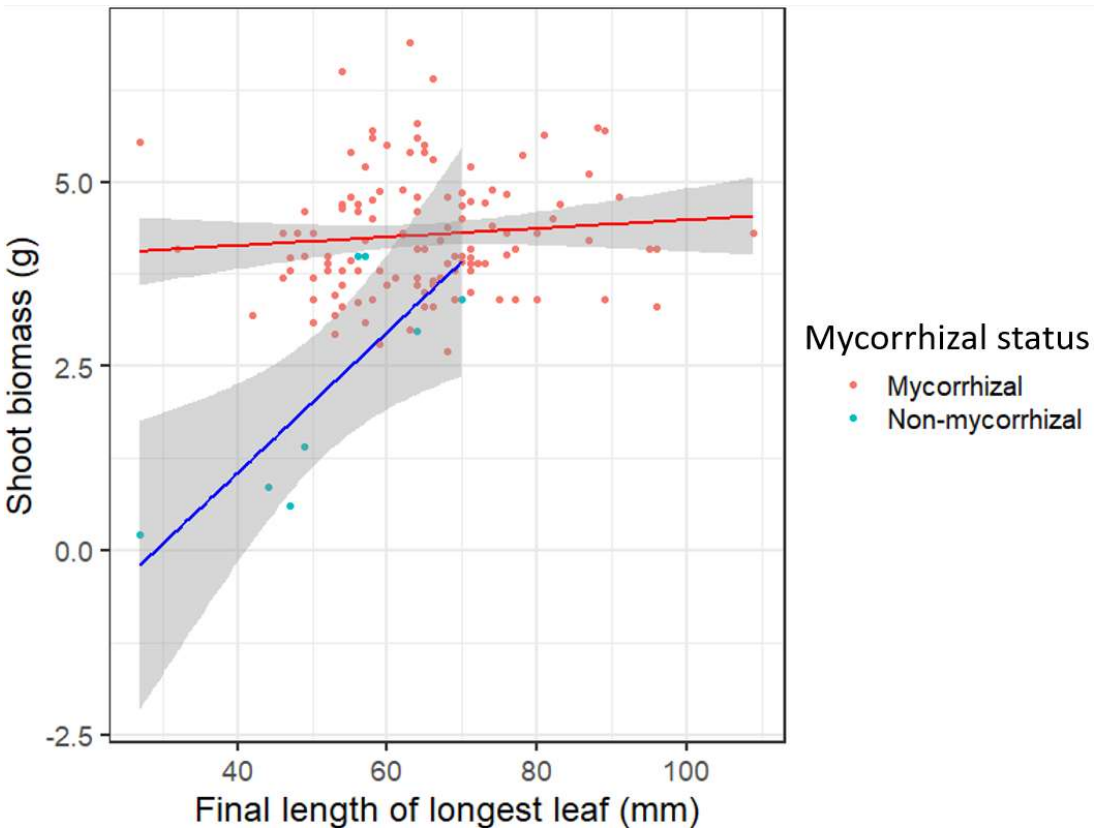

Figure E7. Relationship between shoot biomass and final length of longest leaf.
Note: Measurements are for *Gaillardia aristata* plants. Seeds from Colorado were grown in the greenhouse in North Dakota, USA with or without mycorrhizas. Each point is an observation. Regression lines describe how response variables change with shoot biomass. Gray region flanking line represents confidence interval.

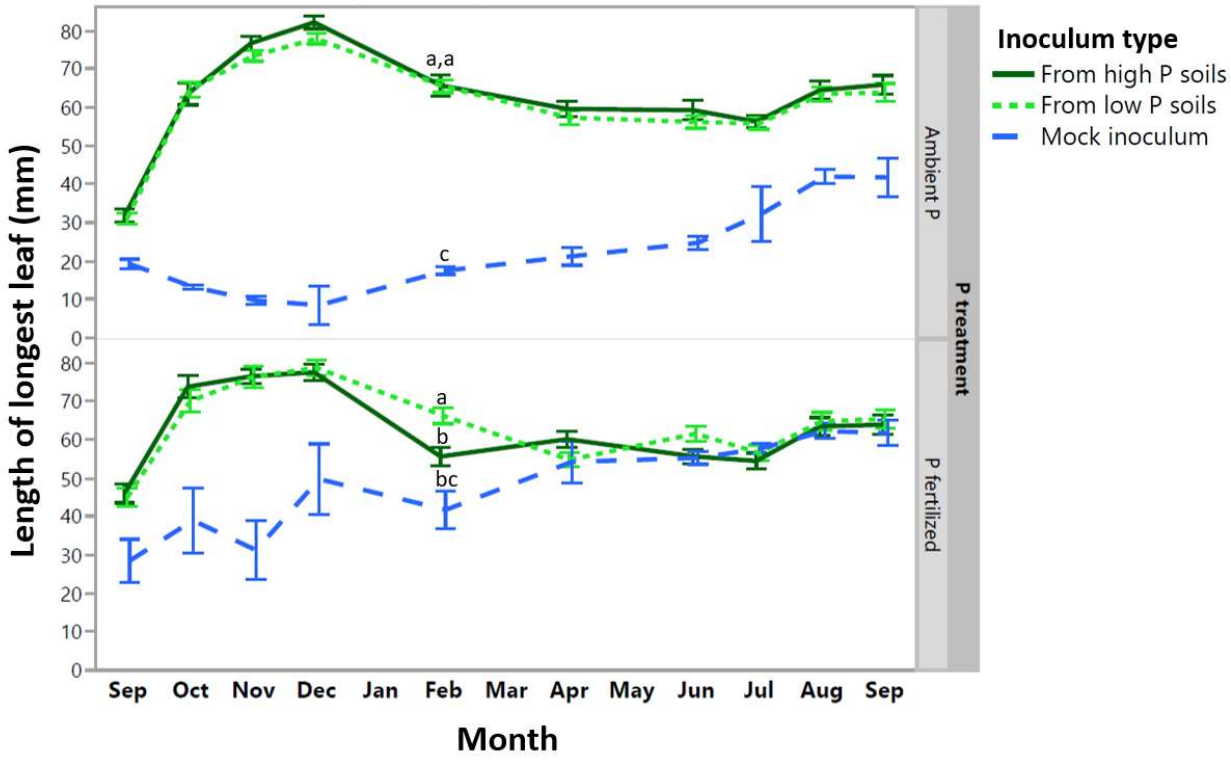

Figure E8. *Gaillardia aristata* growth across treatments and time.
Note: Seeds from Colorado were grown for approximately 14 months in the greenhouse in North Dakota, USA with or without P fertilization and without mycorrhizas (mock inoculum) or with mycorrhizas sourced from low or high P soils. Length of the longest leaf was used as a proxy for plant growth. Measurements were taken approximately once a month throughout the duration of the experiment. No data was collected in January, March, or May. Values are means (N = 30, except for mock inoculum treatment, where N = 4). Each error bar is constructed using 1 standard error from the mean. Groups with the same letter above error bar for February time point were not statistically different.